2

NUSC Technical Report 8121
21 September 1987

Operating Characteristics for Indicator Or-ing of Incoherently Combined Matched-Filter Outputs

Albert H. Nuttall
Surface Ship Sonar Department

Naval Underwater Systems Center

Newport, Rhode Island / New London, Connecticut

Approved for public release: distribution is unlimited.

DISCLAIMER NOTICE

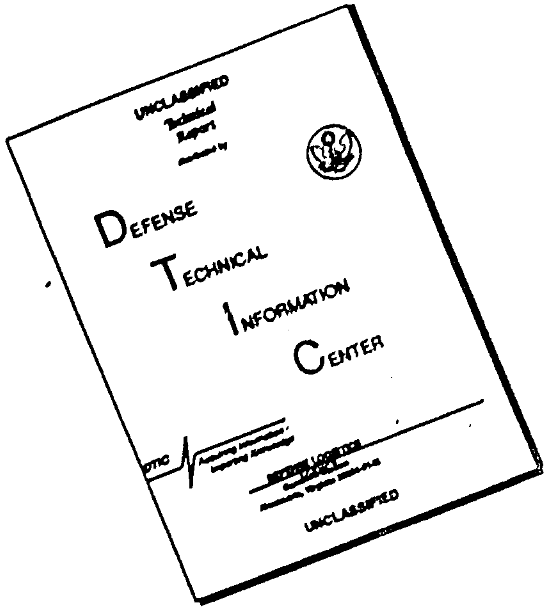

THIS DOCUMENT IS BEST QUALITY AVAILABLE. THE COPY FURNISHED TO DTIC CONTAINED A SIGNIFICANT NUMBER OF PAGES WHICH DO NOT REPRODUCE LEGIBLY.

REPORT DOCUMENTATION PAGE

1a. REPORT SECURITY CLASSIFICATION
UNCLASSIFIED

1b. RESTRICTIVE MARKINGS

2a. SECURITY CLASSIFICATION AUTHORITY

2b. DECLASSIFICATION / DOWNGRADING SCHEDULE

3. DISTRIBUTION / AVAILABILITY OF REPORT
Approved for public release; distribution is unlimited.

4. PERFORMING ORGANIZATION REPORT NUMBER(S)
TR 8121

5. MONITORING ORGANIZATION REPORT NUMBER(S)

6a. NAME OF PERFORMING ORGANIZATION
Naval Underwater Systems Center

6b. OFFICE SYMBOL *(If applicable)*

7a. NAME OF MONITORING ORGANIZATION

6c. ADDRESS *(City, State, and ZIP Code)*
New London Laboratory
New London, CT 06320

7b. ADDRESS *(City, State, and ZIP Code)*

8a. NAME OF FUNDING / SPONSORING ORGANIZATION

8b. OFFICE SYMBOL *(If applicable)*

9. PROCUREMENT INSTRUMENT IDENTIFICATION NUMBER

8c. ADDRESS *(City, State, and ZIP Code)*

10. SOURCE OF FUNDING NUMBERS

PROGRAM ELEMENT NO.	PROJECT NO.	TASK NO.	WORK UNIT ACCESSION NO.
	A75205		

11. TITLE *(Include Security Classification)*
OPERATING CHARACTERISTICS FOR INDICATOR OR-ING OF INCOHERENTLY COMBINED MATCHED-FILTER OUTPUTS

12. PERSONAL AUTHOR(S)
Albert H. Nuttall

13a. TYPE OF REPORT

13b. TIME COVERED FROM ______ TO ______

14. DATE OF REPORT *(Year, Month, Day)*
1987 September 21

15. PAGE COUNT

16. SUPPLEMENTARY NOTATION

17. COSATI CODES

FIELD	GROUP	SUB-GROUP

18. SUBJECT TERMS *(Continue on reverse if necessary and identify by block number)*
Operating Characteristics
Indicator Or-ing
Matched Filters
Incoherent Combination
Detection Probability
False Alarm Probability

19. ABSTRACT *(Continue on reverse if necessary and identify by block number)*

The false alarm and detection probabilities for a processor that incoherently combines M matched filter outputs and then subjects these summed quantities to or-ing amongst N channels are derived for general M, N, and signal-to-noise ratios. A probability of correct detection occurs only when the signal channel output exceeds a threshold and all other noise channel outputs. Receiver operating characteristics are plotted for the 40 possible combinations of M = 1(1)10 with N = 1, 10, 100, 1000, for signal-to-noise ratios ranging over values diverse enough to cover false-alarm, detection probability pairs from (.01,.5) to (1E-10,.999). Also, the required signal-to-noise ratio to realize specified false alarm and detection probabilities are plotted versus N, for several values of M.

The signal-to-noise ratio parameter employed is related to the total received

20. DISTRIBUTION / AVAILABILITY OF ABSTRACT
☒ UNCLASSIFIED/UNLIMITED ☐ SAME AS RPT. ☐ DTIC USERS

21. ABSTRACT SECURITY CLASSIFICATION
UNCLASSIFIED

22a. NAME OF RESPONSIBLE INDIVIDUAL
Albert H. Nuttall

22b. TELEPHONE *(Include Area Code)*
(203) 440-4618

22c. OFFICE SYMBOL
Code 3302

18. Subject Terms (Con'td.)

Correct Detection
Energy Fractionalization
Multipath

19. Abstract (Cont'td.)

signal energy to Gaussian noise spectral density ratio. This allows for consideration of arbitrary fractionalization of the received signal energy and for investigation of mismatch as well as frequency offset and time desynchronization, if desired. Programs for all procedures are listed.

TABLE OF CONTENTS

Page

LIST OF ILLUSTRATIONS ii

LIST OF SYMBOLS v

INTRODUCTION 1

STATISTICS OF FILTER ENVELOPE-SQUARED OUTPUT 7

FALSE ALARM AND DETECTION PROBABILITIES 13

FALSE ALARM PROBABILITY 13

DETECTION PROBABILITY 14

TIGHTNESS OF BOUND 18

GRAPHICAL RESULTS 19

SUMMARY 21

APPENDICES

A. Q_M-FUNCTION RELATIONSHIPS A-1

B. TABULATION OF P_{CD} AND $Q_M(d,T)$ B-1

C. PROGRAM LISTING C-1

REFERENCES R-1

LIST OF ILLUSTRATIONS

Figure		Page
1.	Preprocessing for n-th Channel	3
2.	Indicator Or-ing of N Channels	3
3.	ROC for M = 1, N = 1	23
4.	ROC for M = 1, N = 10	24
5.	ROC for M = 1, N = 100	25
6.	ROC for M = 1, N = 1000	26
7.	ROC for M = 2, N = 1	27
8.	ROC for M = 2, N = 10	28
9.	ROC for M = 2, N = 100	29
10.	ROC for M = 2, N = 1000	30
11.	ROC for M = 3, N = 1	31
12.	ROC for M = 3, N = 10	32
13.	ROC for M = 3, N = 100	33
14.	ROC for M = 3, N = 1000	34
15.	ROC for M = 4, N = 1	35
16.	ROC for M = 4, N = 10	36
17.	ROC for M = 4, N = 100	37
18.	ROC for M = 4, N = 1000	38
19.	ROC for M = 5, N = 1	39
20.	ROC for M = 5, N = 10	40
21.	ROC for M = 5, N = 100	41

LIST OF ILLUSTRATIONS (CONT'D)

Figure		Page
22.	ROC for M = 5, N = 1000	42
23.	ROC for M = 6, N = 1	43
24.	ROC for M = 6, N = 10	44
25.	ROC for M = 6, N = 100	45
26.	ROC for M = 6, N = 1000	46
27.	ROC for M = 7, N = 1	47
28.	ROC for M = 7, N = 10	48
29.	ROC for M = 7, N = 100	49
30.	ROC for M = 7, N = 1000	50
31.	ROC for M = 8, N = 1	51
32.	ROC for M = 8, N = 10	52
33.	ROC for M = 8, N = 100	53
34.	ROC for M = 8, N = 1000	54
35.	ROC for M = 9, N = 1	55
36.	ROC for M = 9, N = 10	56
37.	ROC for M = 9, N = 100	57
38.	ROC for M = 9, N = 1000	58
39.	ROC for M = 10, N = 1	59
40.	ROC for M = 10, N = 10	60
41.	ROC for M = 10, N = 100	61
42.	ROC for M = 10, N = 1000	62

LIST OF ILLUSTRATIONS (CONT'D)

Figure		Page
43.	Required d Values for M=1, $P_{CD} = .5$	63
44.	Required d Values for M=1, $P_{CD} = .9$	63
45.	Required d Values for M=2, $P_{CD} = .5$	64
46.	Required d Values for M=2, $P_{CD} = .9$	64
47.	Required d Values for M=4, $P_{CD} = .5$	65
48.	Required d Values for M=4, $P_{CD} = .9$	65
B-1	Comparison of Probabilities	B-2

LIST OF SYMBOLS

M	number of filter outputs added, figure 1
N	number of channels subject to or-ing, figure 2, (2)
$h(\tau)$	impulse response of filter, figure 1
underline	complex envelope
t_{nm}	sampling time in n-th channel on m-th filter output, figure 1
v_n	summer output of n-th channel, figure 1, (9)
w	maximum output from or-ing device, (2), (3)
$\hat{n}$	channel indication from or-ing device, (2)
$s(t)$	real signal function of time t, (4)
$n(t)$	real noise process, (5)
a,b	real, imaginary parts of signal output, (4)
x,y	real, imaginary parts of noise, (4)
c	complex envelope of filter output, (4)
N_d	double-sided noise spectral density (watts/Hz), (12)
N_o	single-sided noise spectral density (= $2N_d$), (12)
σ^2	noise power, (14)
d	total output signal-to-noise ratio measure, (15)
E_m	received signal energy in m-th component, (17)
P	cumulative distribution function, (18)
Q_M	Marcum's Q_M - function, (19)
E_n	auxiliary function, (22)
e_n	partial exponential, (23)

LIST OF SYMBOLS (CONT'D)

P_F	false alarm probability, (25)
P_{SD}	probability of signal detection, (26)
P_{AD}	probability of any detection, (27)
P_{CD}	probability of correct detection, (28)
ROC	Receiver Operating Characteristic

OPERATING CHARACTERISTICS FOR INDICATOR OR-ING OF INCOHERENTLY COMBINED MATCHED-FILTER OUTPUTS

INTRODUCTION

When multiple pulses are transmitted, in an effort to detect the presence of a target, the multiple echoes should be optimally processed and combined before a decision is reached. For received signals that are deterministic, except for independent random phases between pulses, the ideal processing consists of matched filtering, envelope detection, and combination according to a $\ln I_0$ rule [1; chapter VII, (1.7)]. Since the receiver input signal-to-noise ratio must be known in order to apply this rule, the slightly suboptimum alternative of combining (adding) squared envelopes is often adopted [1; ch. VII, (1.12)]; this is the situation to be considered here.

In addition, if the target has some movement in the radial direction, causing a Doppler shift of the echoes, a search must be conducted over frequency at the receiver, in order not to miss the received signal energy. For example, suppose a series of M tone bursts at a common center frequency are transmitted and echoed off a moving point target. Since the received center frequency will be unknown, groups of matched filters will be necessary, in order to cover the expected range of frequency shifts. Each one of the possible received center frequencies that must be processed is called a channel.

In figure 1, a block diagram of the processing in the n-th channel is depicted. The M narrowband filters in the n-th channel are indicated by impulse responses $\left\{h_{nm}(\tau)\right\}_{m=1}^{M}$. They are followed by detectors which extract the squared envelopes of the filter outputs. These detector outputs are then sampled at times $\left\{t_{nm}\right\}_{m=1}^{M}$, which should correspond to the times of peak signal at each filter output. The sampled outputs are then added, to yield channel output v_n.

The block diagram in figure 1 is not restricted to a transmitted sequence of M tone bursts at a common center frequency. In fact, due to the general filter impulse responses and sampling times allowed, it encompasses any sequence of orthogonal deterministic signals transmitted at arbitrary time delays and frequency offsets, provided they are known to the receiver. The processor in figure 1 also allows for unknown time delay to the target range and unknown frequency shift due to target movement, by virtue of the sampling times not being optimum, and the filter impulse responses not being matched to each received signal component. An example is afforded by the case where the filters are time-delayed and/or frequency-shifted versions of one another,

$$\underline{h}_{nm}(\tau) = \underline{h}(\tau - \tau_{nm}) \exp(i2\pi f_{nm}\tau), \tag{1}$$

corresponding to a time sequence of frequency-stepped pulses; here $\underline{h}$ is the complex envelope corresponding to impulse response h [1; pages 65-72].

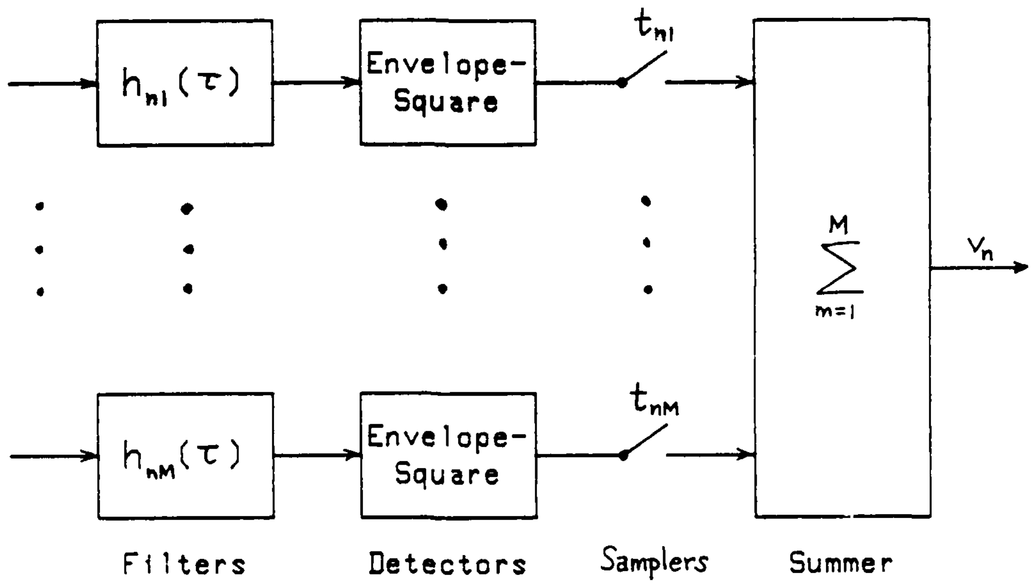

Figure 1. Pre-Processing for n-th Channel

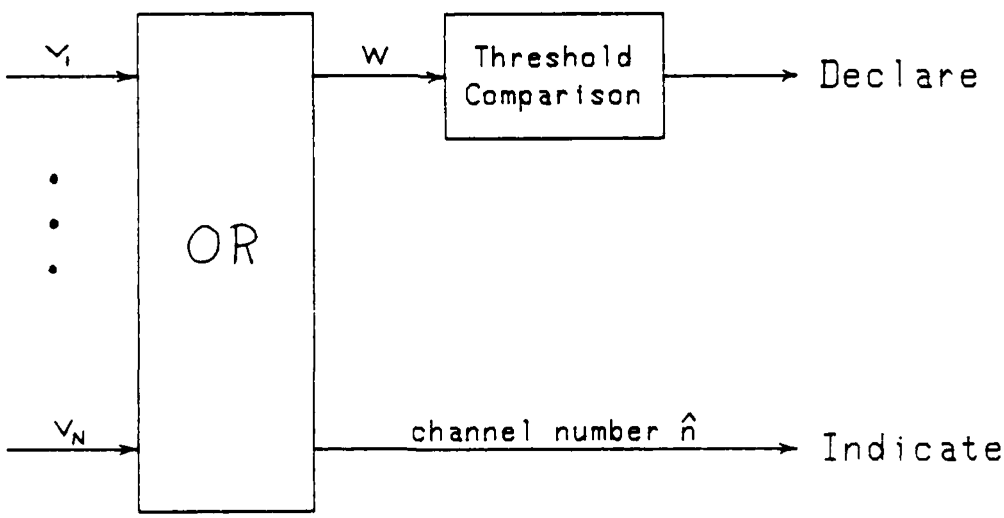

Figure 2. Indicator Or-ing of N Channels

Another instance which is covered by the processing indicated in figure 1 is where the transmitted signal encounters multipath and/or separated target highlight structure. For example, a single transmitted tone burst might be received as four pulses, due to two multipaths and two target highlights. Thus, the number M of filters employed in figure 1 is be interpreted as the total number of <u>received</u> signal components. Some results for the receiver operating characteristics of this processor are given in [1] and [2].

When the processing in the n-th channel indicated in figure 1 is completed, the total of N channels that must be considered is subjected to the indicator or-ing depicted in figure 2. Namely, the maximum of the N channel outputs is extracted, along with its identity,

$$w = \max\left(v_1, v_2, \ldots, v_N\right) = v_{\hat{n}} , \tag{2}$$

and compared with a fixed threshold:

$$\left\{\begin{array}{l} w < \text{threshold: declare no signal present} \\ w > \text{threshold: declare signal present in channel } \hat{n} \end{array}\right\} . \tag{3}$$

Thus, there are two possible outputs from figure 2, the first being a declaration of no signal present, and the second being a declaration of a signal present along with an indication of which channel contains the signal. (This latter information is useful for identifying the Doppler shift, for example, of a moving target.)

A false alarm occurs when output w in (2) exceeds the threshold, but there is no signal present at the input. On the other hand, a correct detection occurs only when the signal channel output exceeds the threshold and all the noise channel outputs. That is, we insist on accurately identifying the signal channel, in order to achieve a correct detection. The performance characteristics of the processor combination in figures 1 and 2 are of interest, namely the false alarm probability and the probability of correct detection, in terms of M, the number of filter outputs summed, N, the number of channels or-ed, and some signal-to-noise ratio measure at the receiver.

It should be observed that the M received signal components have been presumed to have undergone no fading. The only randomness in the received signals are the independent random phase shifts between components. Some results on fading signals, including partial fading between pulses, are given in [3]; however, or-ing was not considered there.

It is also assumed that the individual signal components are orthogonal with respect to each other, perhaps due to time separation and/or frequency shift. That is, at sampling instant t_{nm}, there is only one signal component contributing, with all the other signal components yielding no output at that filter at that time.

The processor considered in this study has undergone some analysis in the past [4]; however, several significant extensions have been made here. First, a different definition of detection probability has been adopted here, namely one which counts as correct detections only those events for which the signal channel output exceeds both the threshold <u>and</u> all the other undesired noise channel outputs. Second, results are extended from a sinusoidal signal to arbitrary orthogonal deterministic signals and filters, with arbitrary sampling instants; this allows for analysis of the effects of filter-signal mismatch, Doppler offset, time desynchronization, multiple highlights, etc. Third, a fundamentally different signal-to-noise ratio parameter, d, is used here to characterize performance, namely, a measure of the total received signal energy to noise spectral density ratio, rather than the signal-to-noise ratio per pulse (usually assumed identical for all pulses); this allows for arbitrary fractionalization of the total received signal energy into component pulses. Fourth, the detection probability vs. false alarm probability curves are plotted on normal probability paper with total signal-to-noise ratio, d, as a parameter; this straightens out the curves, makes them nearly equi-spaced in d, and affords easy accurate interpolation in signal-to-noise ratio values. Finally, the current results are extended to much larger values of the number, N, of or-ing channels and much smaller false alarm probabilities P_F; in particular, values of N up to 1000, and values of P_F as small as 1E-10, are considered.

STATISTICS OF FILTER ENVELOPE-SQUARED OUTPUT

In this section, we derive the statistical properties of the output of figure 1. Suppose a real narrowband deterministic signal s(t) and a real random noise process n(t) have complex envelopes $\underline{s}(t)$ and $\underline{n}(t)$, respectively. Let the sum of these two processes excite a narrowband filter $h(\tau)$ with complex envelope impulse response $\underline{h}(\tau)$. The complex envelope of the filter output at time t is proportional to

$$c(t) = [\underline{s}(t) + \underline{n}(t)] \bullet \underline{h}(t) = a(t) + ib(t) + x(t) + iy(t), \qquad (4)$$

where

$$a(t) + ib(t) = \int d\tau \; \underline{s}(\tau) \; \underline{h}(t-\tau) \qquad (5)$$

is the deterministic signal output, and

$$x(t) + iy(t) = \int d\tau \; \underline{n}(\tau) \; \underline{h}(t-\tau) \qquad (6)$$

is the random noise output process. Then the filter squared-envelope output at time t is

$$|c(t)|^2 = |a(t) + ib(t) + x(t) + iy(t)|^2 =$$

$$= [a(t) + x(t)]^2 + [b(t) + y(t)]^2. \qquad (7)$$

More generally, for M filters, if signal $s_m(t)$ excites filter $h_m(\tau)$, the m-th filter squared-envelope output at sample time t_m is

$$|c_m(t_m)|^2 = [a_m(t_m) + x_m(t_m)]^2 + [b_m(t_m) + y_m(t_m)]^2 \quad \text{for } 1 \le m \le M. \tag{8}$$

Sample times $\{t_m\}_1^M$ can be selected arbitrarily; each individual t_m should be chosen to maximize the size of the m-th signal output, $a_m^2(t_m) + b_m^2(t_m)$.

If we sum these squared-envelope filter output samples, we have channel output

$$v = \sum_{m=1}^{M} |c_m(t_m)|^2 =$$

$$= \sum_{m=1}^{M} \left\{ [a_m(t_m) + x_m(t_m)]^2 + [b_m(t_m) + y_m(t_m)]^2 \right\} . \tag{9}$$

The signal and noise outputs, given in (5) and (6), apply for an arbitrary complex envelope signal $\underline{s}_m(t)$ and filter $\underline{h}_m(\tau)$ in the m-th branch of the receiver. The instantaneous output signal squared-envelope is

$$a_m^2(t) + b_m^2(t) = |a_m(t) + ib_m(t)|^2 = \left| \int d\tau\, \underline{s}_m(\tau)\, \underline{h}_m(t-\tau) \right|^2 , \tag{10}$$

while the instantaneous output noise squared-envelope is

$$x_m^2(t) + y_m^2(t) = |x_m(t) + iy_m(t)|^2 = \left| \int d\tau\, \underline{n}(\tau)\, \underline{h}_m(t-\tau) \right|^2 . \tag{11}$$

Here, we presume that a common broadband noise n(t) excites all the filters $\{h_m(\tau)\}$ in the receiver bank. Observe that if the m-th signal is subject to a random phase shift, according to the factor $\exp(i\theta_m)$, this cancels out of the envelope-squared signal term. Thus, all the results here apply not only to a deterministic signal, but also to one with an arbitrary phase shift. However, no fading of the received signal is allowed in any of the current results.

If the real input noise n(t) is white with double-sided spectral level N_d watts/Hz, then the correlation of complex envelope $\underline{n}(t)$ is [1; ch. II, (3.11) and (6.22)]

$$\overline{\underline{n}(t)\ \underline{n}^*(t-\tau)} = 4N_d\ \delta(\tau) = 2N_o\ \delta(\tau); \tag{12}$$

N_o is the single-sided noise spectral density level in watts/Hz. By use of (6), this results in average noise powers for the m-th components, as

$$\overline{x_m^2(t)} = \overline{y_m^2(t)} = 2N_d \int d\tau\ \left|\underline{h}_m(\tau)\right|^2 . \tag{13}$$

We presume that all the filters have the same level (energy); thus, we define

$$\sigma^2 = \overline{x_m^2(t)} = \overline{y_m^2(t)} = 2N_d \int d\tau \left|\underline{h}_m(\tau)\right|^2 \quad \text{for } 1 \le m \le M. \tag{14}$$

This is an important restriction; greater generality is given in [2; appendices B and C].

We are now in position to employ the general results listed in appendix A, when the noise is Gaussian. Namely, define, as in (A-1),

$$d^2 = \frac{1}{\sigma^2} \sum_{m=1}^{M} \left[a_m^2(t_m) + b_m^2(t_m) \right] =$$

$$= \frac{1}{\sigma^2} \sum_{m=1}^{M} \left| \int d\tau \; \underline{s}_m(\tau) \; \underline{h}_m(t_m - \tau) \right|^2 =$$

$$= \frac{\sum_{m=1}^{M} \left| \int d\tau \; \underline{s}_m(\tau) \; \underline{h}_m(t_m - \tau) \right|^2}{2N_d \int d\tau \left| \underline{h}_m(\tau) \right|^2} . \tag{15}$$

Observe that the absolute level of each filter, $\underline{h}_m$, cancels out in this ratio. However, d^2 does depend on the scale of each signal $\underline{s}_m$ and inversely on noise level N_d.

The maximum value of each term in these ratios is realized by choosing the m-th filter such that its impulse response

$$\underline{h}_m(\tau) = k \; \underline{s}_m^*(T_m - \tau), \tag{16}$$

where k is a complex constant selected to guarantee the equal energy requirement in (14), and T_m is a delay inserted for realizability, and by choosing sample time t_m equal to T_m. This is the matched filter to the m-th signal, sampled at the time of peak output. Thus, we have, in the best situation,

$$\max d^2 = \frac{1}{2N_d} \sum_{m=1}^{M} \int dt \, \left| \underline{s}_m(t) \right|^2 = \frac{1}{N_d} \sum_{m=1}^{M} E_m = \frac{E_T}{N_d} = \frac{2E_T}{N_o} , \qquad (17)$$

where E_m is the received signal energy in the m-th real signal component $s_m(t)$, and E_T is the total received signal energy over all M paths (branches). Additional interpretations of d^2 are available in (A-21) et seq.

This maximum value of d^2 in (17) is realized only if the receiving filters are the matched filters (16), and if the filter outputs are sampled at the correct time instants. More generally, the generic value of d^2 in (15) allows for arbitrary signals, filters, and sampling instants, thereby affording the possibility of considering losses due to mismatch and desynchronization. The signals can be time-delayed and/or frequency-shifted versions of each other, if desired. A more thorough analysis and comparison is presented in [2; appendices B and C]. The received signals have undergone no fading in any of these considerations; thus the current analysis applies to a deterministic signal, except for random phase.

Reference to (A-2) and (A-6) now allows us to state the exceedance distribution function of channel output v in (9) as

$$\mathrm{Prob}(v > u) = 1 - P_v(u) = Q_M\left(d, \sqrt{u}/\sigma\right) \text{ for } u > 0, \tag{18}$$

where the Q_M-function is

$$Q_M(\alpha, \beta) = \int_{\beta}^{\infty} dx\ x \left(\frac{x}{\alpha}\right)^{M-1} I_{M-1}(\alpha x) \exp\left(\frac{x^2 + \alpha^2}{-2}\right) . \tag{19}$$

Parameters d and σ in (18) are given by (15) and (14), respectively. These results pertain to the signal-bearing channel; the noise-only channel outputs correspond to setting d = 0.

FALSE ALARM AND DETECTION PROBABILITIES

The exceedance distribution function of the processor output v_n for the n-th channel (see figure 1) is given by (18) for signal present in that channel. For those channels with no signal present, the exceedance distribution is

$$1 - P_v^{(o)}(u) = Q_M(0,T) = E_{M-1}(T^2/2) \quad \text{for } u > 0, \tag{20}$$

where we have let

$$T = \sqrt{u}\,/\sigma \tag{21}$$

for notational convenience, and defined

$$E_n(x) = \exp(-x)\ e_n(x), \tag{22}$$

where

$$e_n(x) = \sum_{k=0}^{n} x^k/k! \tag{23}$$

is the partial exponential [5; 6.5.11].

FALSE ALARM PROBABILITY

Since the noises in the N channels subject to or-ing in figure 2 are presumed independent, the probability that all N outputs do not exceed a threshold value u is

$$[P_V^{(o)}(u)]^N = \left[1-E_{M-1}\left(\frac{u}{2\sigma^2}\right)\right]^N , \tag{24}$$

where cumulative distribution function $P_V^{(o)}$ was obtained from (20). The false alarm probability is then

$$P_F = 1 - [1 - E_{M-1}(T^2/2)]^N, \tag{25}$$

where we used (21).

DETECTION PROBABILITY

When signal is present in one channel, we have several alternative definitions of a detection probability. For example, we could define the probability of signal detection, P_{SD}, as the probability that the *signal* channel output exceeds threshold u, disregarding the noise channels completely; then directly from (18) and (21),

$$P_{SD} = Q_M(d,T), \tag{26}$$

which is, of course, independent of N.

However, it is possible that the noise channels could also cause a threshold crossing, even when the signal channel does not. We can then define a probability of any detection, P_{AD}, as the probability that *any* channel output exceeds the threshold u. This quantity is given by

$$P_{AD} = 1 - [P_v^{(o)}(u)]^{N-1}\ P_v(u) =$$

$$= 1 - [1 - E_{M-1}(T^2/2)]^{N-1}\ [1 - Q_M(d,T)], \tag{27}$$

by use of (20) and (18). This is the case considered in [4; see (9) and (4)].

The problem with this latter definition is that, since we are interested in knowing which channel contains the signal, the probability P_{AD} contains some (rare) events which indicate the incorrect channel to contain the signal. The best alternative appears to be to define the probability of correct detection, P_{CD}, as the probability that the signal channel output exceeds the threshold u <u>and</u> exceeds all the noise outputs. In this case, the signal will be detected and its channel number correctly indicated. This probability is given by

$$P_{CD} = \int_u^{\infty} dt\ p_v(t)\ [P_v^{(o)}(t)]^{N-1}, \tag{28}$$

where probability density function p_v and cumulative distribution function $P_v^{(o)}$ are given by (A-4) and (A-9), respectively. Substituting these expressions, letting $x = \sqrt{t}\,/\sigma$, and using (21), there follows the integral result

$$P_{CD} = \int_T^\infty dx\ x\ (\frac{x}{d})^{M-1}\ I_{M-1}(dx)\ \exp\left(\frac{x^2+d^2}{-2}\right)\ [1-E_{M-1}(x^2/2)]^{N-1}\ . \qquad (29)$$

From physical reasoning or mathematical manipulations, it follows that

$$P_{CD} < P_{SD} < P_{AD} \quad \text{for } N > 1. \qquad (30)$$

For $N = 1$, no or-ing, all three detection probabilities are equal to $Q_M(d,T)$.

Also, from (29), since the bracketed term is greater than or equal to its value at $x = T$, we have the lower bound

$$P_{CD} > [1 - E_{M-1}(T^2/2)]^{N-1}\ Q_M(d,T) \quad \text{for } N > 1. \qquad (31)$$

Thus we have the tight bounds on the probability of correct detection:

$$[1 - E_{M-1}(T^2/2)]^{N-1}\ Q_M(d,T) < P_{CD} < Q_M(d,T)\ . \qquad (32)$$

To show how tight these bounds are, recall the false alarm probability in (25), in order to express the bounds as

$$(1 - P_F)^{\frac{N-1}{N}} Q_M(d,T) < P_{CD} < Q_M(d,T) . \tag{33}$$

For small false alarm probabilities,

$$(1 - P_F)^{\frac{N-1}{N}} \approx 1 - P_F \frac{N-1}{N} > 1-P_F , \tag{34}$$

leading to

$$(1 - P_F) Q_M(d,T) < P_{CD} < Q_M(d,T); \tag{35}$$

thus the bounds in (32) are very tight for small false alarm probabilities. This is very convenient computationally, since it means that we will not have to evaluate the integral in (29) numerically, but need only compute the simpler quantities Q_M and E_{M-1}.

One special case of P_{CD} can be evaluated in closed form: for d = 0+, (28) yields

$$P_{CD}^{(o)} = \int_u^{\infty} dt \; p_v^{(o)}(t) \left[P_v^{(o)}(t)\right]^{N-1} =$$

$$= \frac{1}{N} \left\{1 - \left[P_v^{(o)}(u)\right]^N\right\} = \frac{1}{N} P_F , \tag{36}$$

the latter relation following from (25). This relation agrees with physical reasoning.

TIGHTNESS OF BOUND

To verify the accuracy afforded by using the upper bound $Q_M(d,T)$, instead of the exact result (29) for P_{CD}, a short comparative study of the two quantities was conducted; the numerical results are tabulated in appendix B. False alarm probabilities near the values .1, .01, .001, and detection probabilities near the values .5, .9, .99, .999 were considered, while M took on values 1,10, and N took on values 2,10,100,1000. These ranges of values encompass most of the cases of practical interest; there is no need to consider smaller P_F values, since the discrepancy is even smaller then. It will be observed that for $P_F < .1$ (the only cases plotted here), the differences between the exact P_{CD} and $Q_M(d,T)$ are inconsequential; in particular, see figure B-1.

GRAPHICAL RESULTS

In this section, we plot the analytical results for the false alarm probability (25) and the tight upper bound on the probability of correct detection (33); see (35). The number of filter outputs summed, M, ranges over the values

$$M = 1,2,3,4,5,6,7,8,9,10 = 1(1)10, \tag{37}$$

while the number of channel or-ed, N, ranges over the values

$$N = 1,\ 10,\ 100,\ 1000. \tag{38}$$

The parameter, d, on the plots is the generic signal-to-noise ratio defined by (15), for general signals and filters. The 40 combinations corresponding to (37) and (38) are plotted on normal probability paper in figures* 3 through 42. Values of d small enough to encompass the (poor quality) operating point $(P_F, P_{CD}) = (.01, .5)$ have been employed; while at the high quality end, values of d extending up to $(P_F, P_{CD}) = (1E\text{-}10, .999)$ have been used. The increment in d is .5 for all the results in figures 3 through 42.

---

*All the figures are collected together, after the Summary section.

It will be observed that the curves are approximately equispaced in parameter d, thereby allowing for ready accurate interpolation in d, given specified P_F and P_{CD}. The curves, for cases in which N = 1, are virtually straight lines, while those for N = 1000 have developed significant curvature; nevertheless, the equispaced nature of the results readily accommodates interpolation in all cases.

From these results, it is possible to extract a different type of performance characteristic, namely the required values of d to achieve a specified quality of performance in terms of false alarm probability and detection probability. In figures 43 through 48, these results are plotted for the six combinations of

$$M = 1,2,4 \quad \text{with } P_{CD} = .5,.9, \tag{39}$$

while N varies over 1(1)1000, and P_F takes on the values 1E-2, 1E-4, 1E-6, 1E-8, 1E-10. (Strictly, only the cases for N = 1, 10, 100, 1000 follow from figures 3 through 42; the remaining values of N were obtained directly from (25) and (33).)

The most striking feature of figures 43 through 48 is their slow increase with N, the number of channels subjected to or-ing. Certainly the increase in required d values was anticipated, since or-ing cannot improve performance capability; however, the amount of increase is not very significant. Thus, from figure 43, for P_F = 1E-10, d need only increase from 6.71 to 7.67 as N increases from 1 (no or-ing) to N = 1000. Greater increases are necessary for the larger P_F values.

SUMMARY

It will be easily observed from the graphical results in figures 3 through 42 that, for a fixed amount of or-ing (fixed N), the performance degrades as M increases. That is, for specified values of P_F and d, the values of P_{CD} decrease as M is increased. Alternatively, to maintain a specified performance pair P_F, P_{CD}, the values of d must be increased as M increases. This is due to the fact that parameter d in (15) or (17) is a total (or output) signal-to-noise ratio measure and that larger M corresponds to increased fractionalization of the received signal energy into more paths or branches. Since the filter-output combination rule is incoherent, namely adding squared envelopes, this fractionalization cannot be made up by summation, and a loss occurs.

On the other hand, if we were to add more paths to a particular system, then both M and d would increase. Whether this results in an improvement or degradation depends on the relative amount of additional energy. Particular cases can be studied quantitatively by referring to figures 3 through 42. In addition, programs for the procedures in this report are listed in BASIC in appendix C, if additional cases of interest to the reader need to be investigated.

The maximum value of d^2 is given by (17) as $2E_T/N_0$; this can be realized only if the matched filters (16) are utilized and if the sampling times are properly selected. If these conditions are not met, the value of d^2 given by (15) must be employed. In any event, the figures are parameterized by quantity d, regardless of what filters and sampling times are used. Thus a desired value of d for a mismatched situation will require larger signal levels for $\{\underline{s}_m\}$ in (15) than the values indicated by the ideal, (17). In this manner, the degradation caused by mismatch and/or desynchronization can be quantitatively assessed.

The received signal was assumed to have undergone no fading in the current analysis. Extensions to fading signals, but without or-ing, are available in [3]. This latter reference presumed a fixed threshold for decision variable comparisons (as did this analysis in (3) and (18)); extensions to a variable threshold, based on a finite sample size noise-level estimation procedure, are currently underway. Results on this normalizer in a fading environment will be reported on shortly by the author.

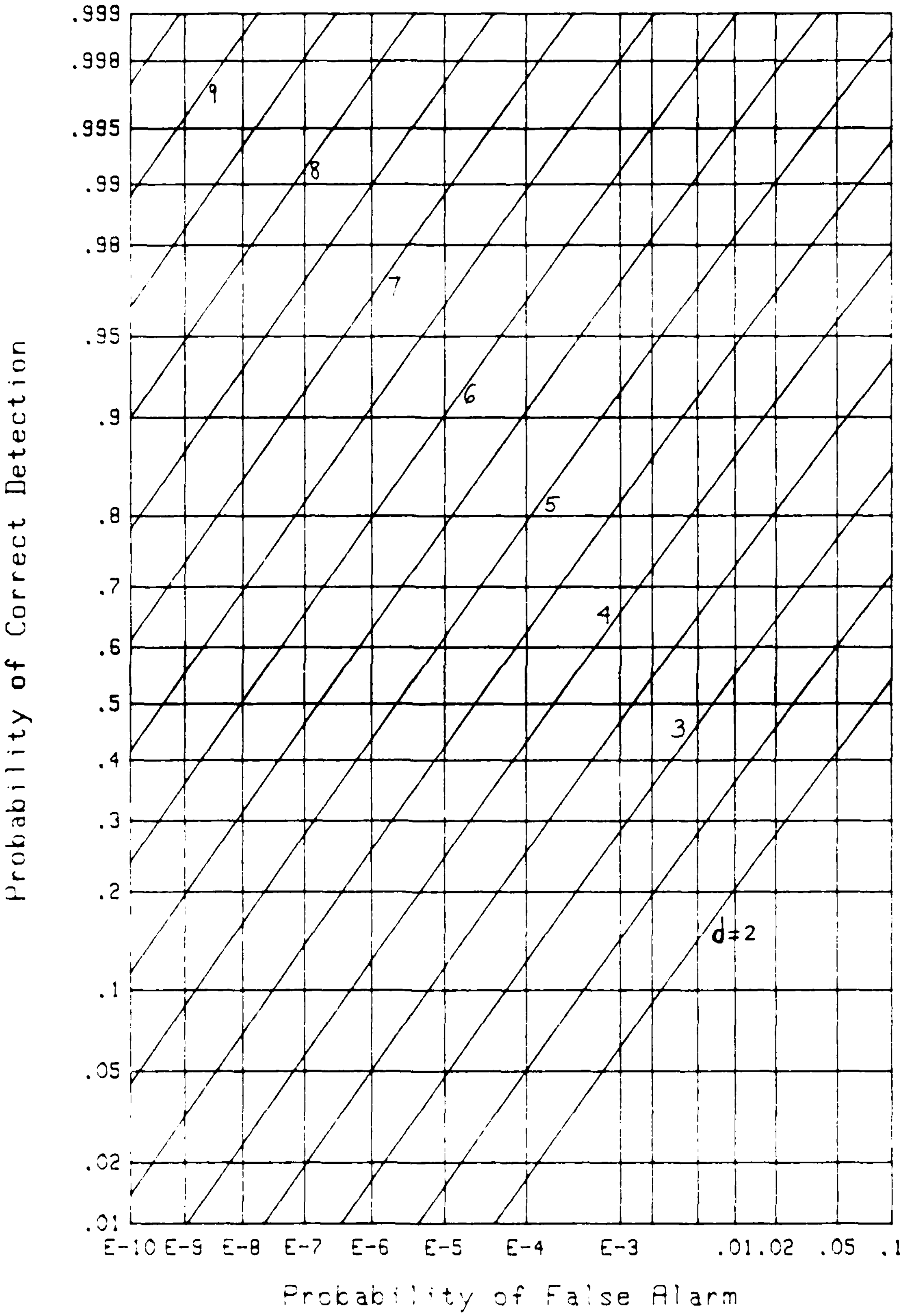

Figure 3. ROC for M=1, N=1

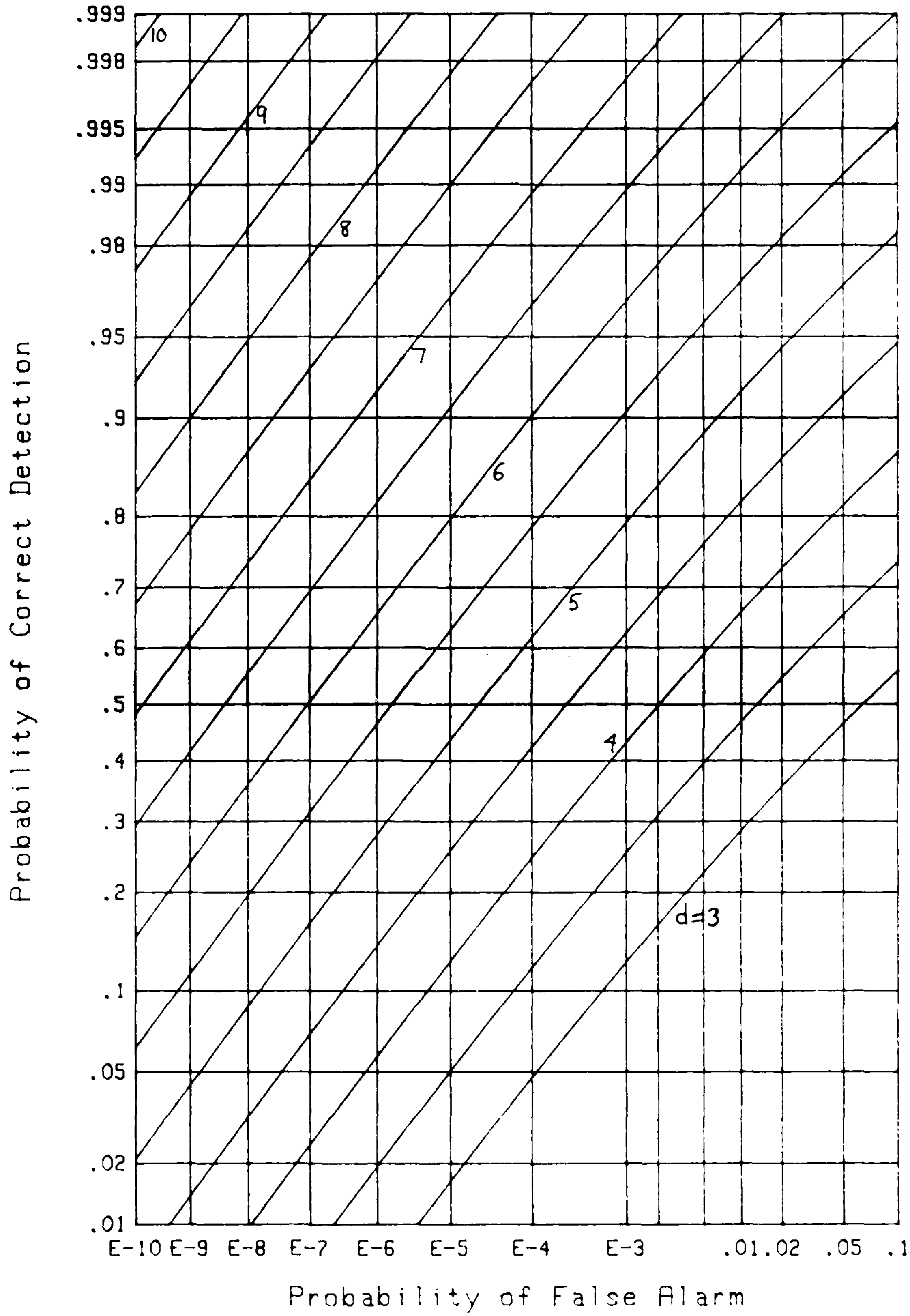

Figure 4. ROC for M=1, N=10

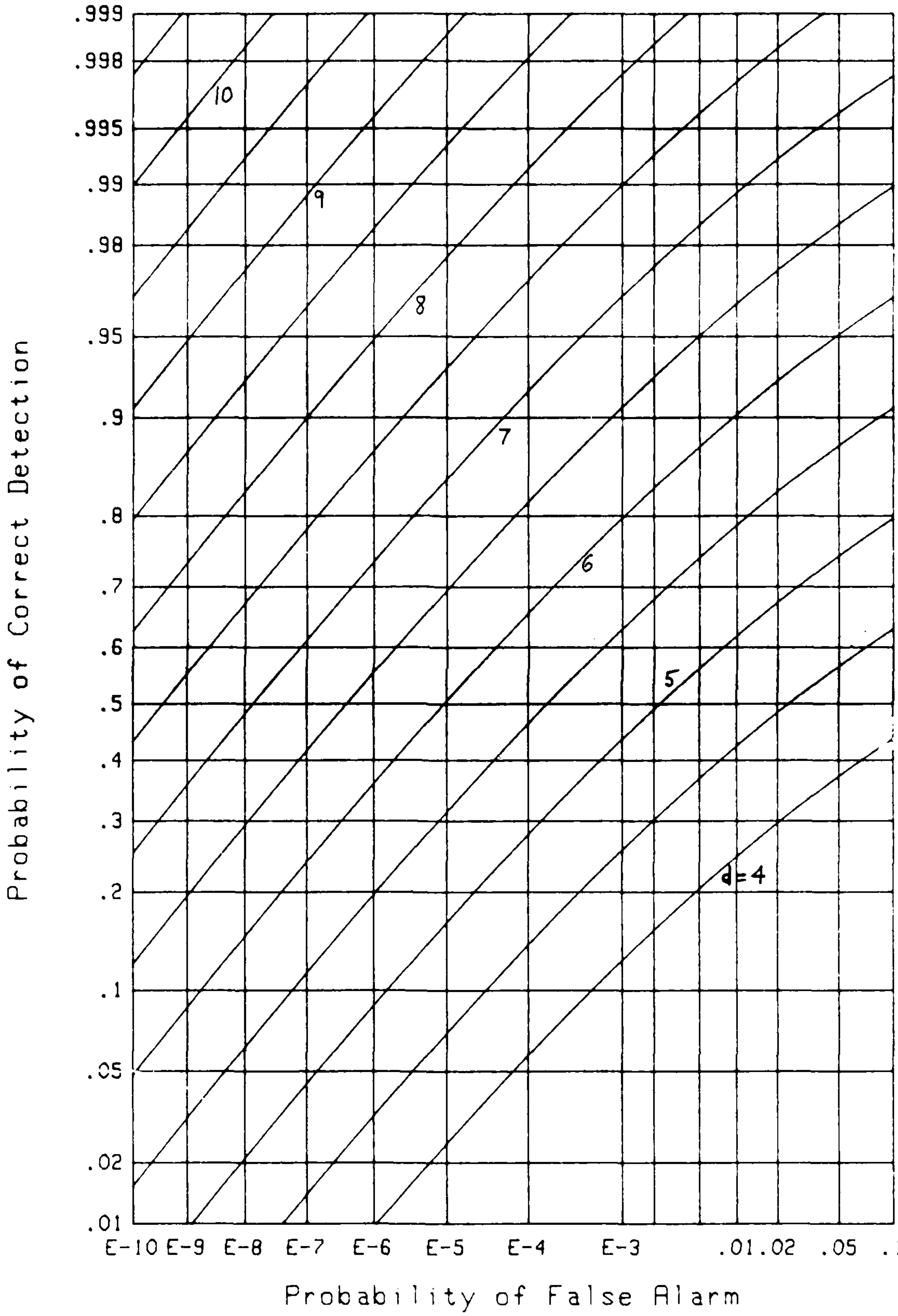

Figure 6. ROC for M=1, N=1000

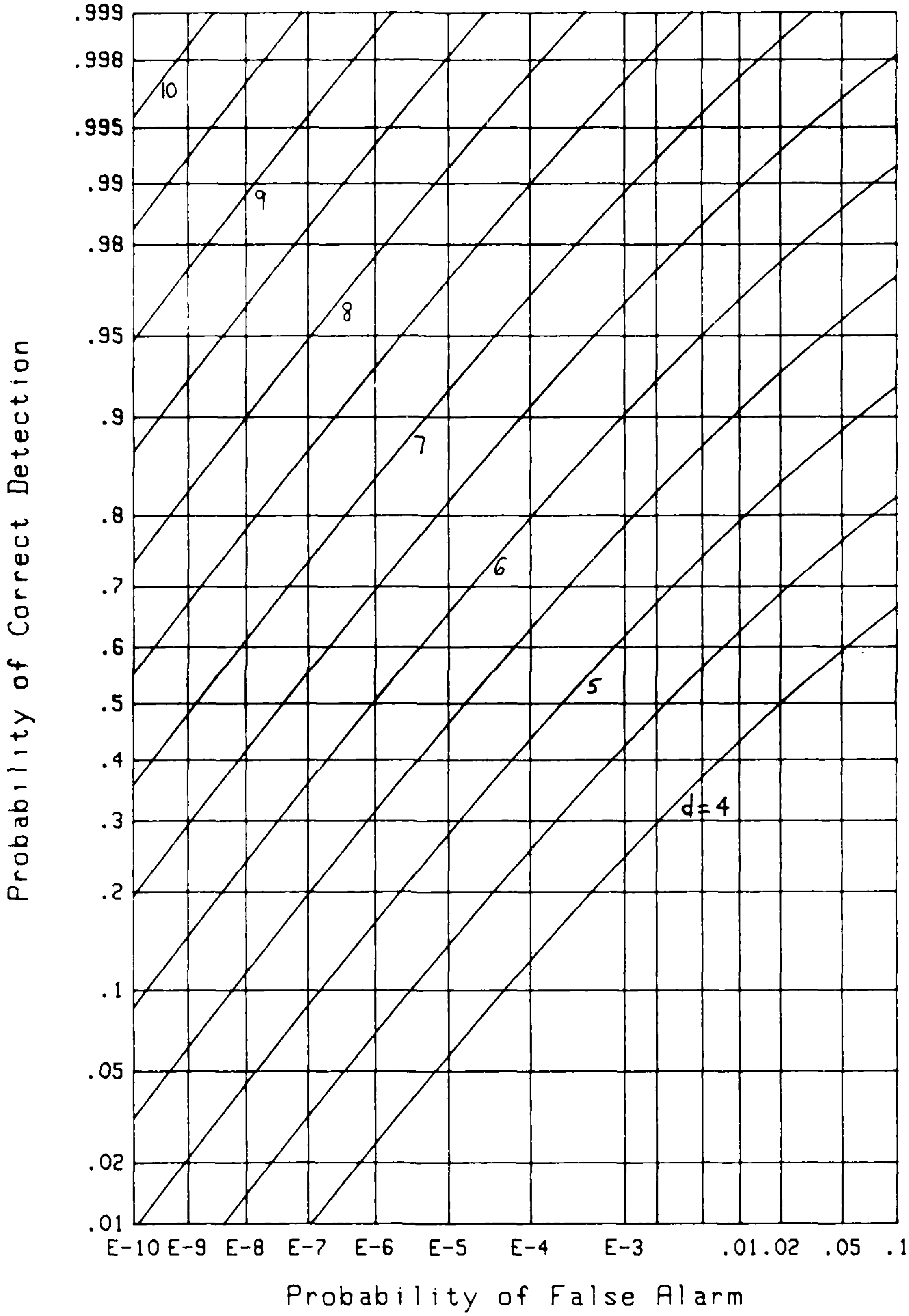

Figure 5. ROC for M=1, N=100

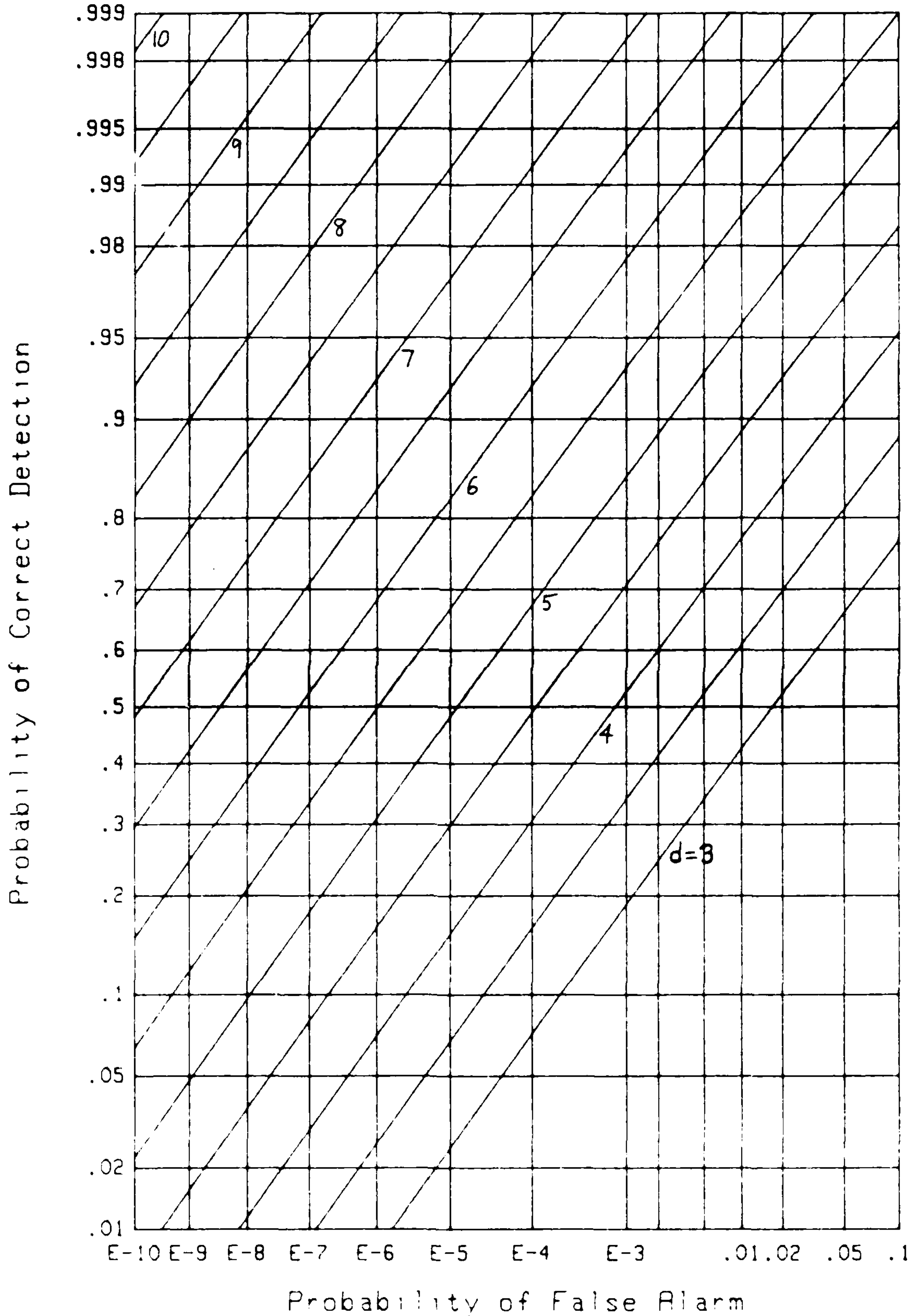

Figure 7. ROC for M=2, N=1

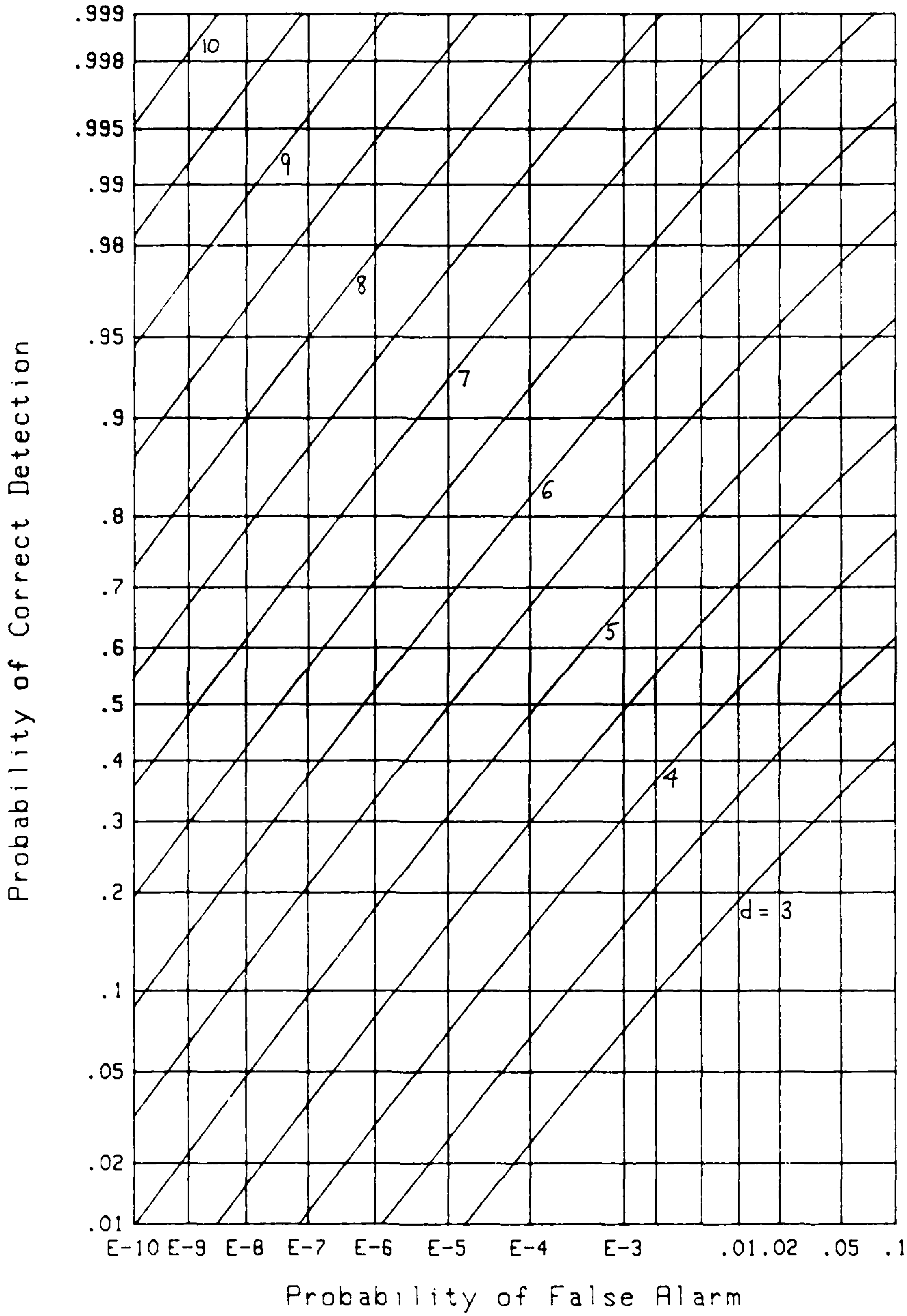

Figure 8. ROC for M=2, N=10

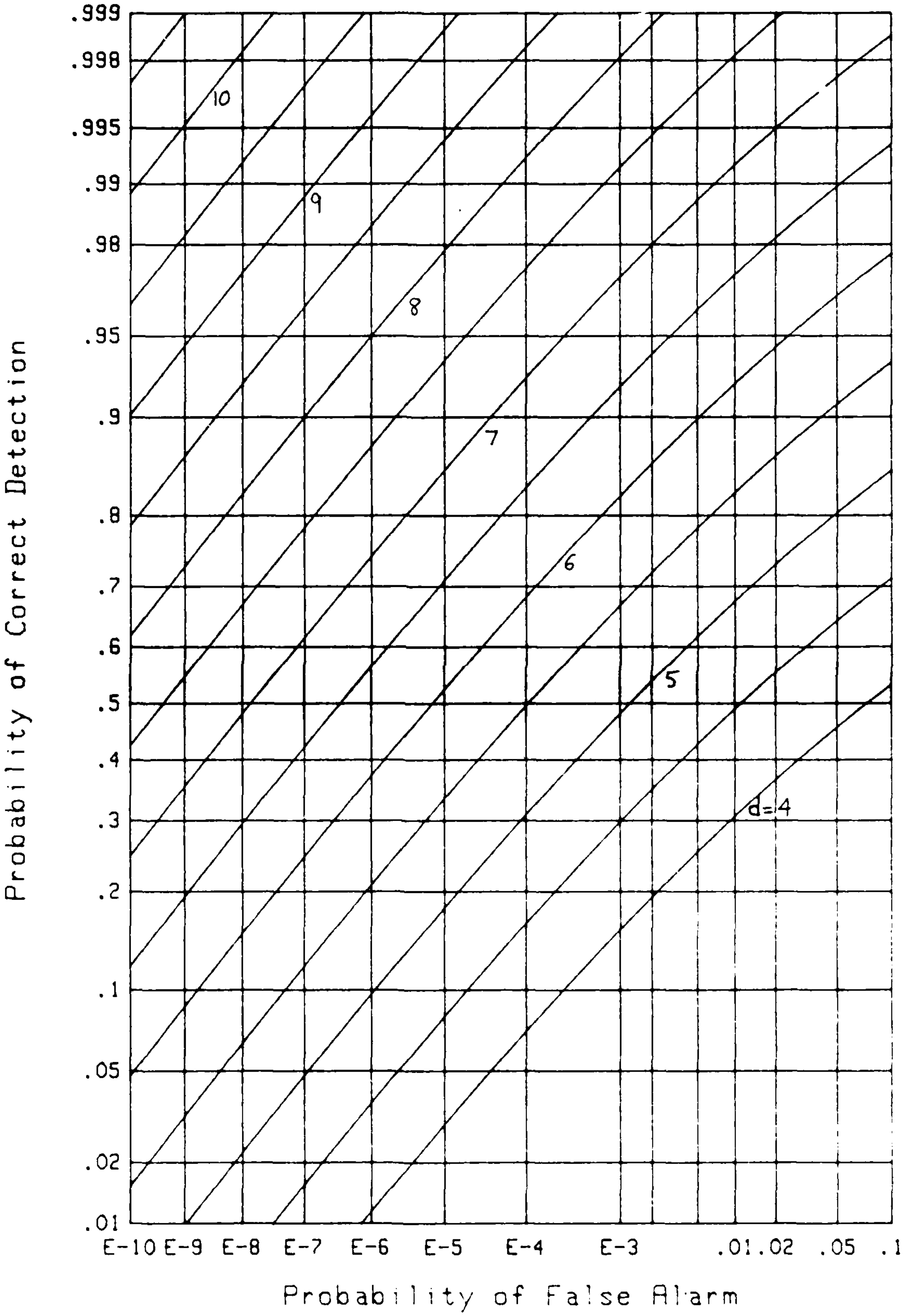

Figure 9. ROC for M=2, N=100

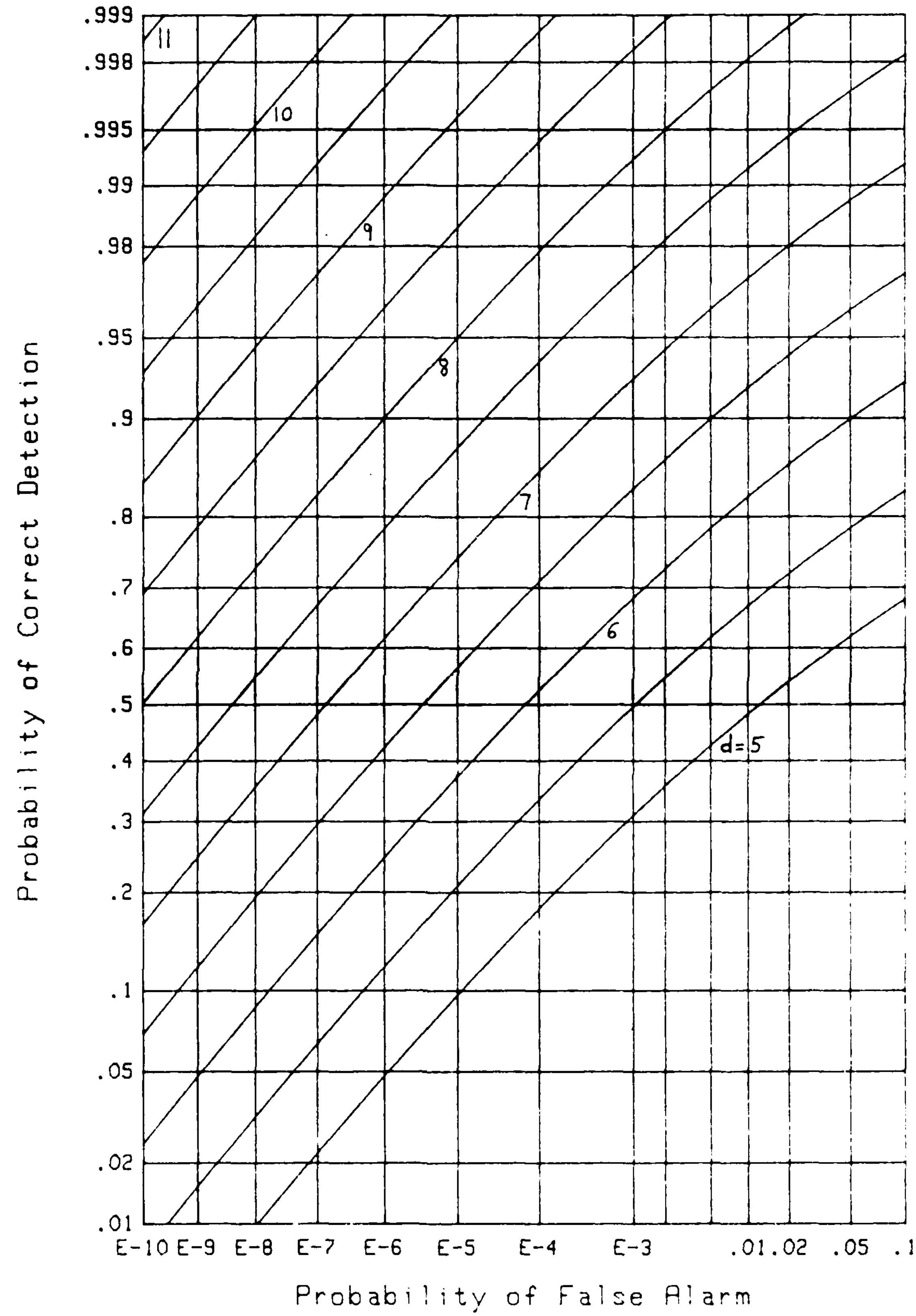

Figure 10. ROC for M=2, N=1000

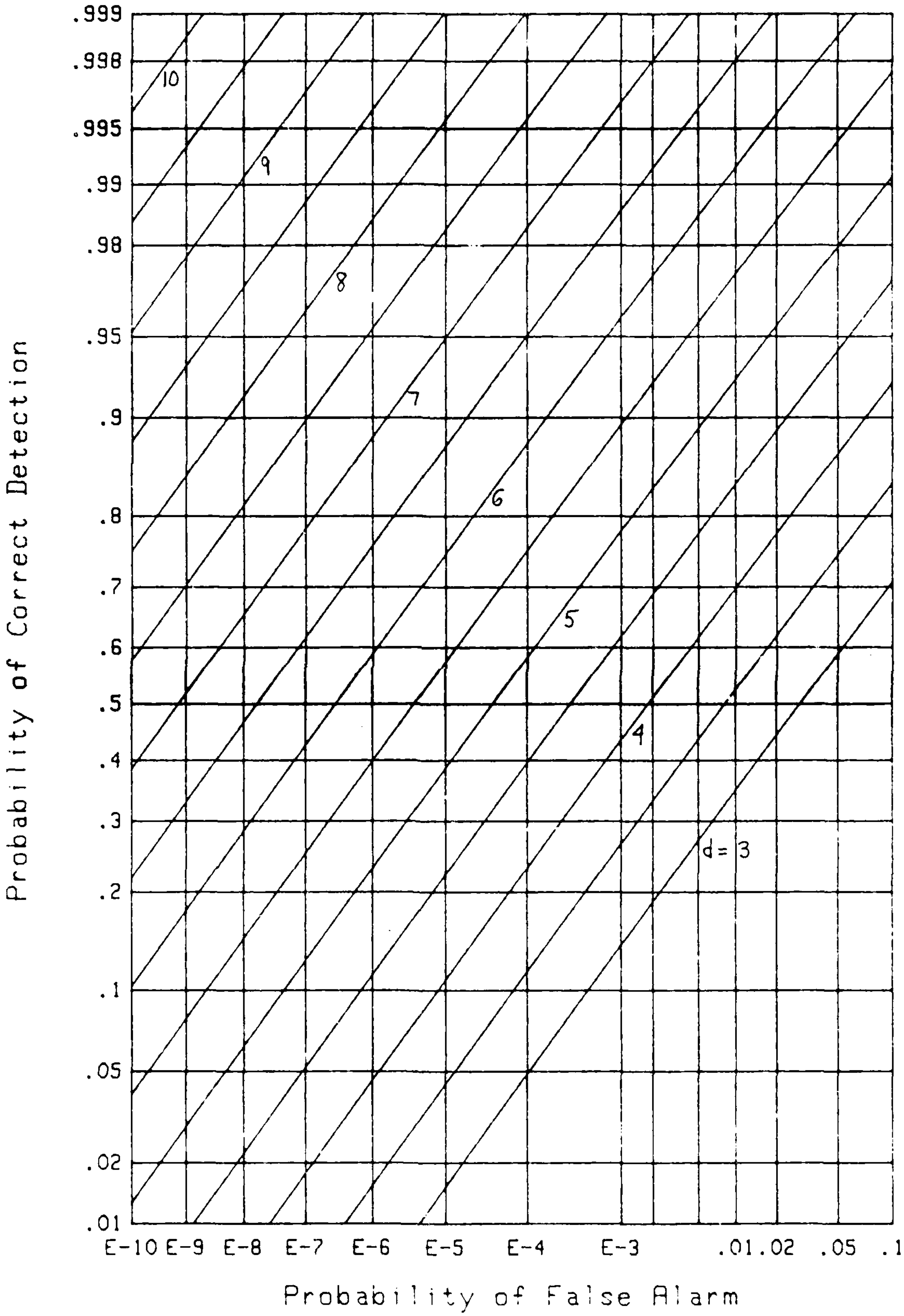

Figure 11. ROC for M=3, N=1

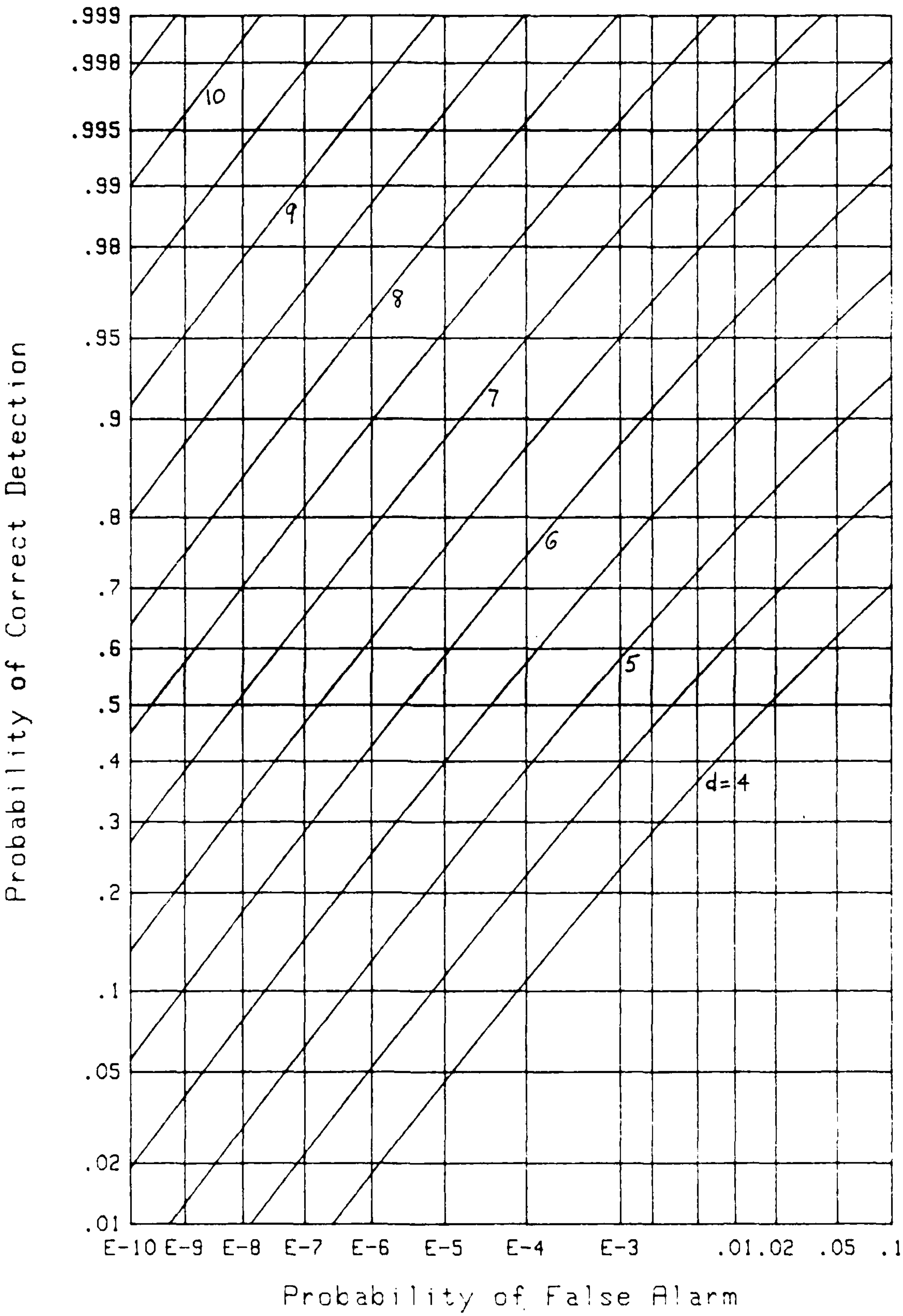

Figure 12. ROC for M=3, N=10

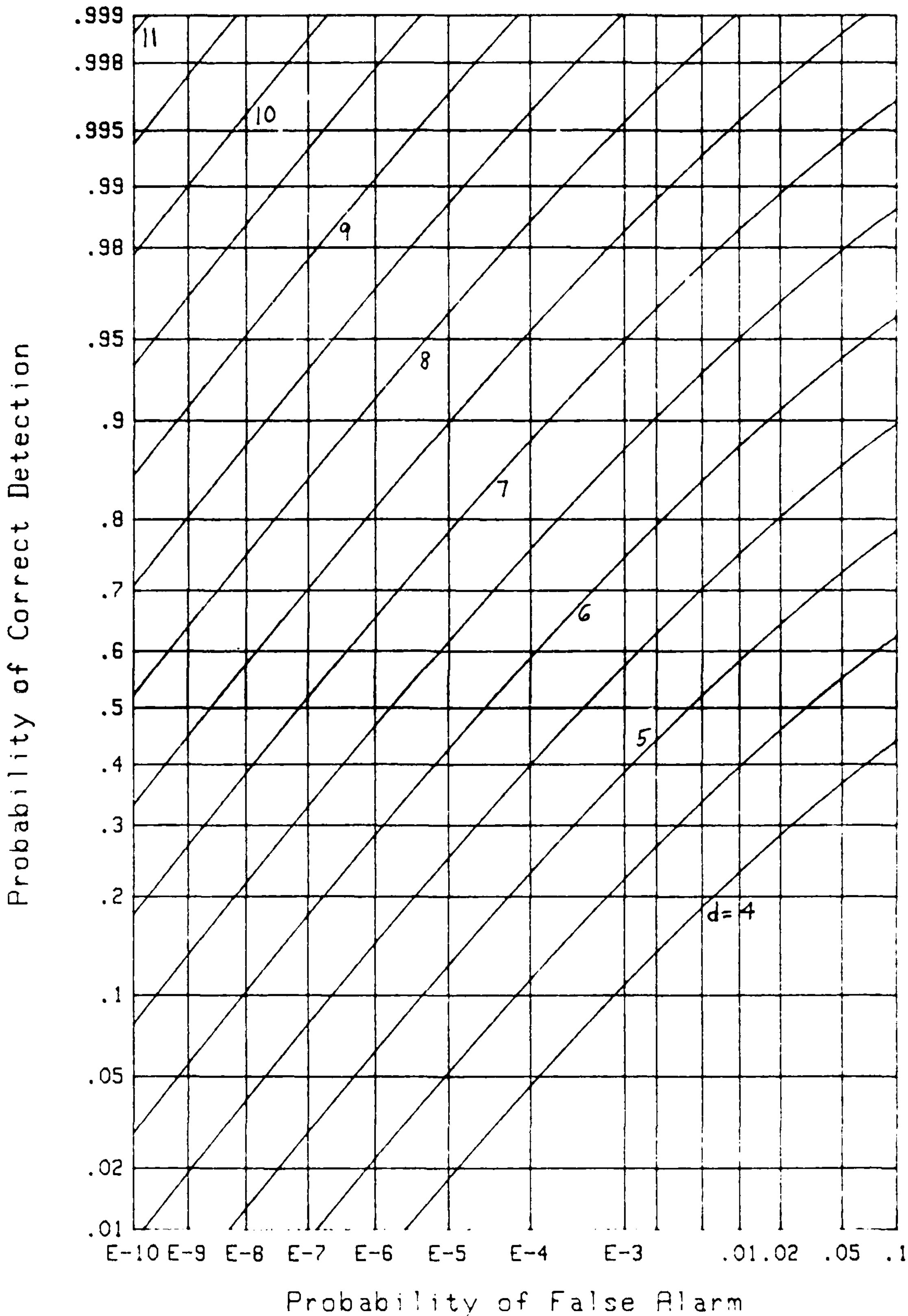

Figure 13. ROC for M=3, N=100

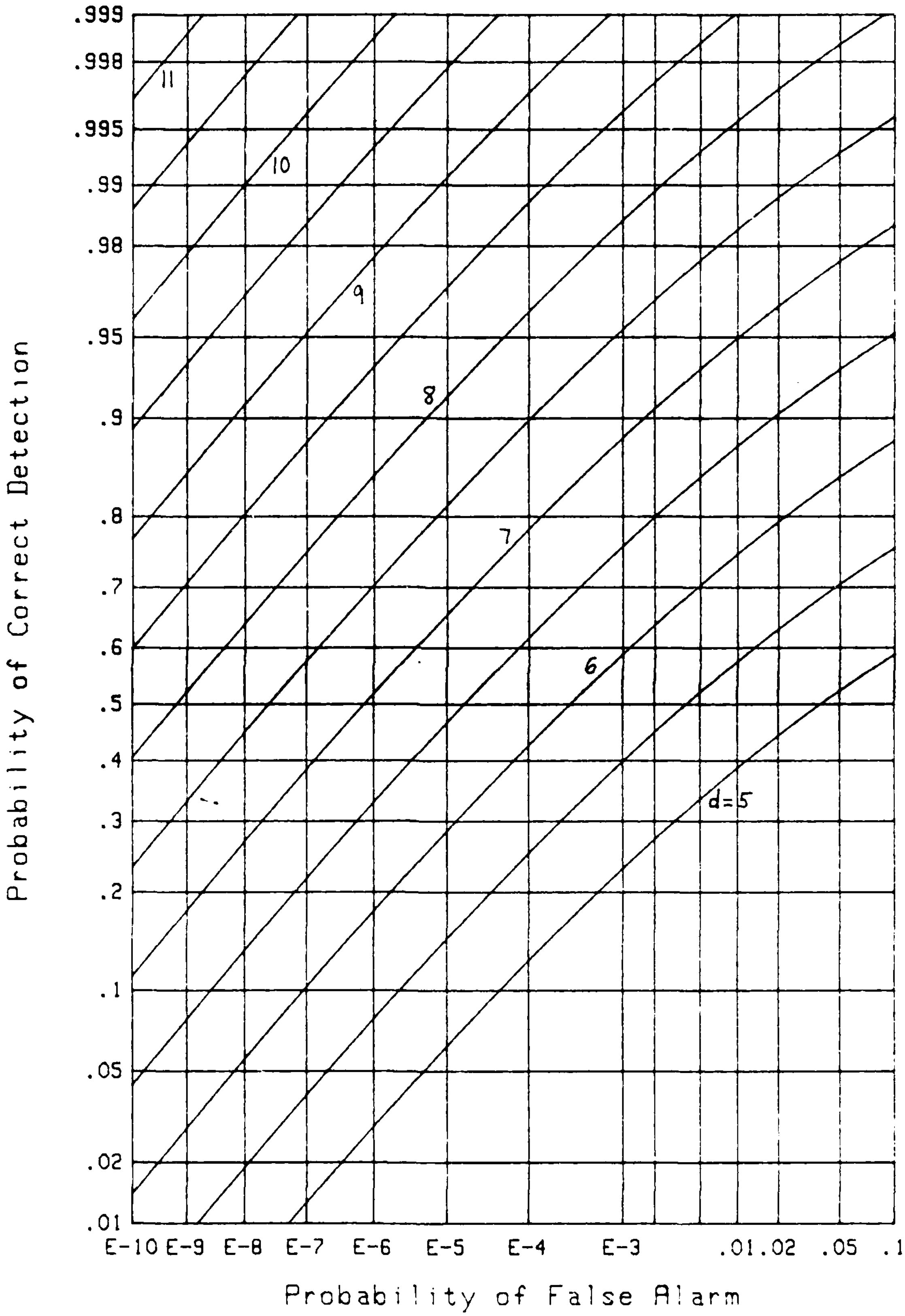

Figure 14. ROC for M=3, N=1000

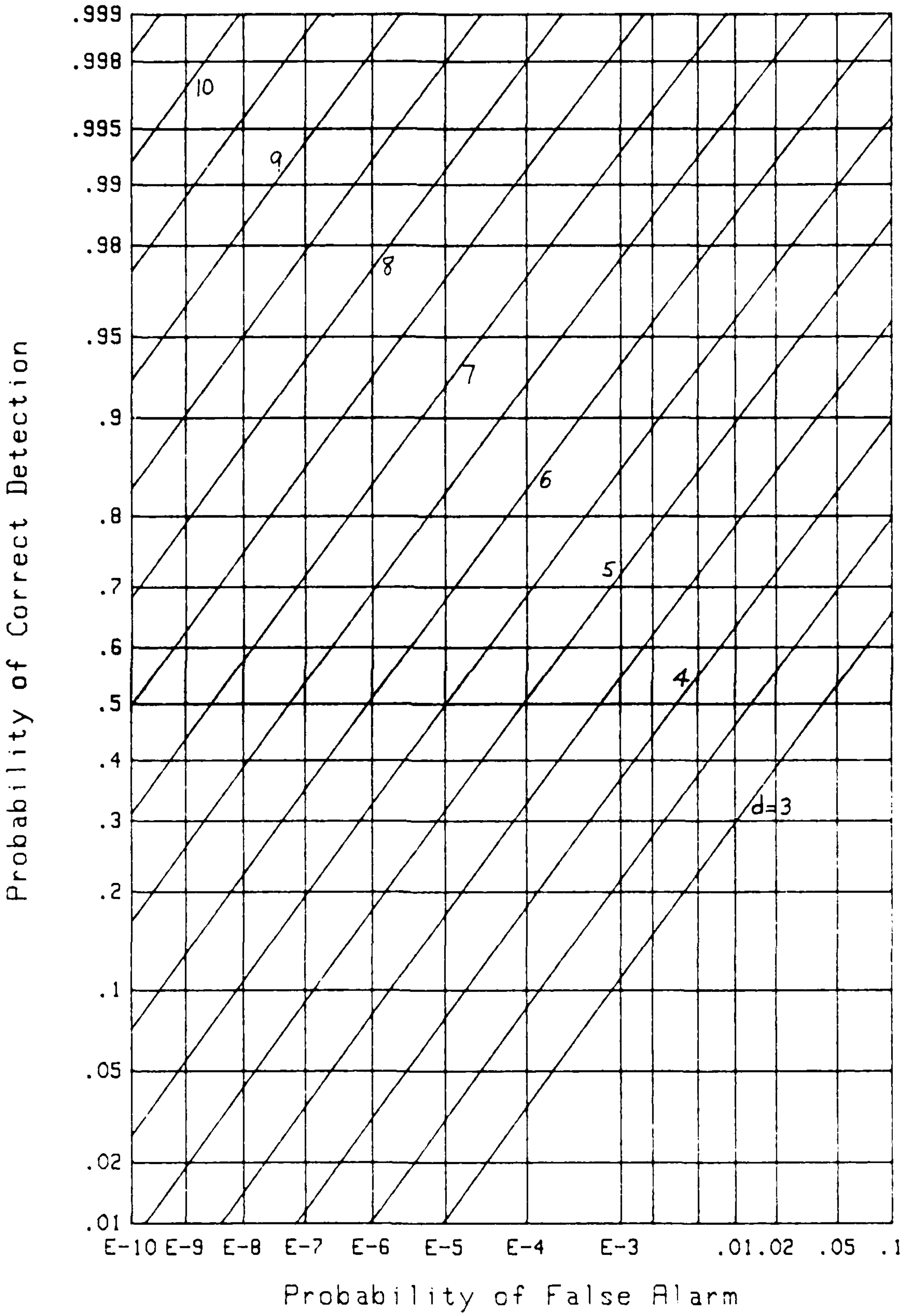

Figure 15. ROC for M=4, N=1

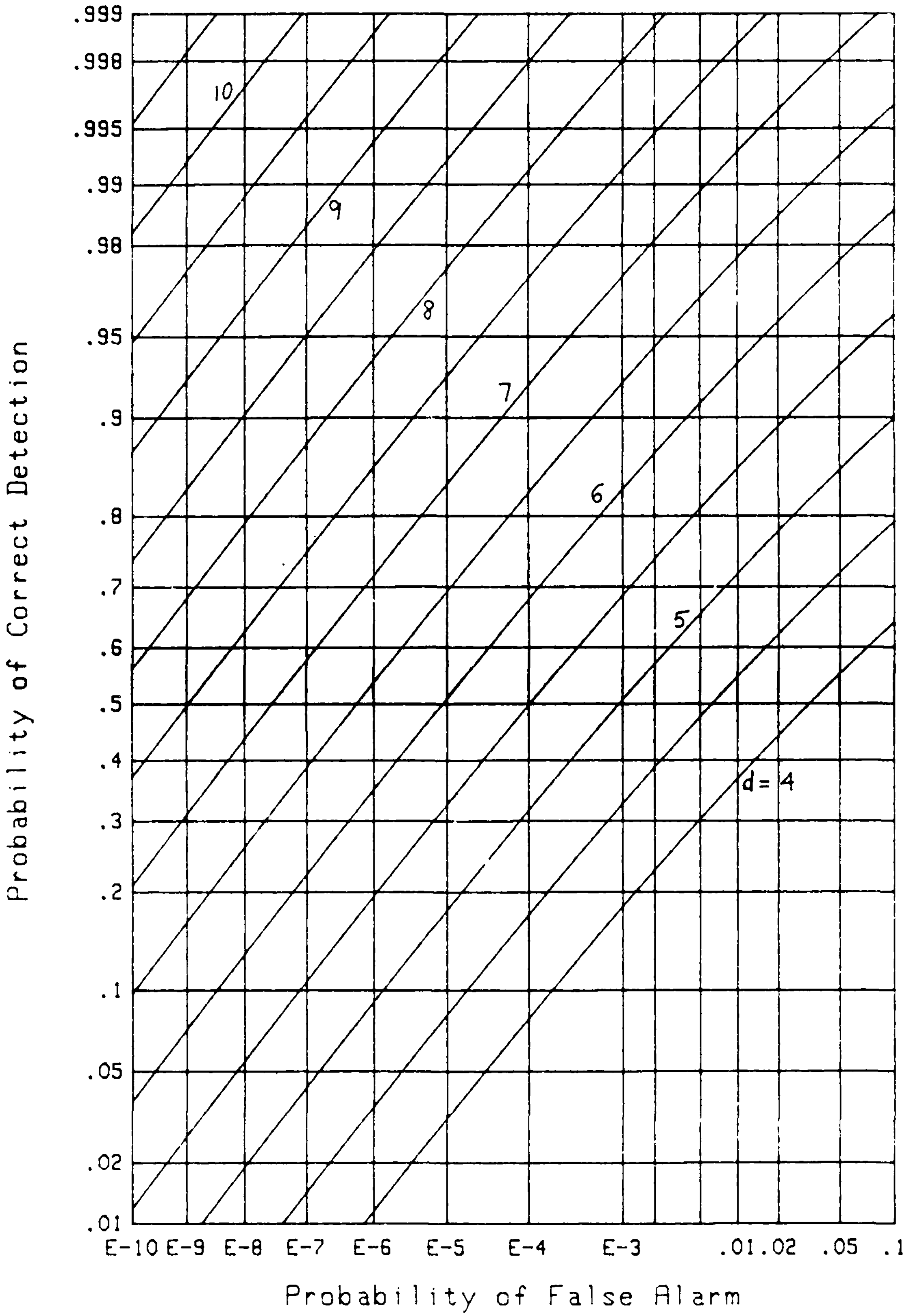

Figure 16. ROC for M=4, N=10

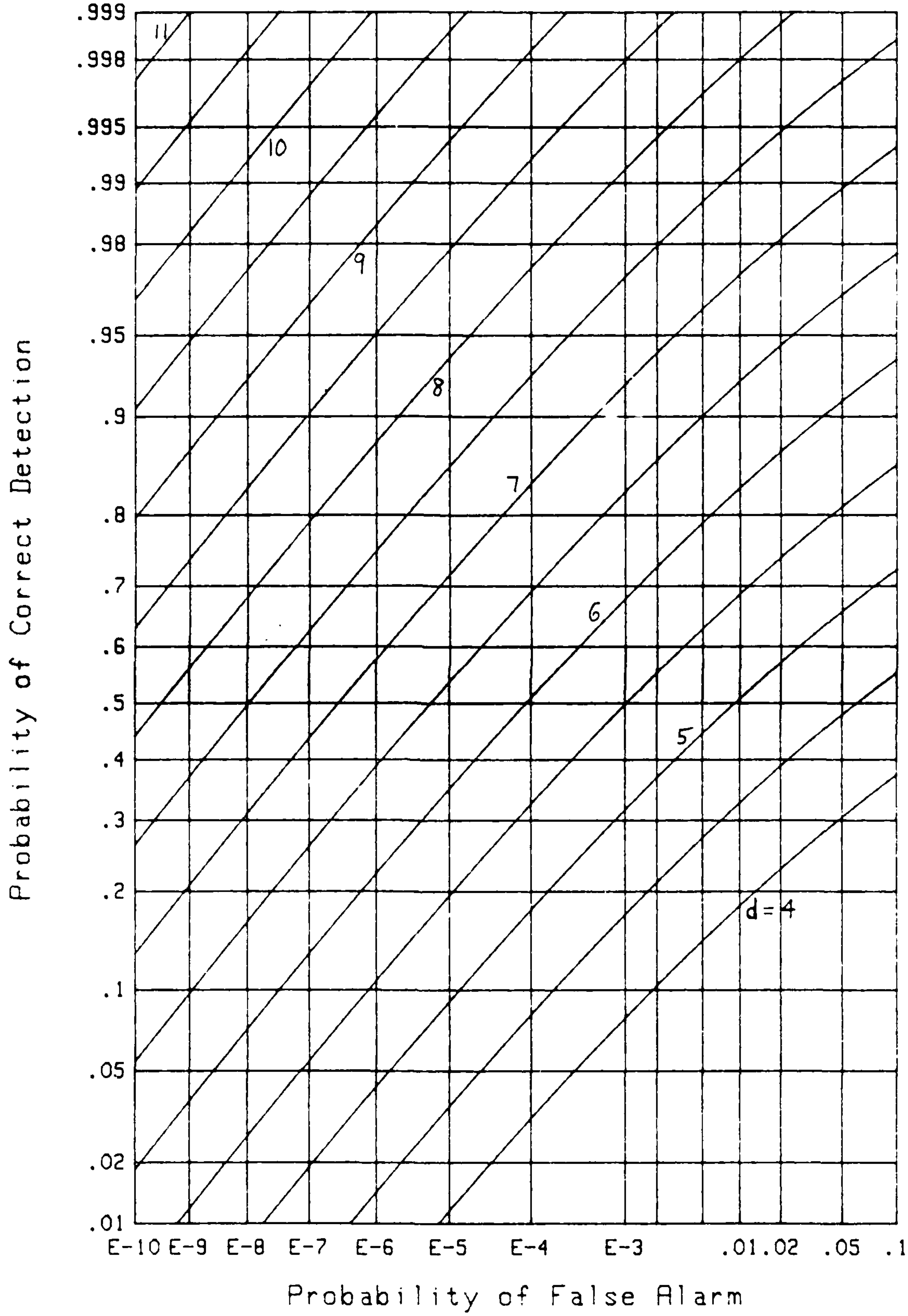

Figure 17. ROC for M=4, N=100

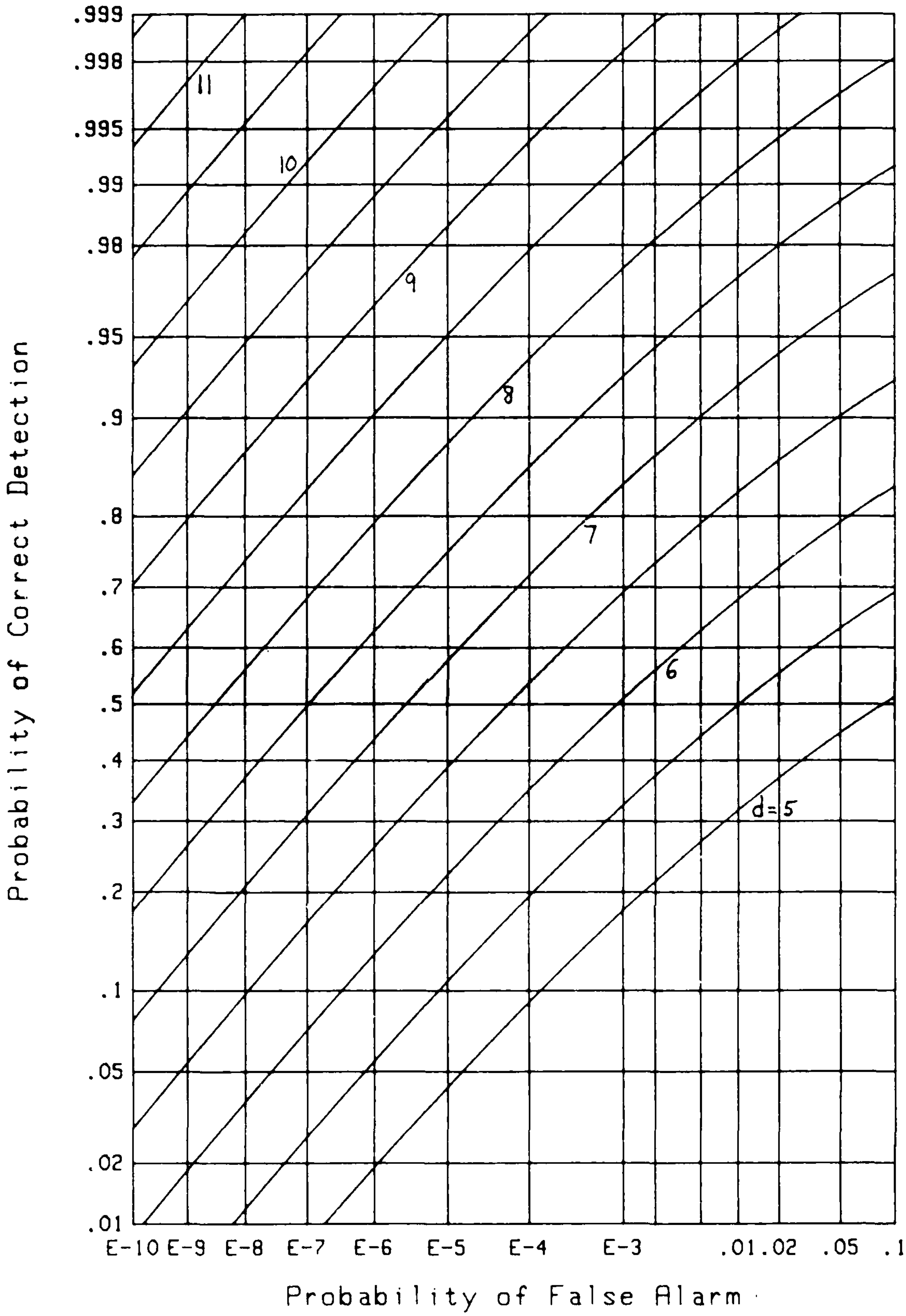

Figure 18. ROC for M=4, N=1000

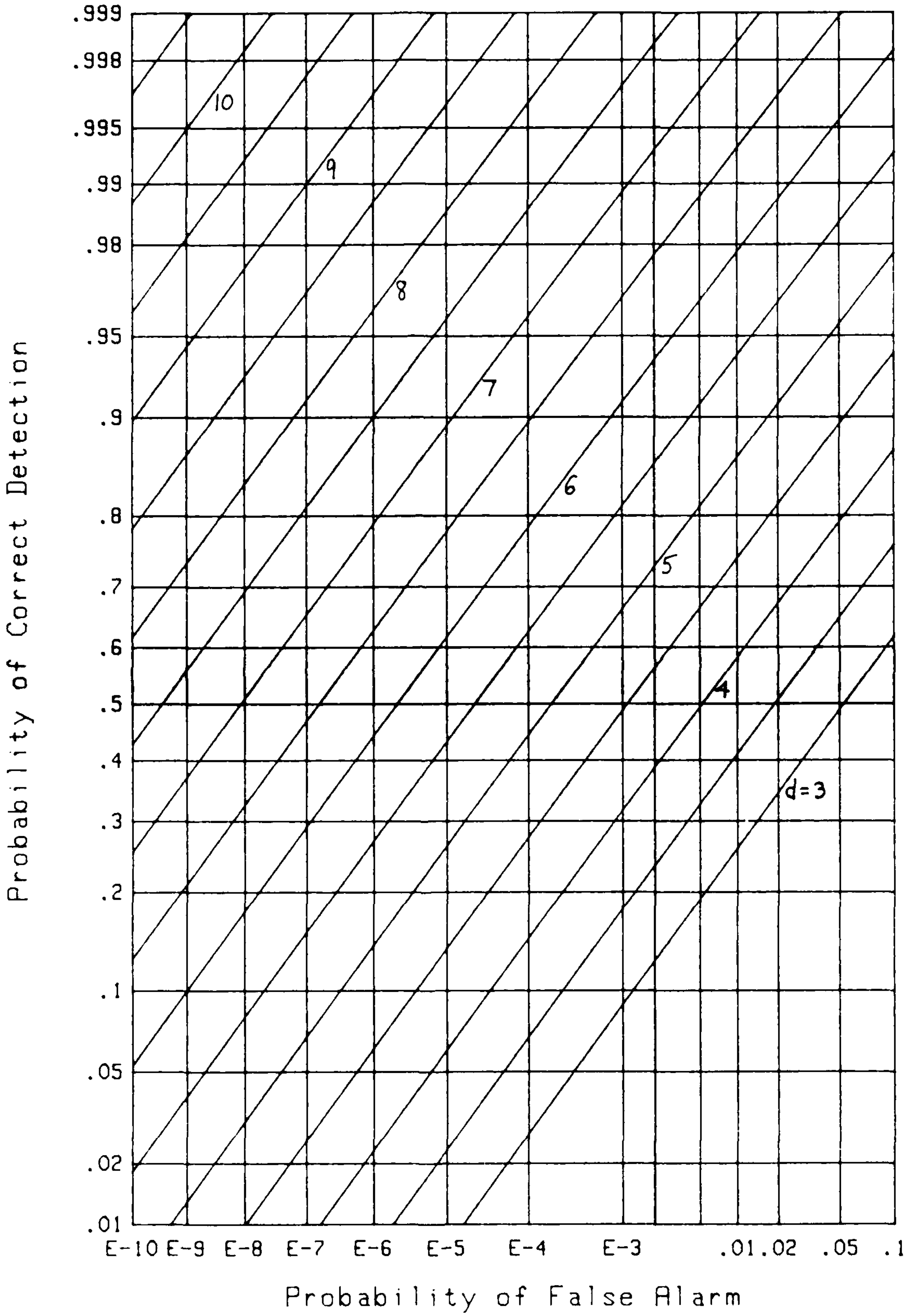

Figure 19. ROC for M=5, N=1

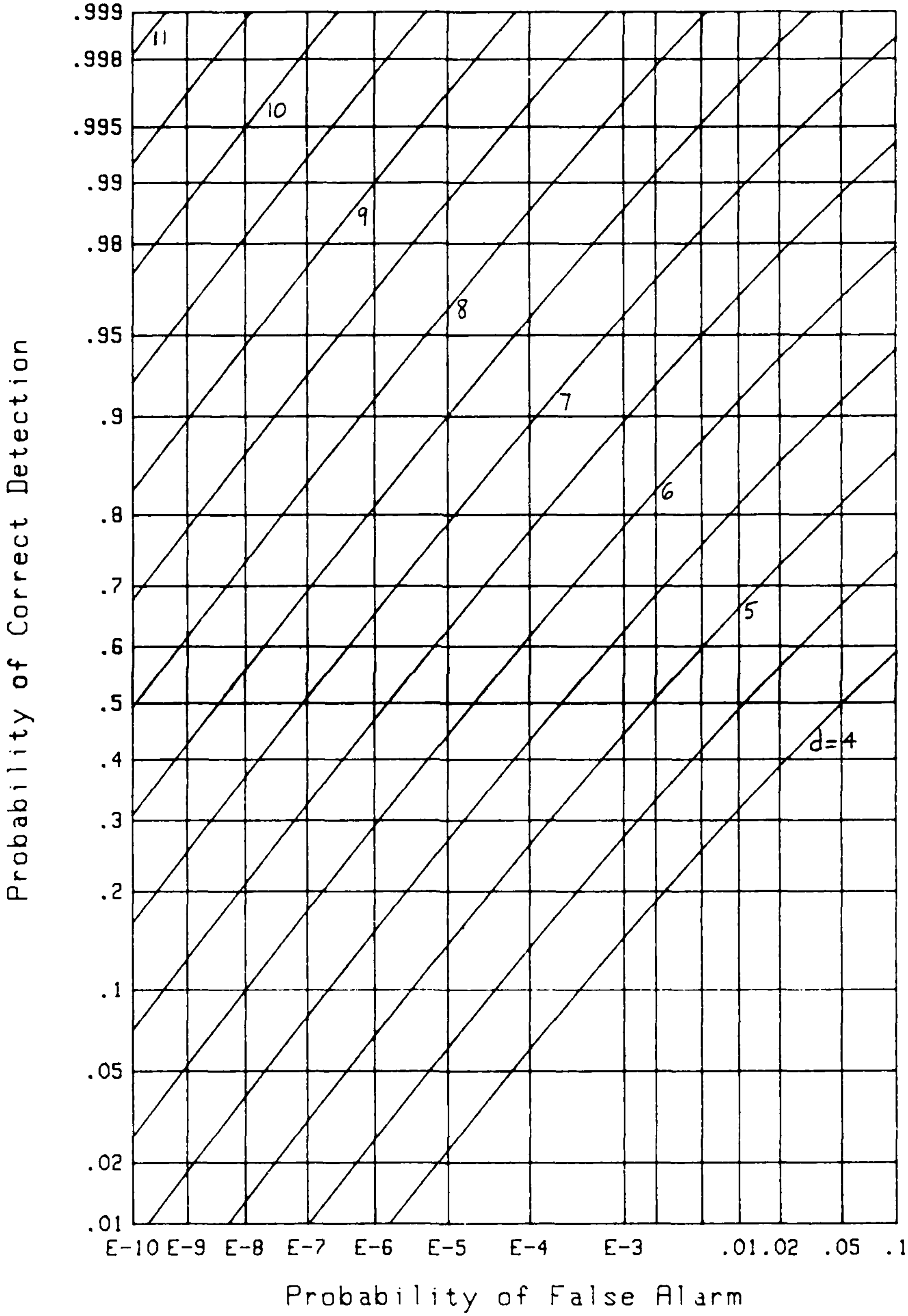

Figure 20. ROC for M=5, N=10

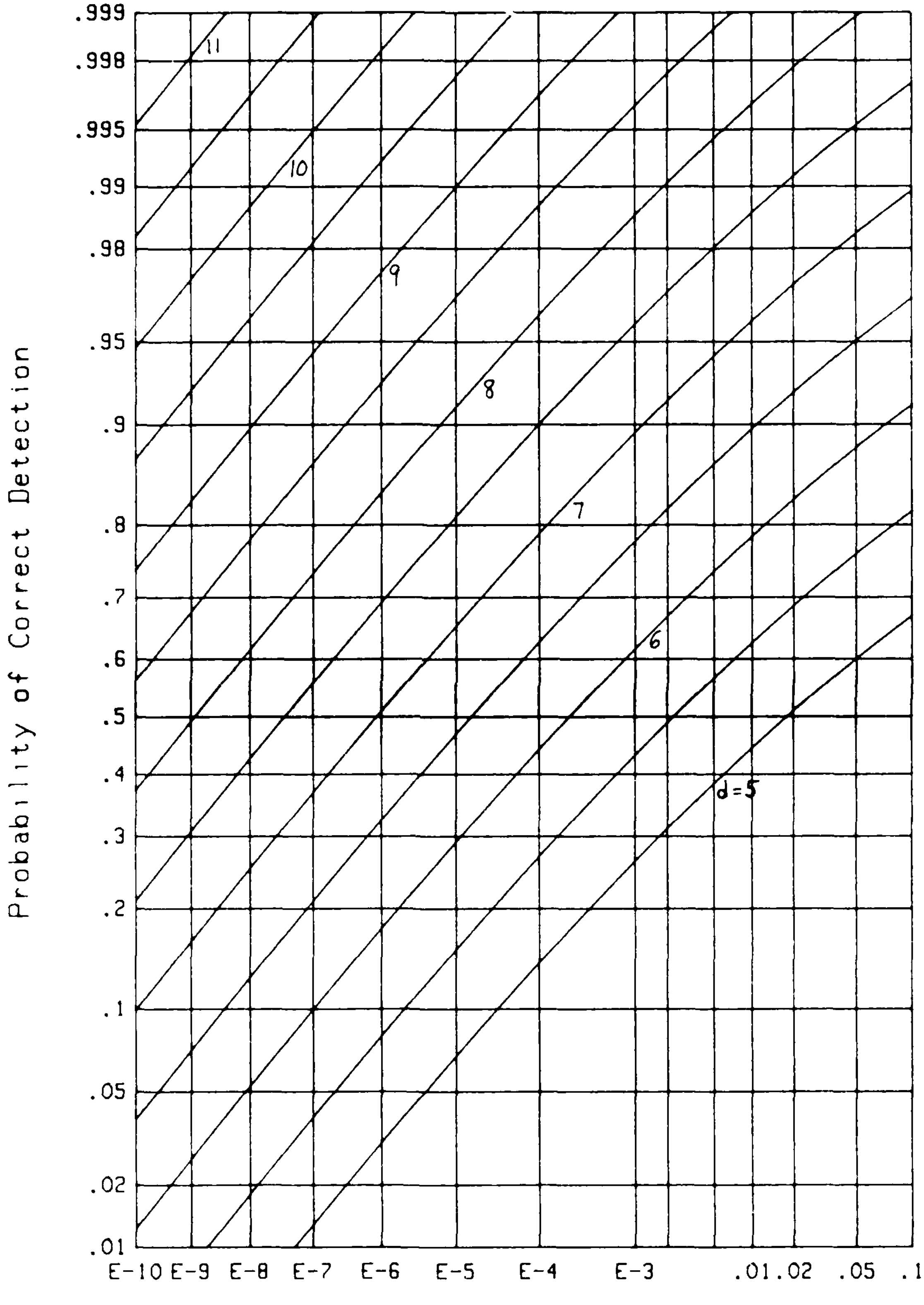

Figure 21. ROC for M=5, N=100

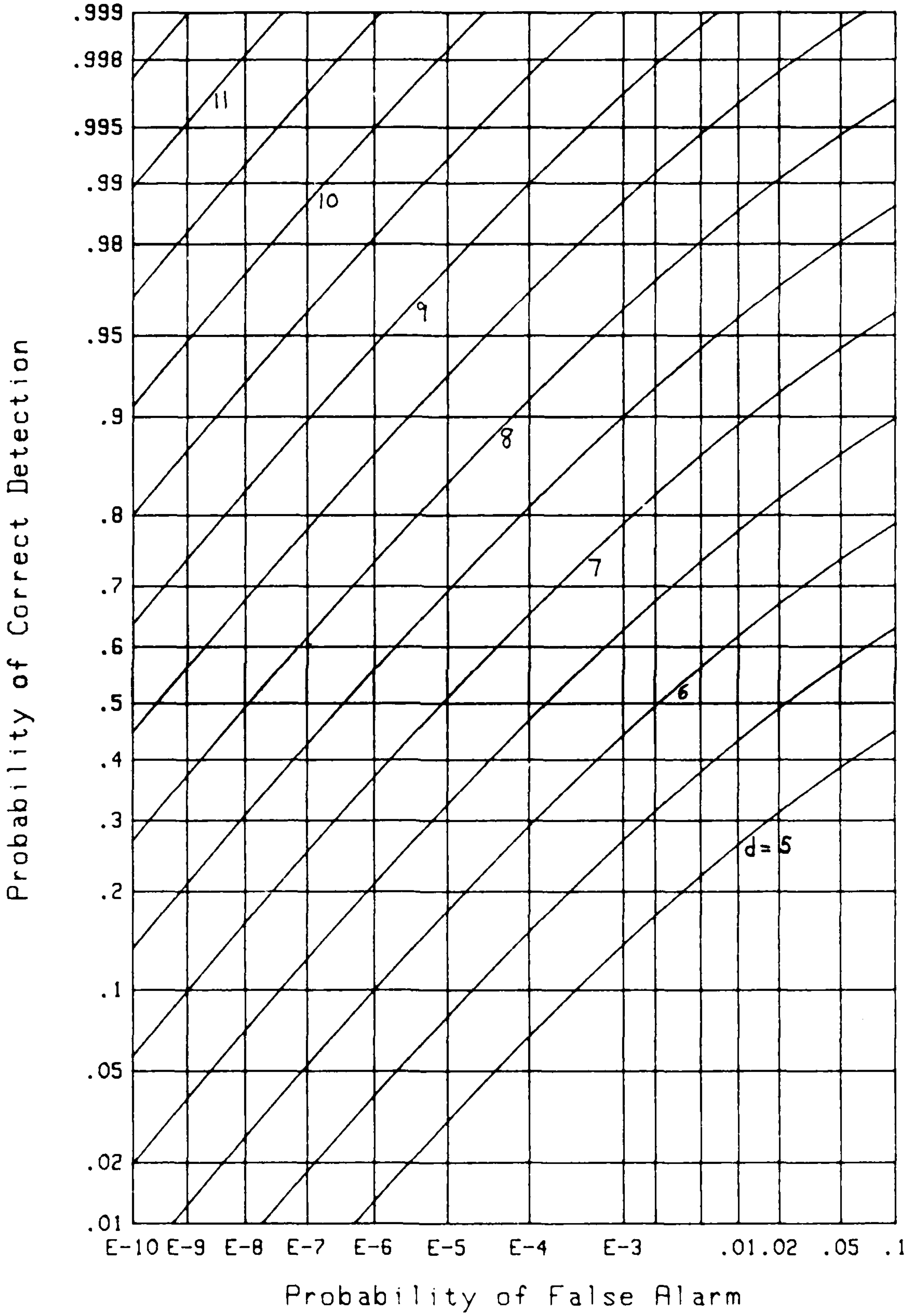

Figure 22. ROC for M=5, N=1000

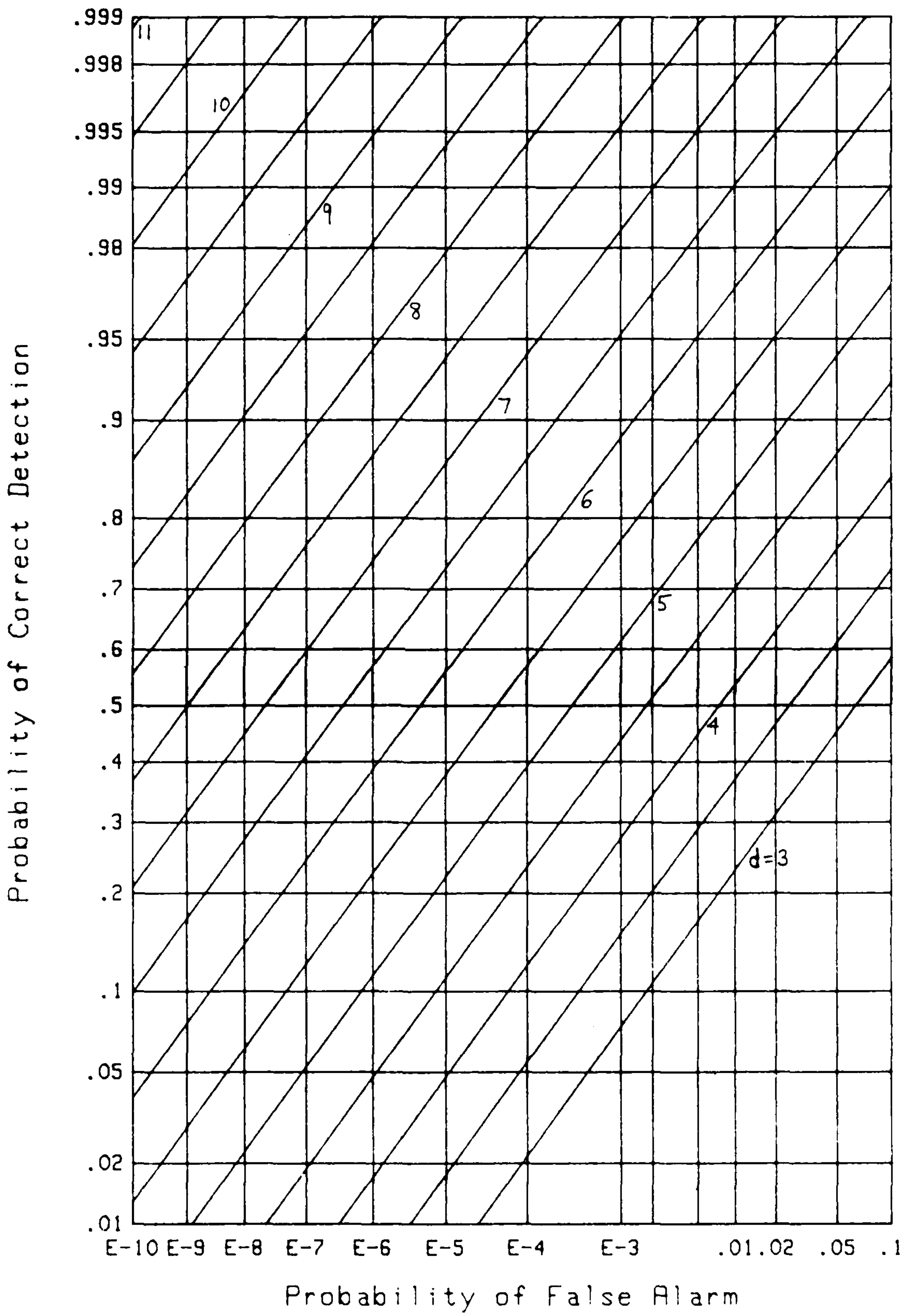

Figure 23. ROC for M=6, N=1

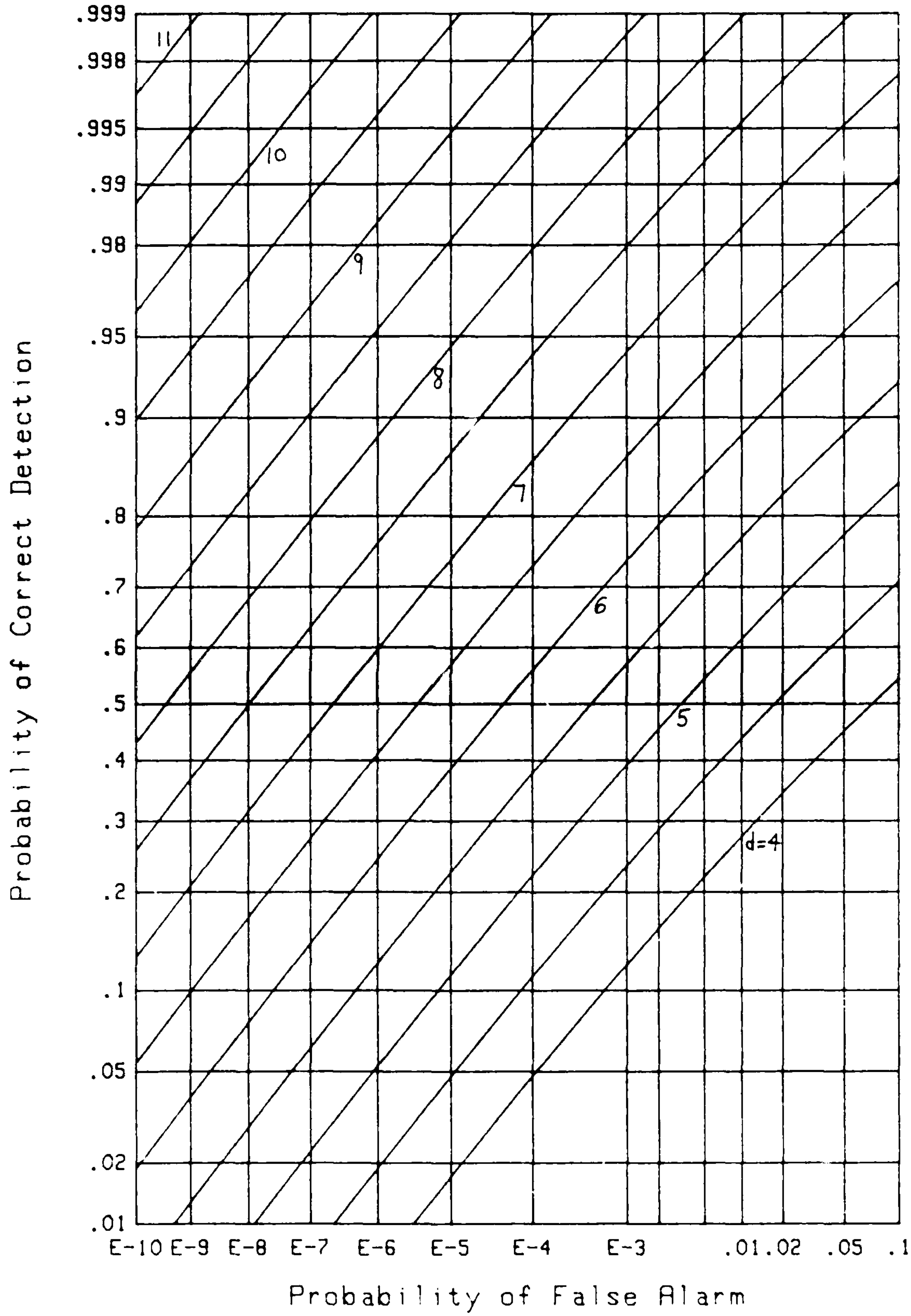

Figure 24. ROC for M=6, N=10

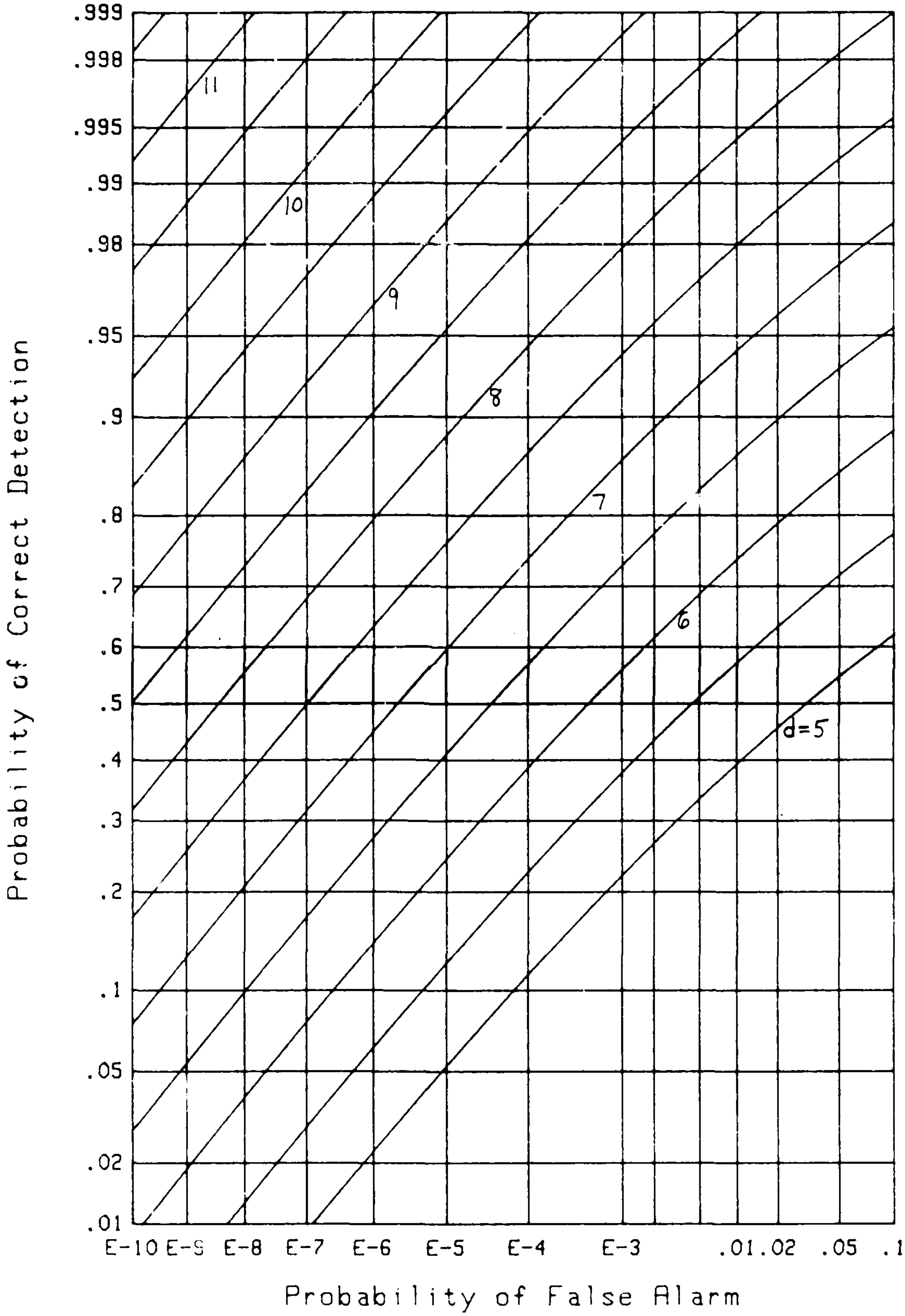

Figure 25. ROC for M=6, N=100

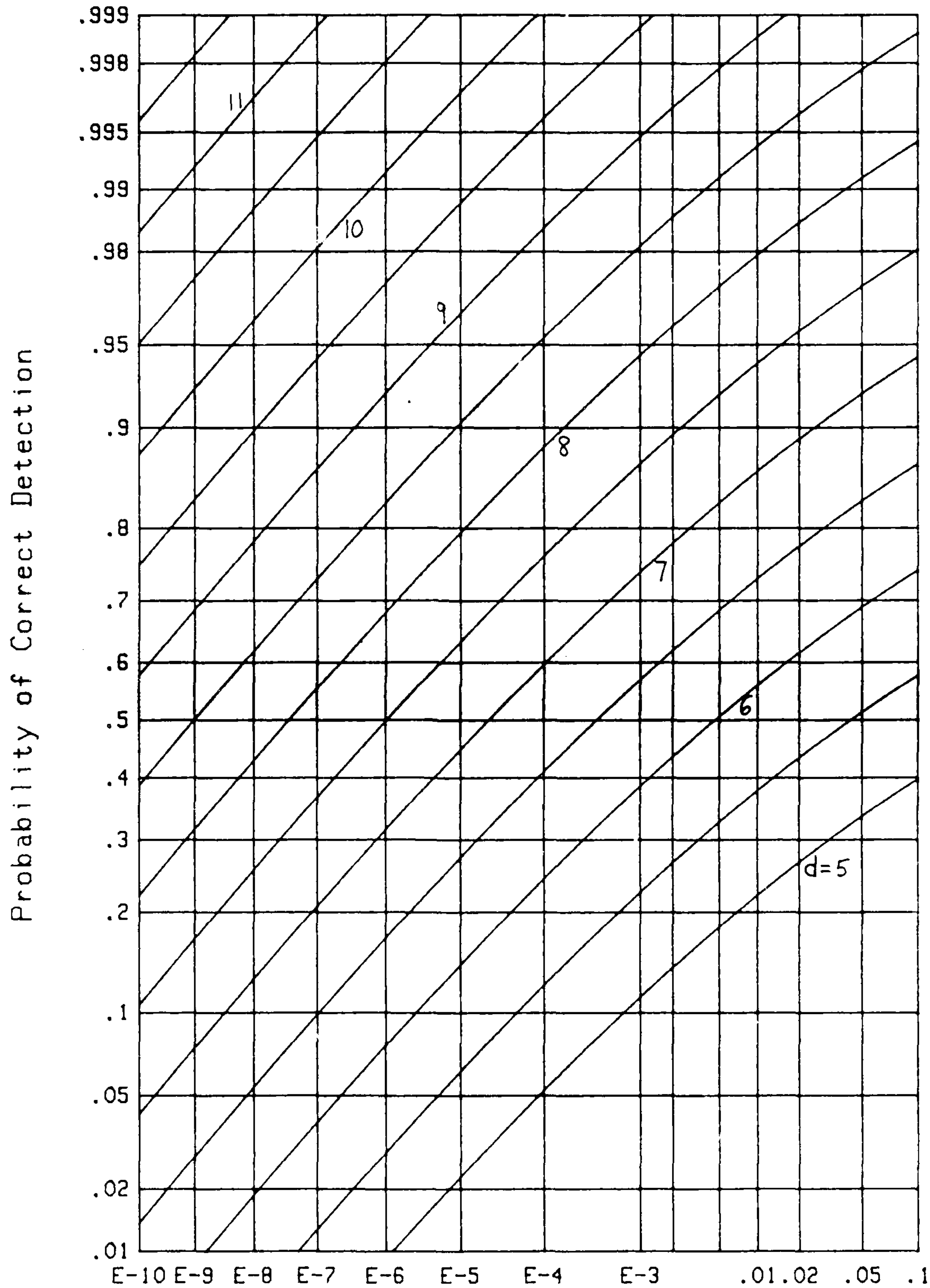

Figure 26. ROC for M=6, N=1000

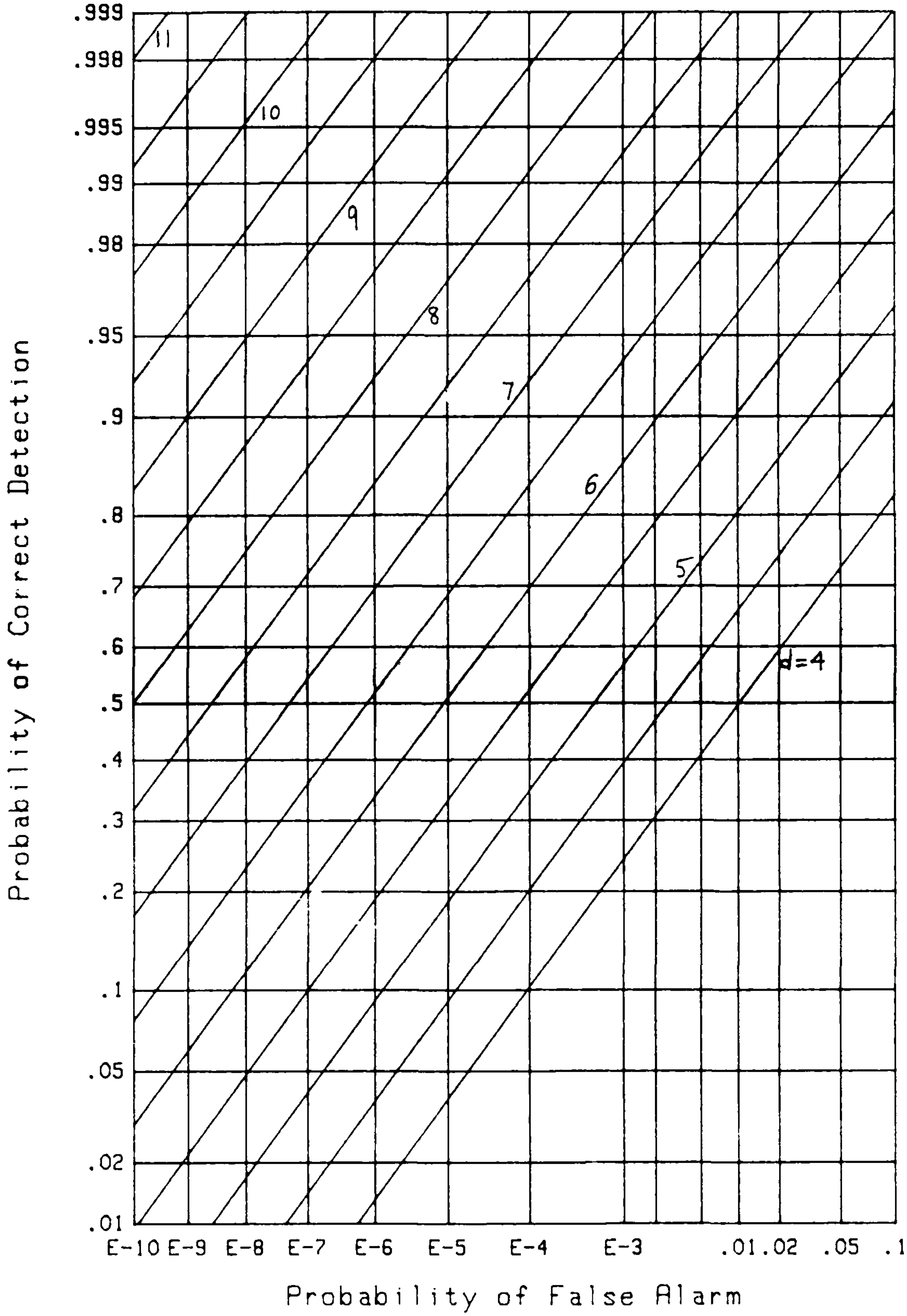

Figure 27. ROC for M=7, N=1

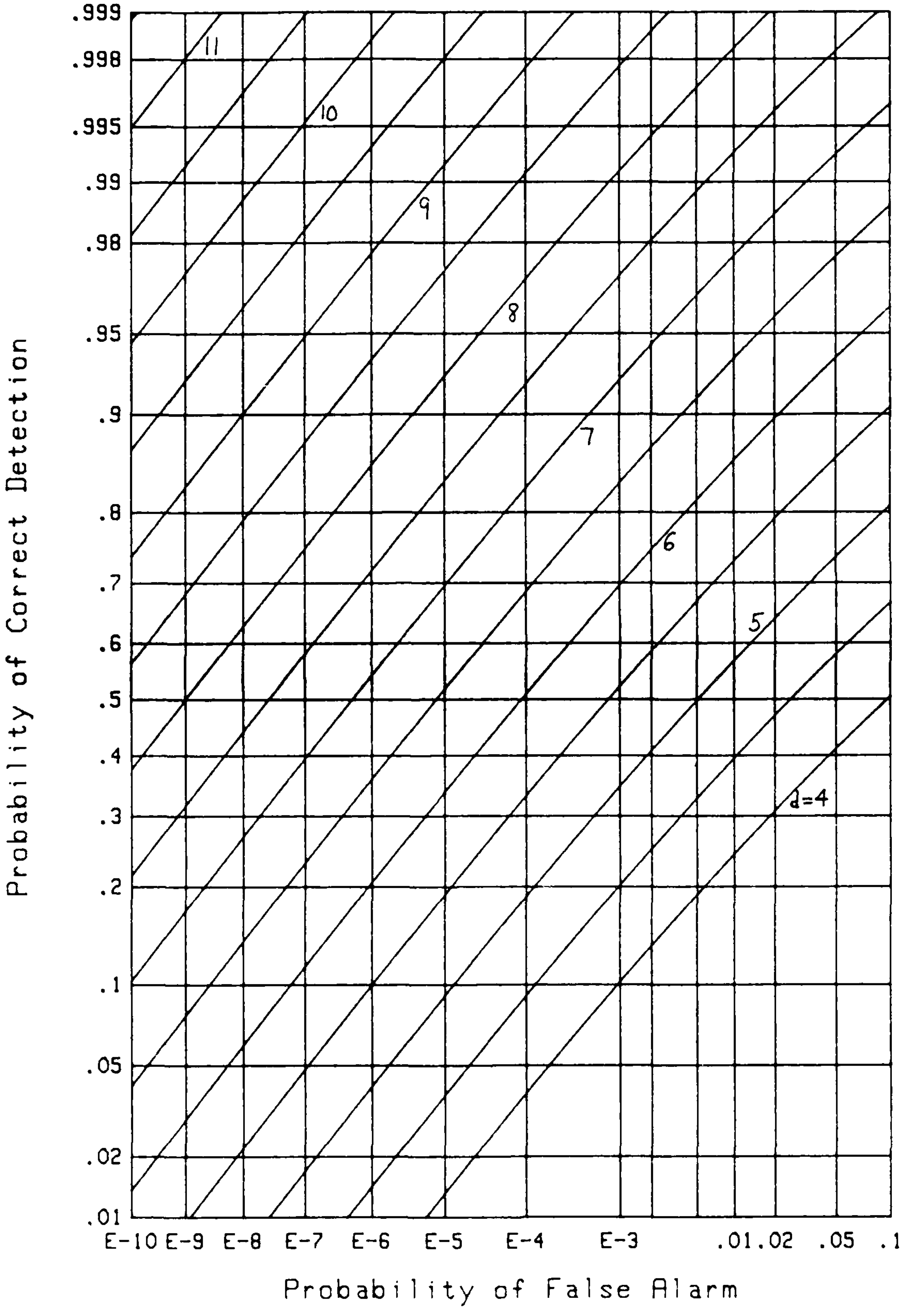

Figure 28. ROC for M=7, N=10

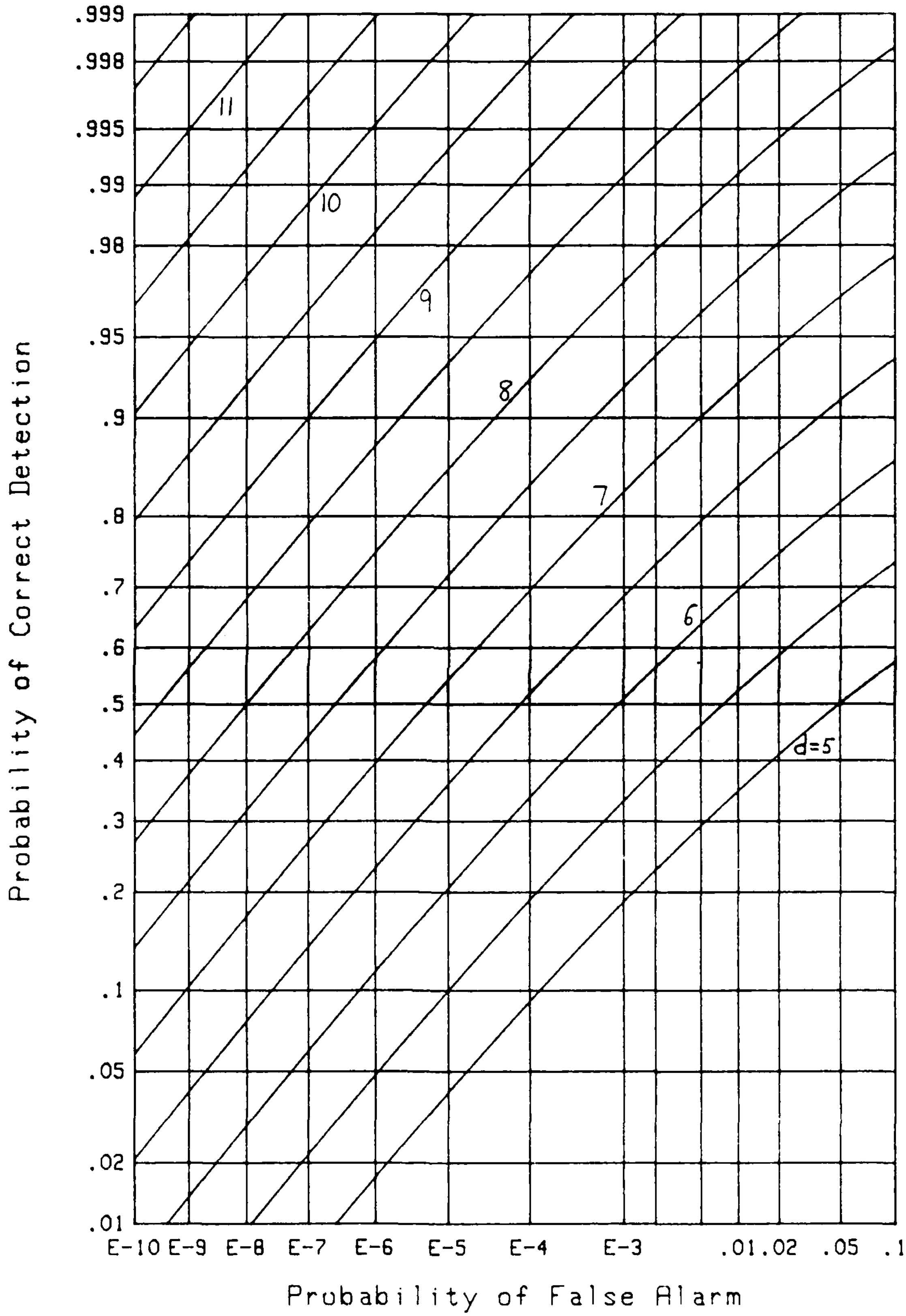

Figure 29. ROC for M=7, N=100

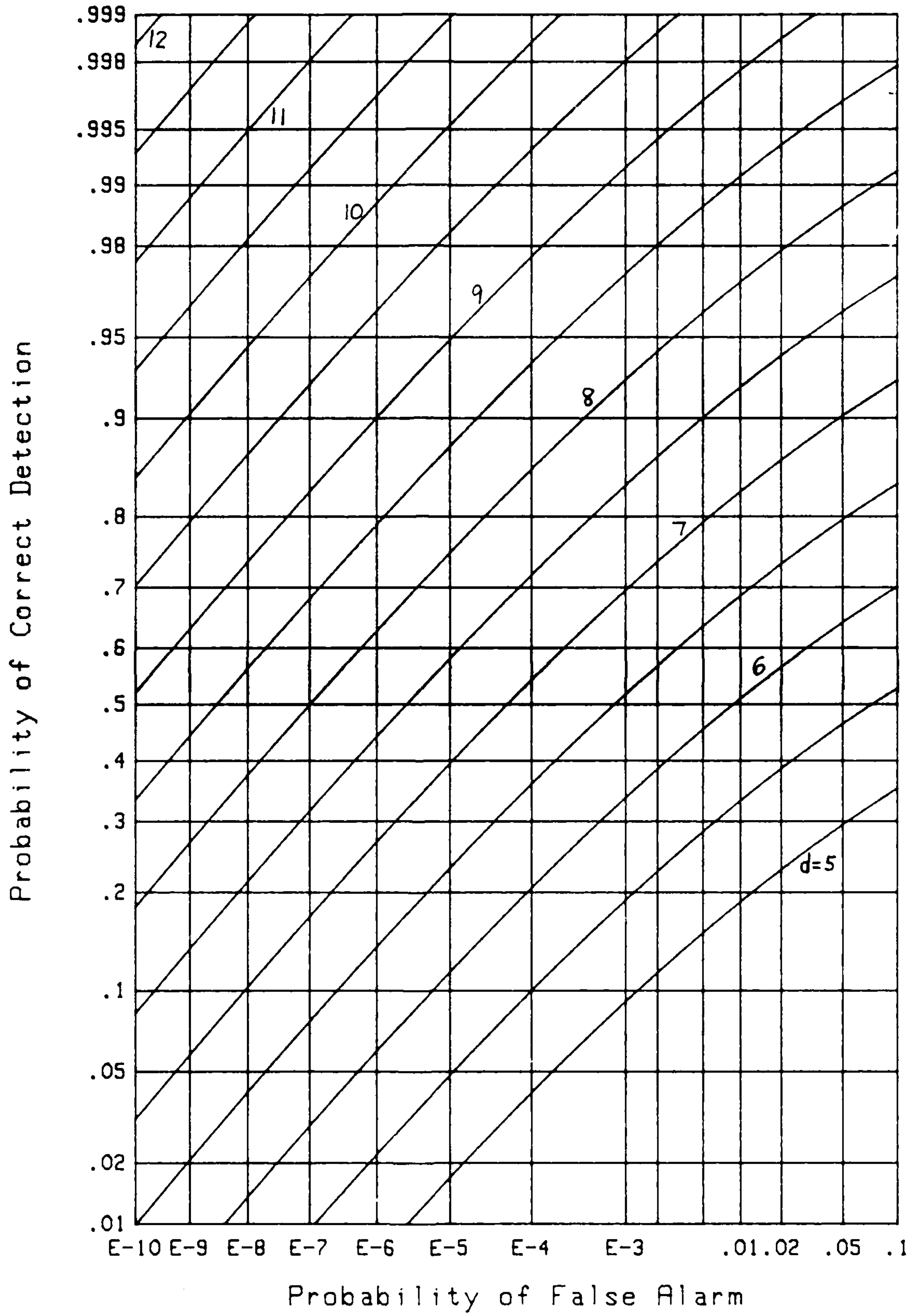

Figure 30. ROC for M=7, N=1000

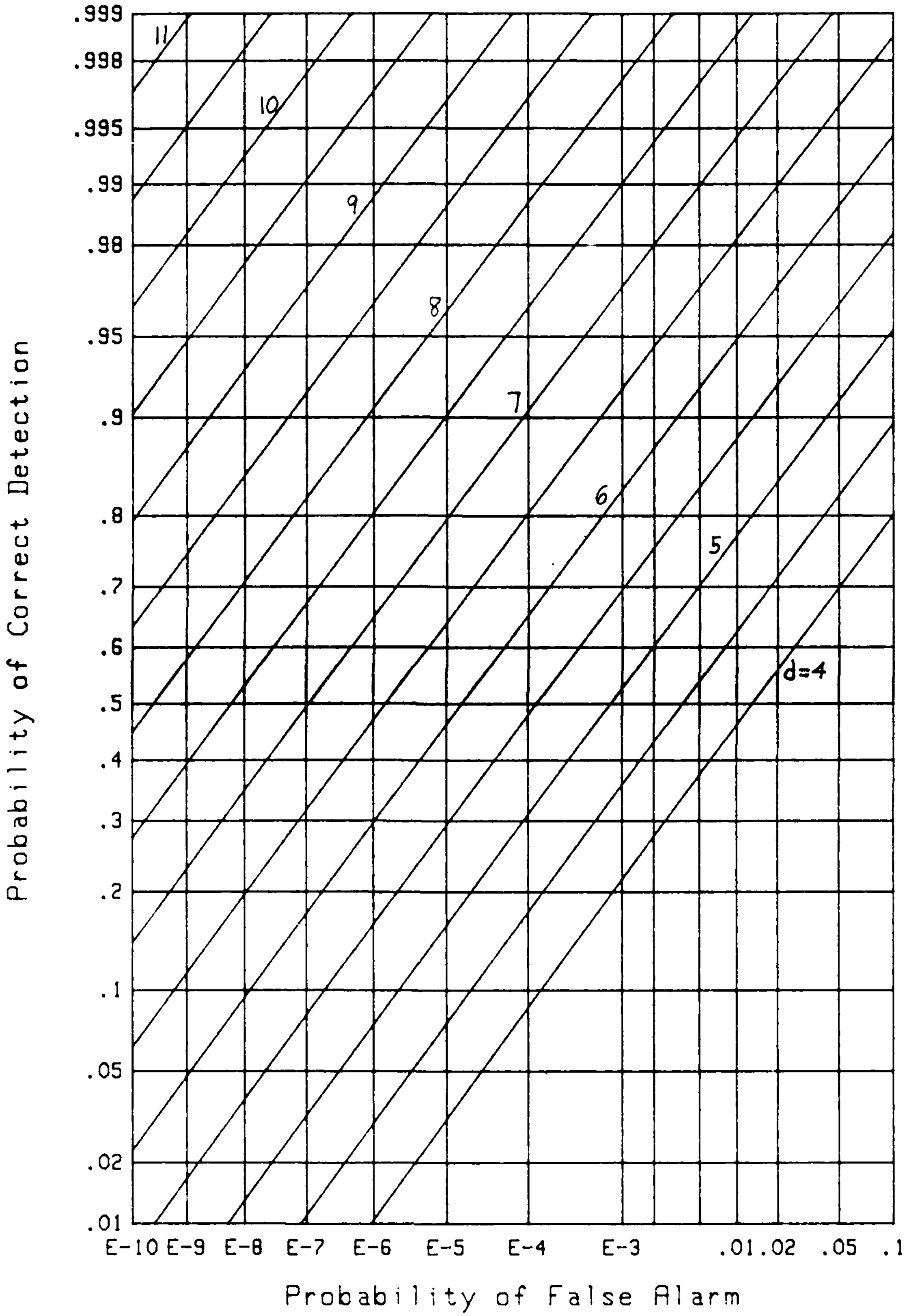

Figure 31. ROC for M=8, N=1

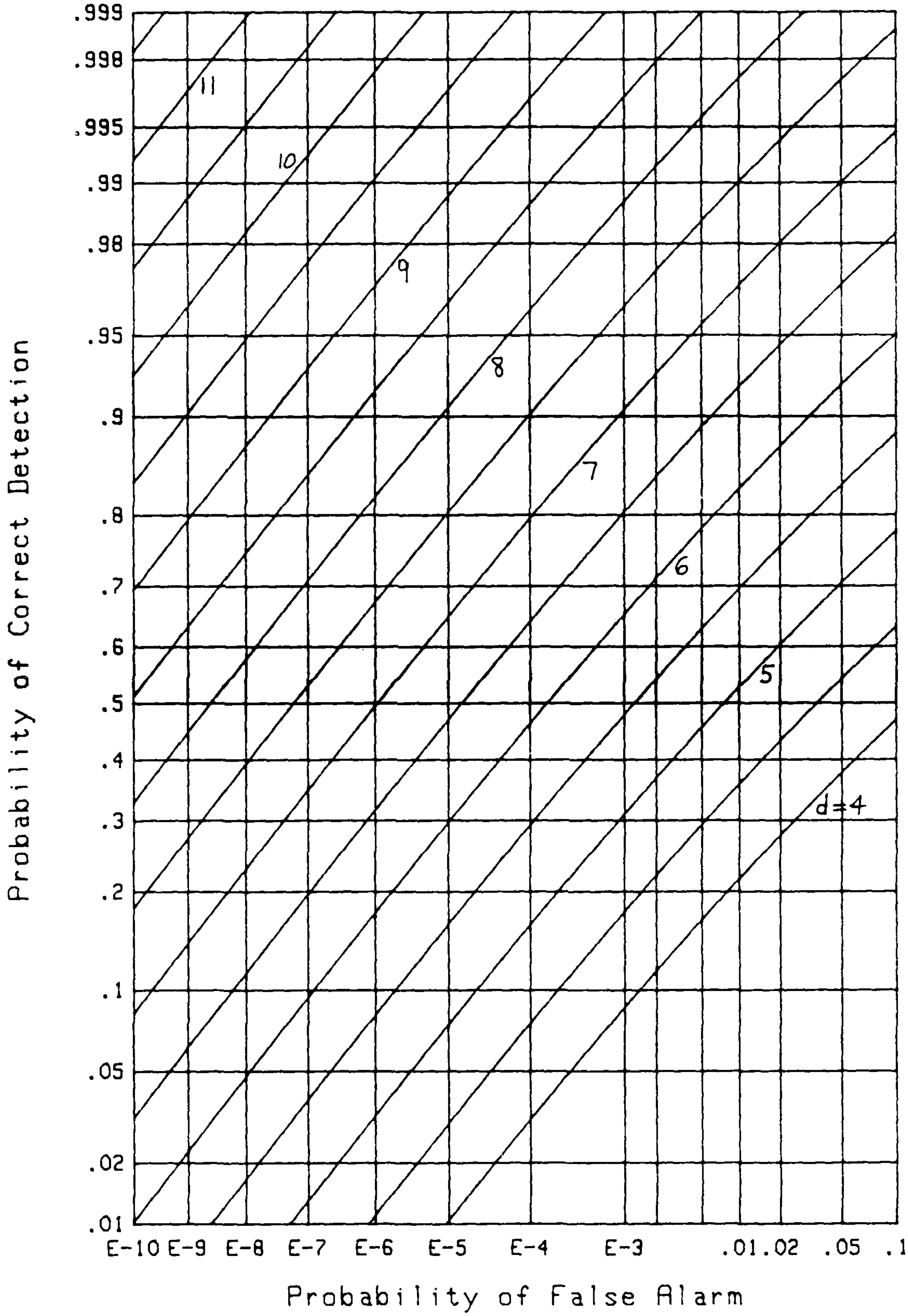

Figure 32. ROC for M=8, N=10

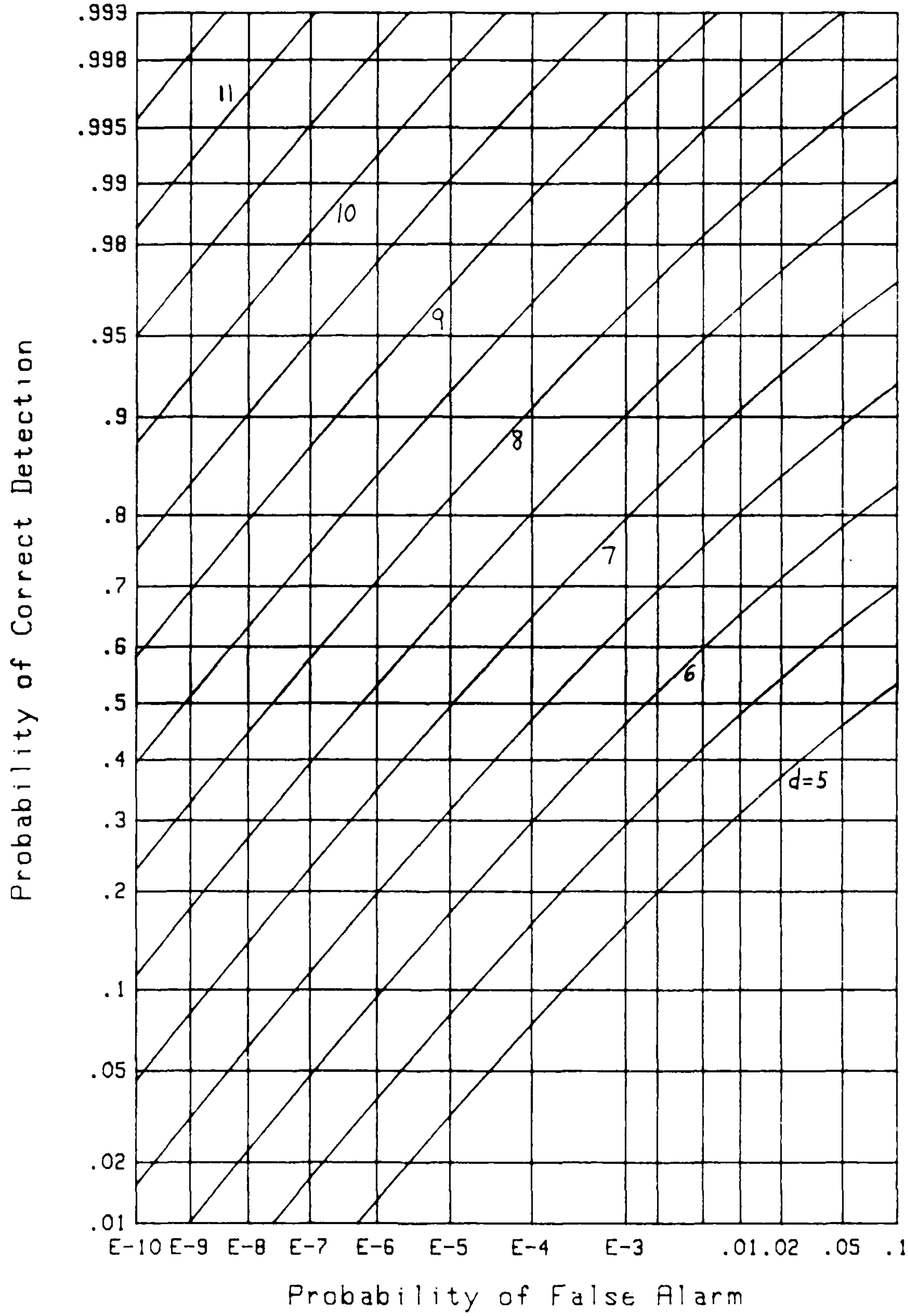

Figure 33. ROC for M=8, N=100

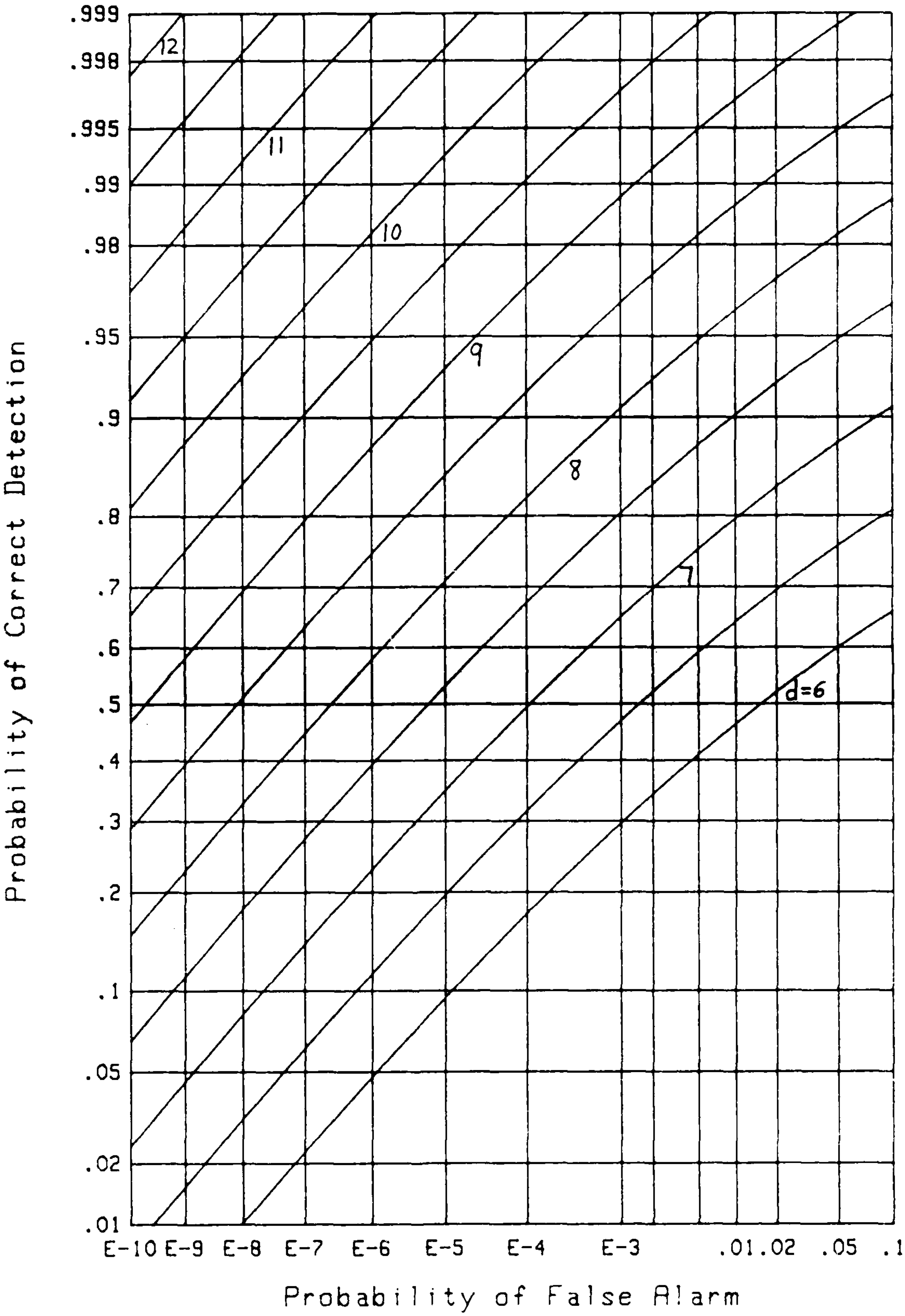

Figure 34. ROC for M=8, N=1000

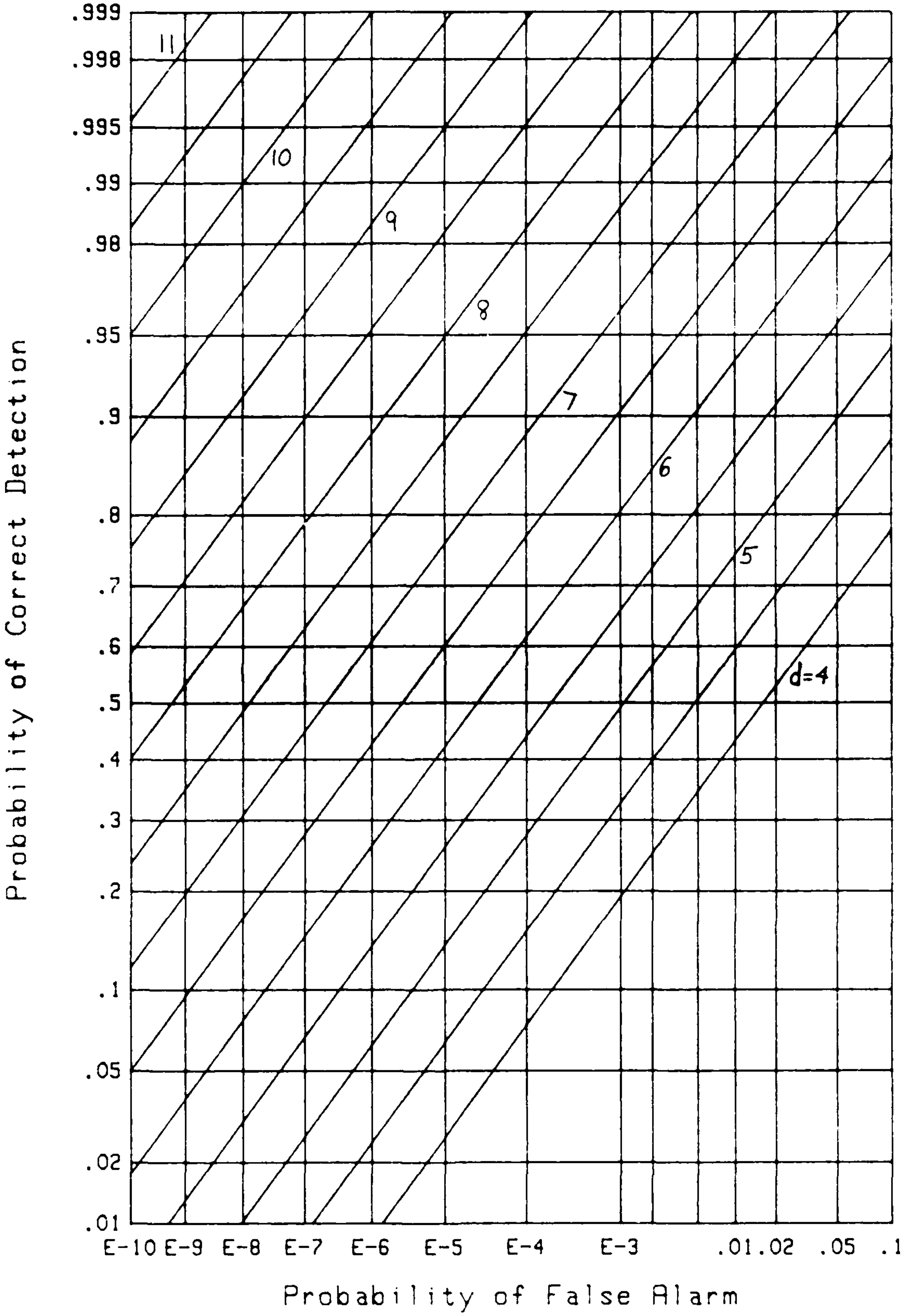

Figure 35. ROC for M=9, N=1

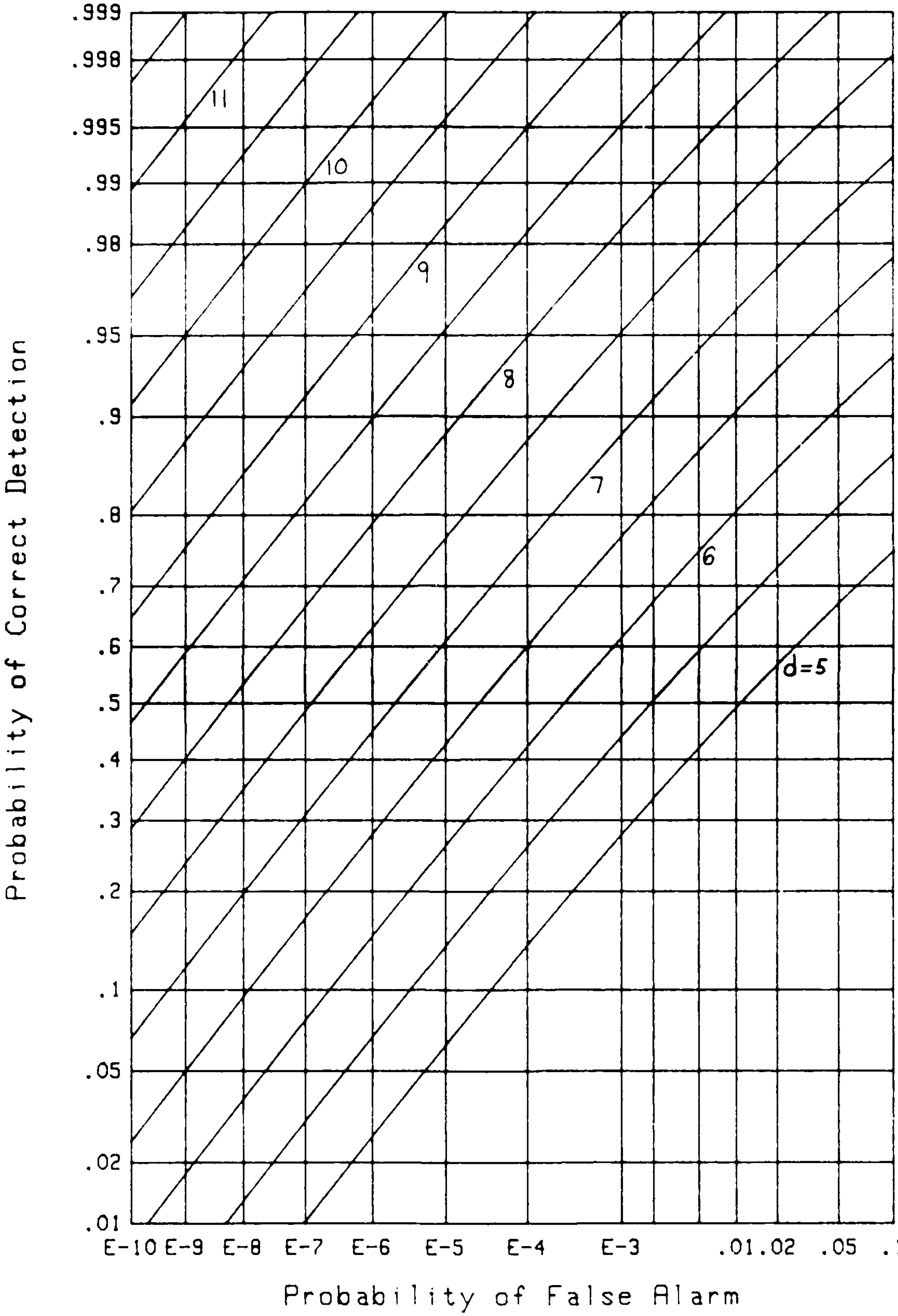

Figure 36. ROC for M=9, N=10

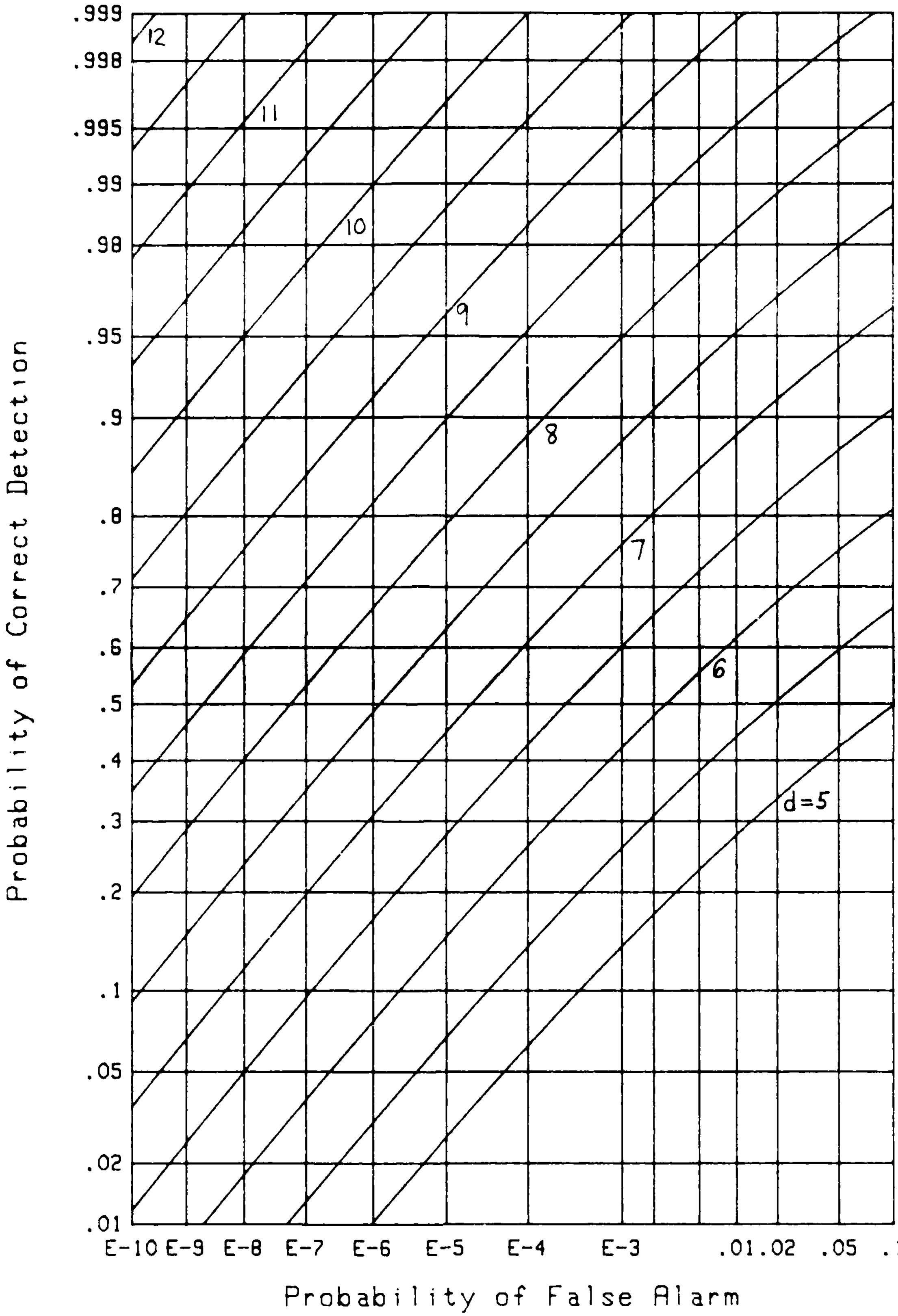

Figure 37. ROC for M=9, N=100

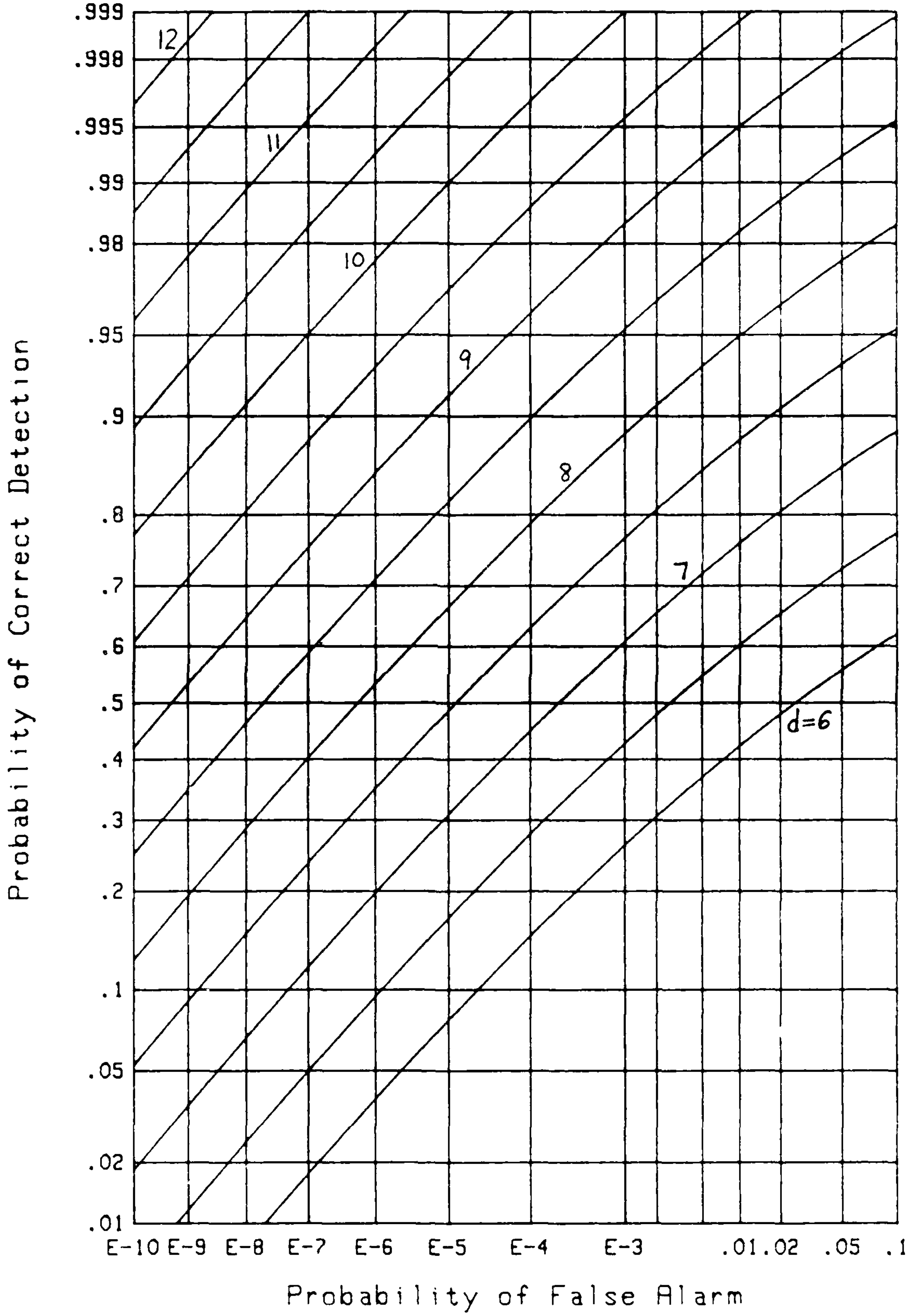

Figure 38. ROC for M=9, N=1000

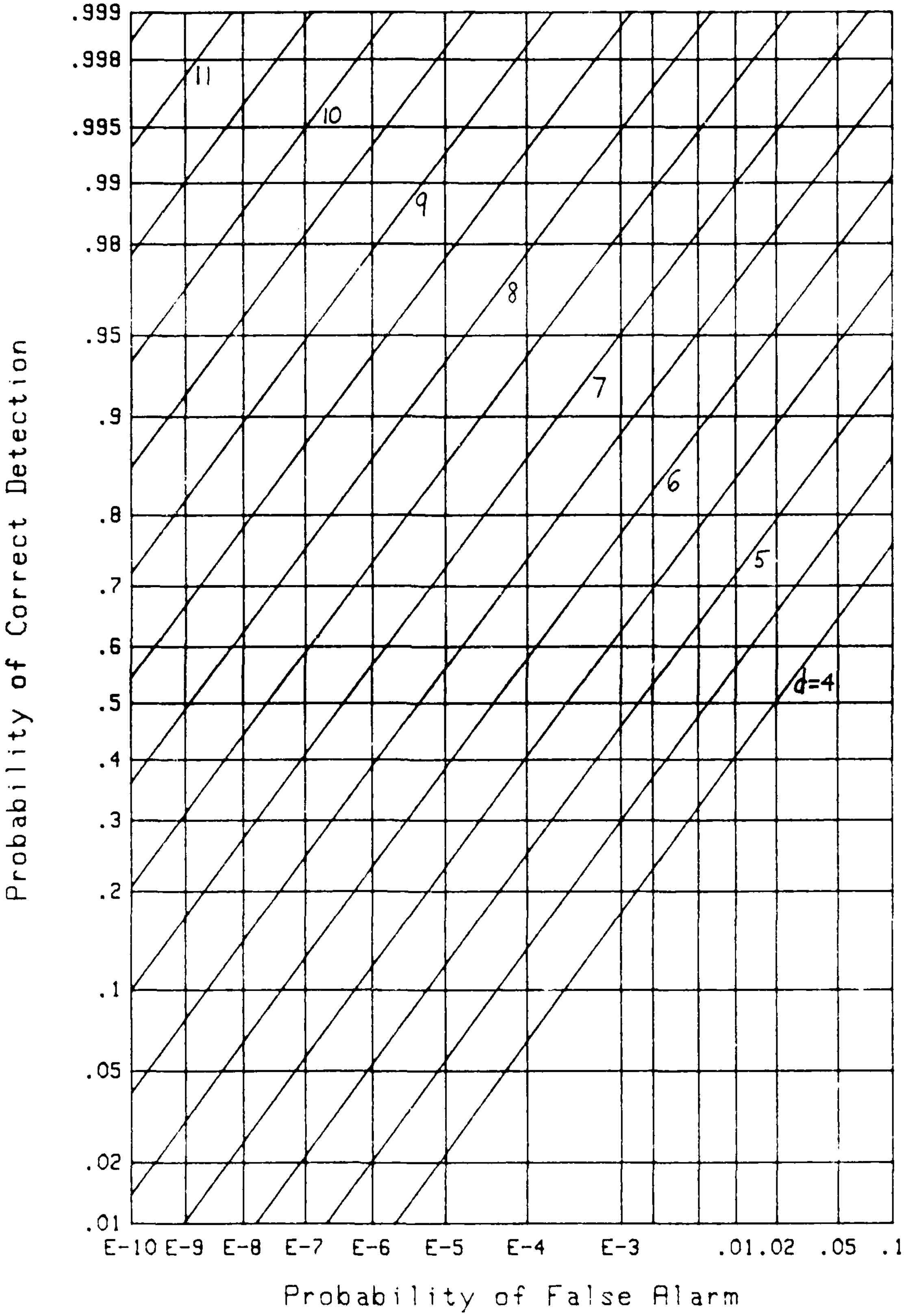

Figure 39. ROC for M=10, N=1

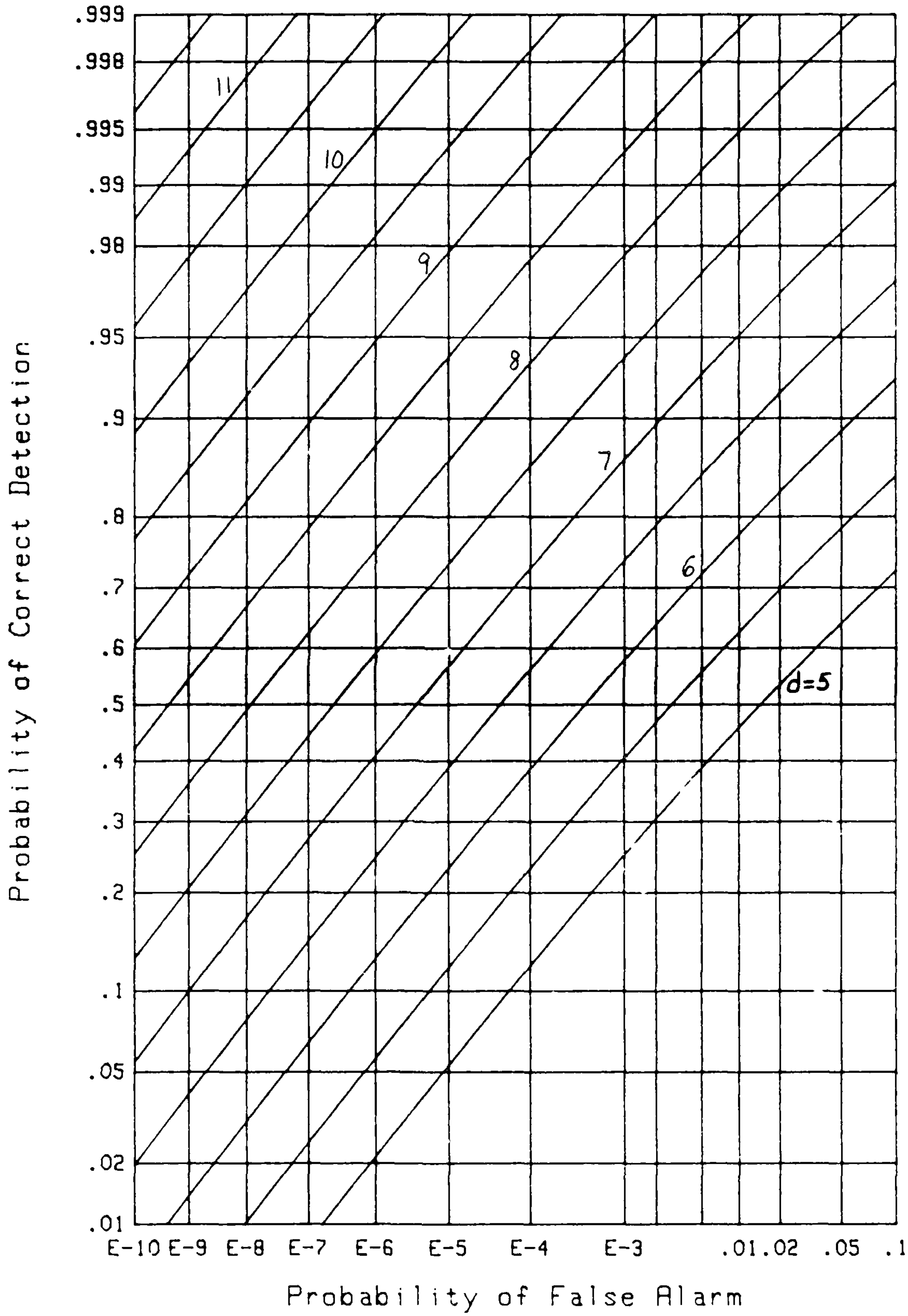

Figure 40. ROC for M=10, N=10

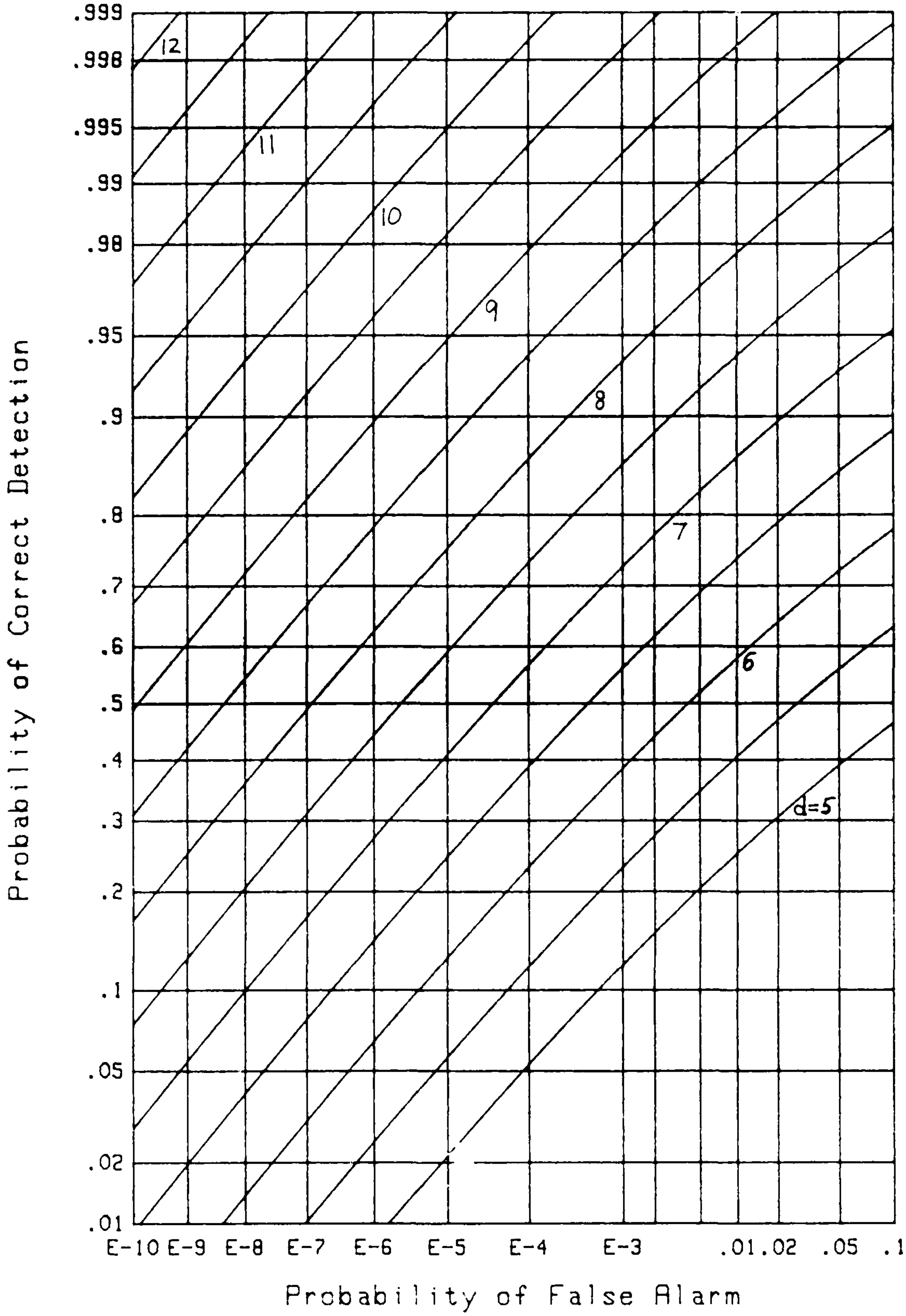

Figure 41. ROC for M=10, N=100

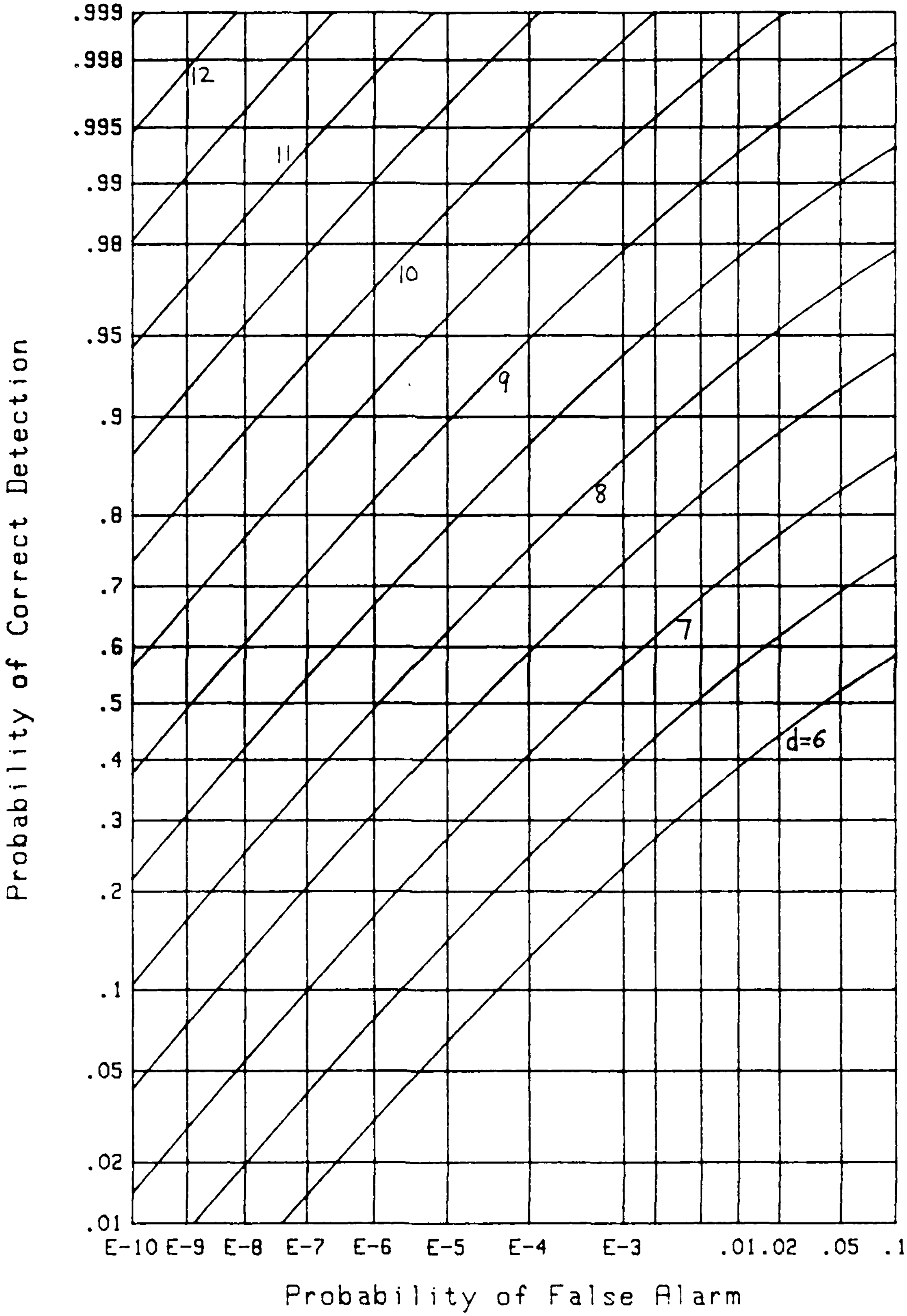

Figure 42. ROC for M=10, N=1000

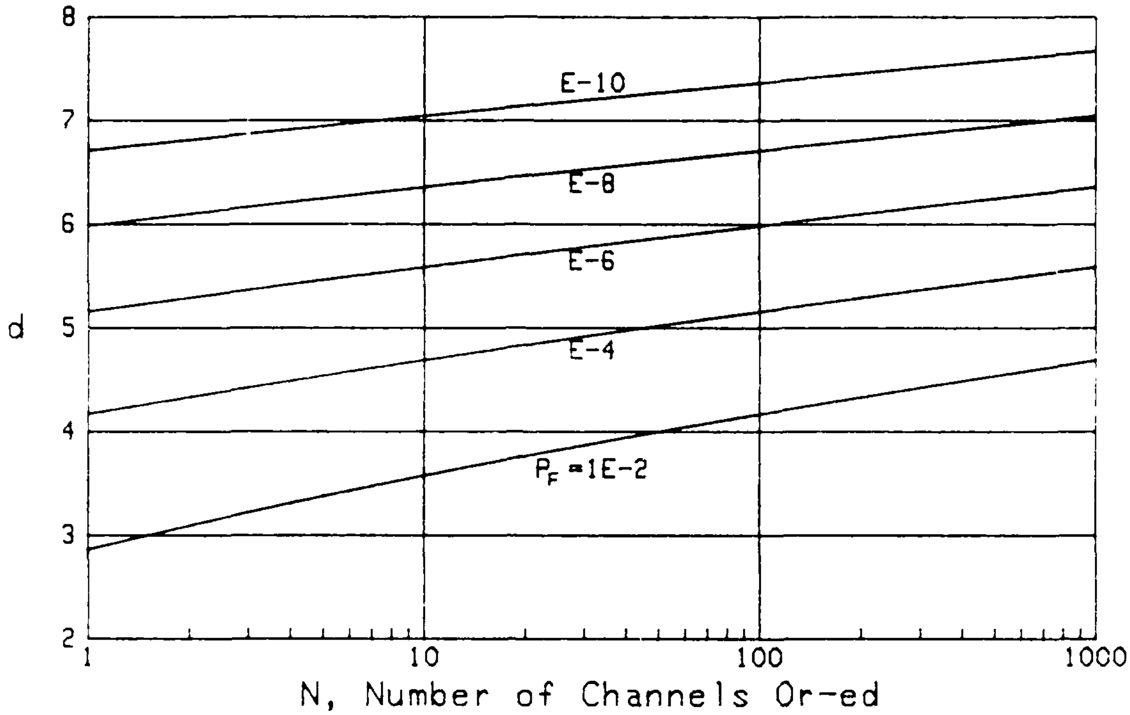

Figure 43. Required d Values for M=1, P_{CD}=.5

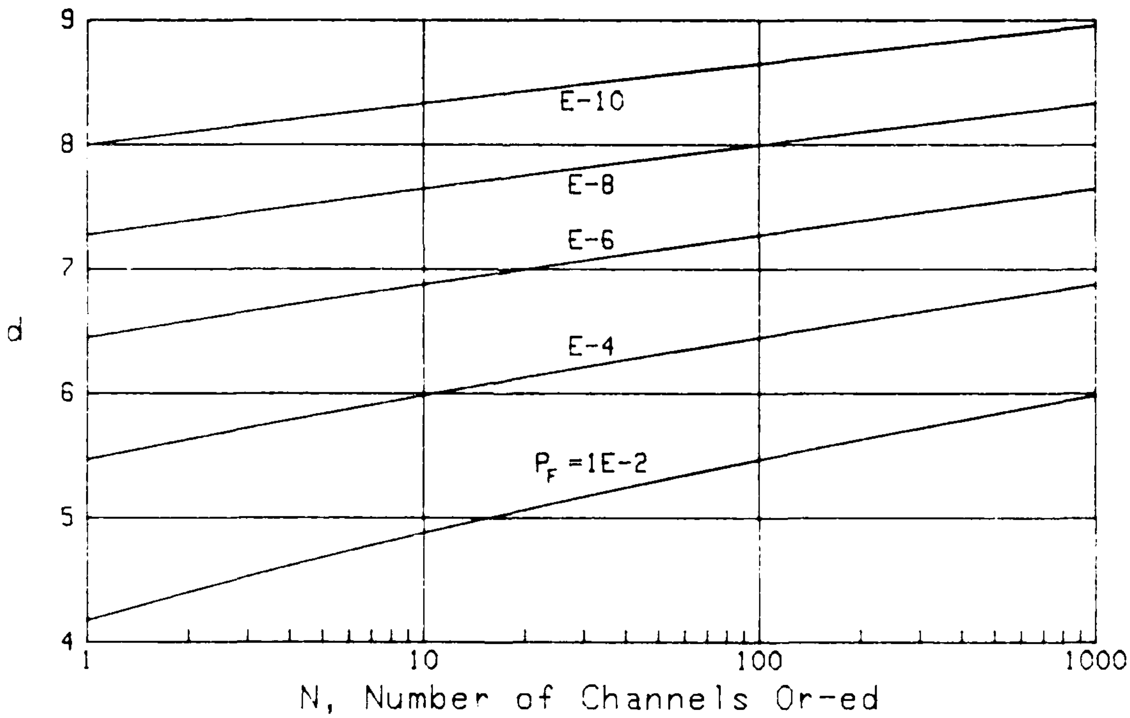

Figure 44. Required d Values for M=1, P_{CD}=.9

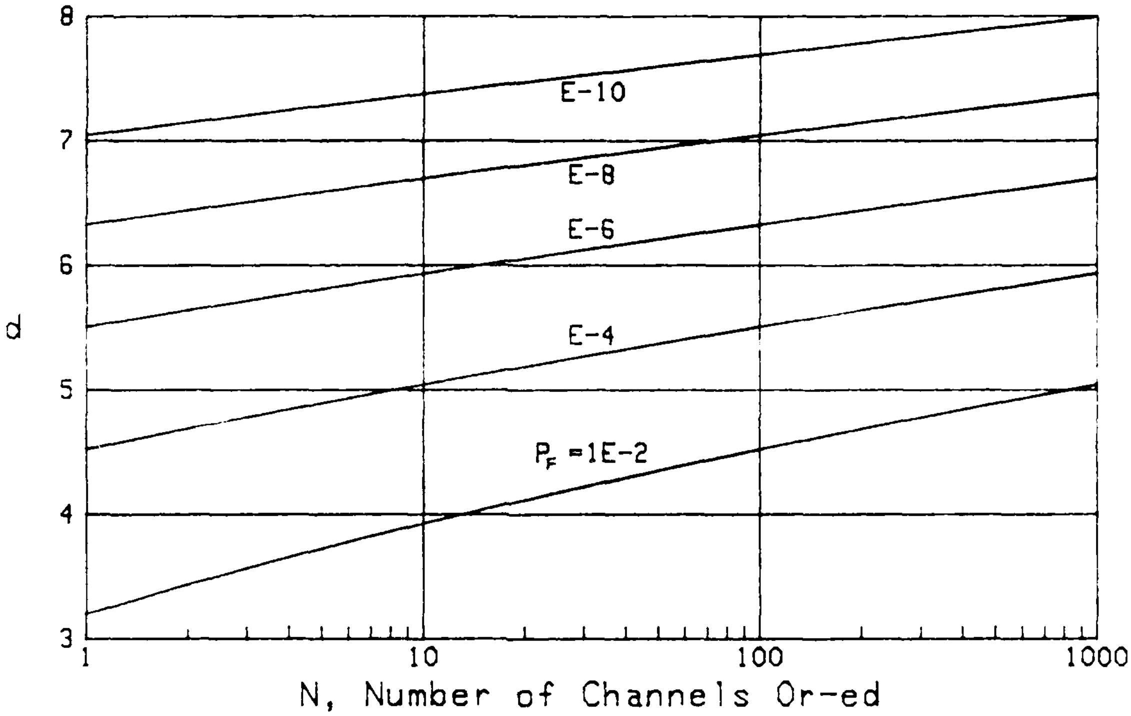

Figure 45. Required d Values for M=2, P_{CD}=.5

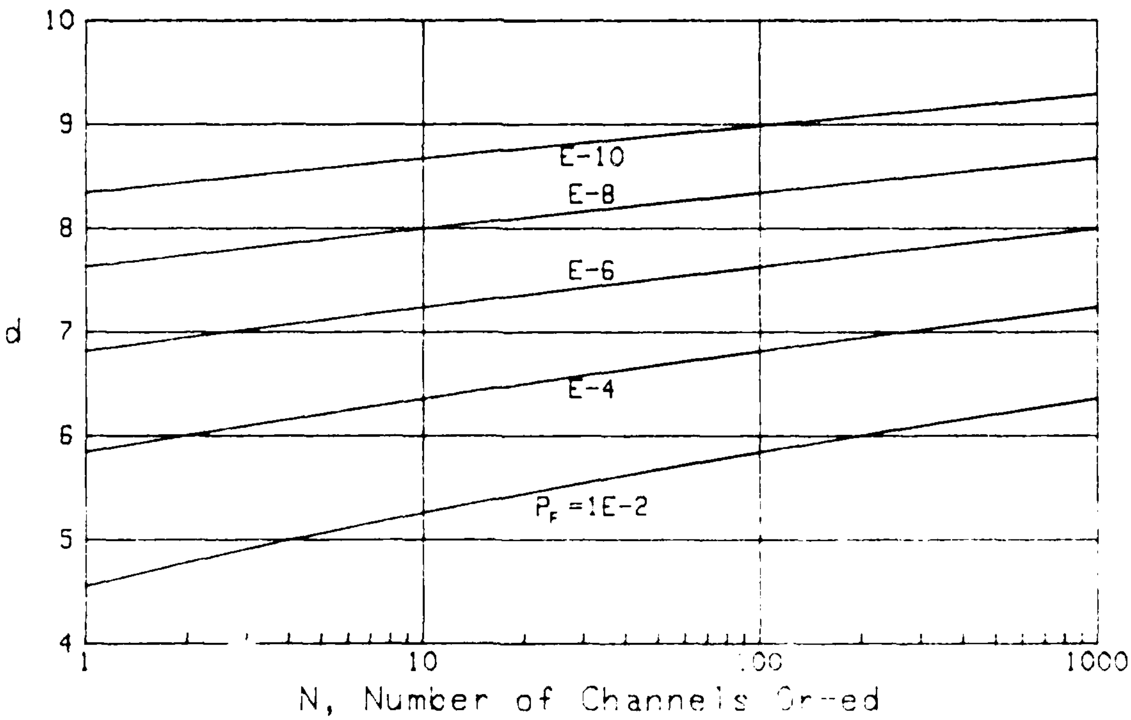

Figure 46. Required d Values for M=2, P_{CD}=.9

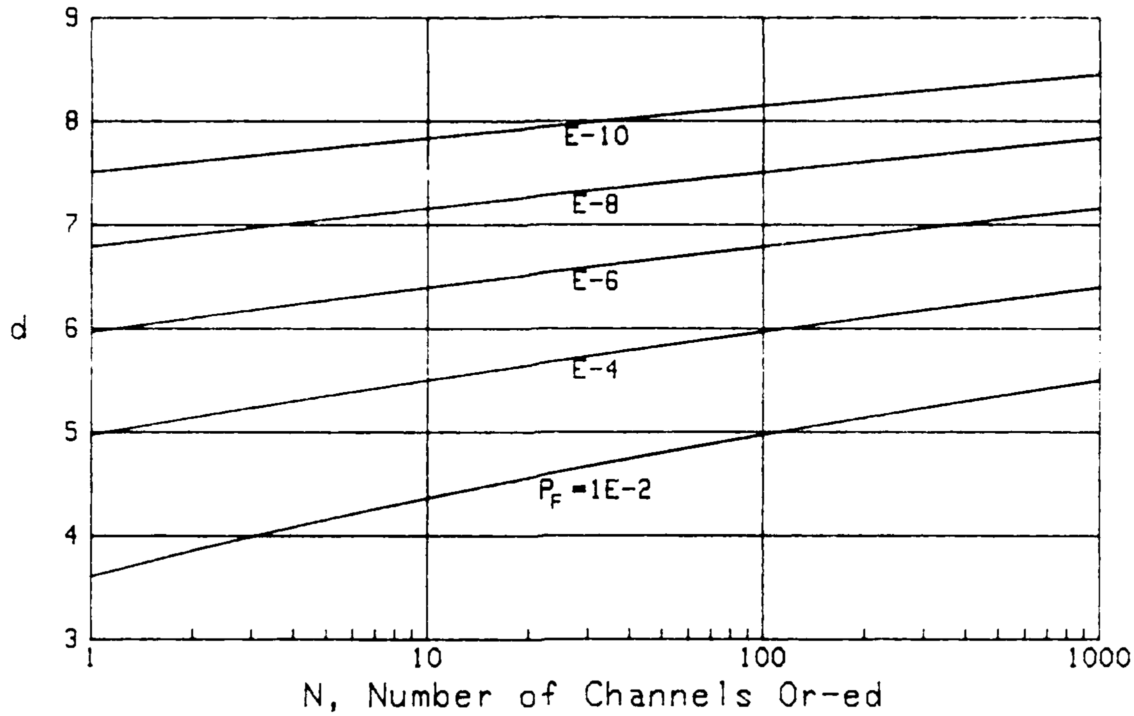

Figure 47. Required d Values for M=4, P_{CD}=.5

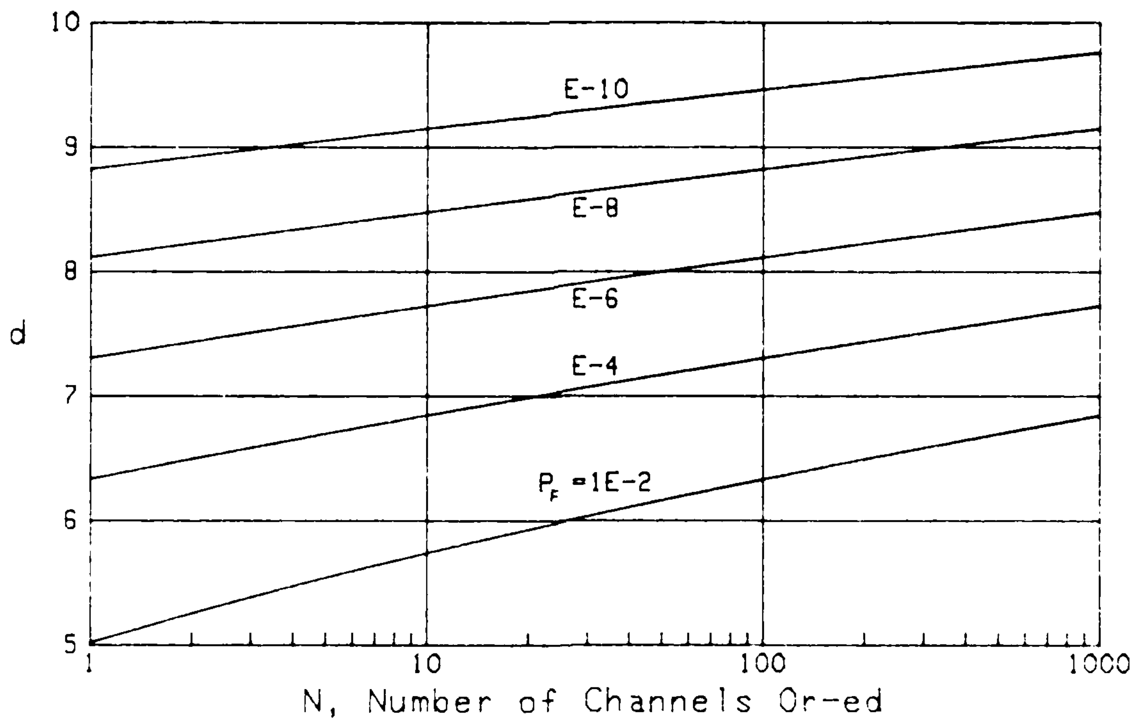

Figure 48. Required d Values for M=4, P_{CD}=.9

APPENDIX A. Q_M-FUNCTION RELATIONSHIPS

Let $\{x_m\}_1^M$ and $\{y_m\}_1^M$ be independent identically distributed Gaussian random variables, each with zero mean and common variance σ^2, and let $\{a_m\}_1^M$ and $\{b_m\}_1^M$ be arbitrary fixed constants. Define "total" parameter

$$d^2 = \frac{1}{\sigma^2} \sum_{m=1}^{M} (a_m^2 + b_m^2) \ . \tag{A-1}$$

Chi-Squared Variate

We are interested in the statistical description of the noncentral chi-squared random variable of 2M degrees of freedom,

$$v = \sum_{m=1}^{M} [(x_m + a_m)^2 + (y_m + b_m)^2] \ . \tag{A-2}$$

We will only list results here, and will not give detailed derivations.

The characteristic function of v is [6; page 11]

$$f_v(\xi) = \overline{\exp(i\xi v)} = (1 - i\xi 2\sigma^2)^{-M} \ \exp\left[\frac{i\xi d^2\sigma^2}{1-i\xi 2\sigma^2}\right], \tag{A-3}$$

which is seen to depend on the arbitrary constants $\{a_m\}$ and $\{b_m\}$ only through the sum d^2 in (A-1). The probability density function of random variable v is [7; 6.631 4]

$$p_v(u) = \frac{1}{2\sigma^2}\left(\frac{\sqrt{u}}{d\sigma}\right)^{M-1} I_{M-1}\left(\frac{d\sqrt{u}}{\sigma}\right)\exp\left(-\frac{u}{2\sigma^2} - \frac{d^2}{2}\right) \quad \text{for } u > 0. \tag{A-4}$$

The cumulative distribution function of random variable v is

$$\text{Prob } (v < u) = P_v(u) = \int_0^u dt\ p_v(t) \ , \tag{A-5}$$

and the exceedance distribution function is

$$1 - P_v(u) = Q_M(d, \sqrt{u}/\sigma) \quad \text{for } u > 0, \tag{A-6}$$

where the Q_M-function is

$$Q_M(\alpha, \beta) = \int_\beta^\infty dx\ x\left(\frac{x}{\alpha}\right)^{M-1} I_{M-1}(\alpha x)\ \exp\left(-\frac{x^2+\alpha^2}{2}\right) . \tag{A-7}$$

As special cases of (A-4) and (A-6), for d = 0, we have probability density function

$$p_v^{(o)}(u) = \frac{u^{M-1}}{(M-1)!\ (2\sigma^2)^M}\ \exp\left(\frac{-u}{2\sigma^2}\right) \quad \text{for } u > 0 \tag{A-8}$$

and exceedance distribution function

$$1-P_v^{(o)}(u) = \exp\left(\frac{-u}{2\sigma^2}\right) e_{M-1}\left(\frac{u}{2\sigma^2}\right) = E_{M-1}\left(\frac{u}{2\sigma^2}\right) \quad \text{for } u > 0, \tag{A-9}$$

where [5; 6.5.11]

$$e_n(x) = \sum_{k=0}^{n} x^k/k! \tag{A-10}$$

is the partial exponential and where we define

$$E_n(x) = \exp(-x)\ e_n(x) \ . \qquad \text{(A-11)}$$

Returning to the general case of $d > 0$ for random variable v again, the cumulants of v are

$$\lambda_v(n) = \left(2\sigma^2\right)^n n!\left(\frac{M}{n} + \frac{d^2}{2}\right) \quad \text{for } n \geq 1 \ , \qquad \text{(A-12)}$$

the υ-th moments are

$$\overline{v^\upsilon} = (2\sigma^2)^\upsilon \frac{\Gamma(M + \upsilon)}{\Gamma(M)}\ {}_1F_1(-\upsilon;M;-\ d^2/2) \quad \text{for } \upsilon > -M, \qquad \text{(A-13)}$$

and the n-th moments are

$$\overline{v^n} = (2\sigma^2)^n\ n!\ L_n^{(M-1)}(-d^2/2). \qquad \text{(A-14)}$$

<u>Chi Variate</u>

The noncentral chi variate of 2M degrees of freedom is

$$z = v^{1/2} = \left\{\sum_{m=1}^{M} [(x_m + a_m)^2 + (y_m + b_m)^2]\right\}^{1/2} . \qquad \text{(A-15)}$$

Its probability density function is

$$p_z(u) = \frac{u}{\sigma^2}\left(\frac{u}{d\sigma}\right)^{M-1} I_{M-1}\left(\frac{du}{\sigma}\right) \exp\left(-\frac{u^2}{2\sigma^2} - \frac{d^2}{2}\right) \quad \text{for } u > 0, \qquad \text{(A-16)}$$

and its exceedance distribution function is

$$1 - P_z(u) = Q_M(d,\ u/\sigma) \quad \text{for } u > 0. \tag{A-17}$$

As special cases of (A-16) and (A-17), for d = 0, we have probability density function

$$p_z^{(o)}(u) = \frac{2\ u^{2M-1}}{(M-1)!\ (2\sigma^2)^M}\ \exp\left(\frac{-u^2}{2\sigma^2}\right) \quad \text{for } u > 0 \tag{A-18}$$

and exceedance distribution function

$$1 - P_z^{(o)}(u) = E_{M-1}\left(\frac{u^2}{2\sigma^2}\right) \text{ for } u > 0, \tag{A-19}$$

in terms of the functions defined in (A-10) and (A-11).

In general, for d > 0, the ν-th moment of random variable z is

$$\overline{z^\nu} = \sigma^\nu\ 2^{\nu/2}\ \frac{\Gamma(M + \nu/2)}{\Gamma(M)}\ {}_1F_1(-\nu/2;M;-d^2/2) \quad \text{for } \nu > -\ 2M. \tag{A-20}$$

The characteristic function and cumulants of z are not available in any compact form.

<u>Special Case</u>

If the constants in random variable v in (A-2), and in random variable z in (A-15), satisfy

$$a_m = A \cos \Theta_m, \quad b_m = A \sin \Theta_m, \tag{A-21}$$

where $\{\Theta_m\}$ are arbitrary, then (A-1) reduces to

$$d^2 = M\,A^2/\sigma^2, \tag{A-22}$$

independent of the particular values of $\{\Theta_m\}$. So if $\{\Theta_m\}$ were random variables instead of constants, the statistics of v and z in (A-2) and (A-15), respectively, would be unaffected. This conclusion follows immediately from (A-3).

In this latter case of random $\{\Theta_m\}$, if they are also uniformly distributed over 2π, it is sometimes useful to define an individual (common) signal-to-noise ratio

$$R = \frac{\overline{a_m^2}}{\overline{x_m^2}} = \frac{\overline{b_m^2}}{\overline{y_m^2}} = \frac{A^2/2}{\sigma^2} \quad \text{for all m.} \tag{A-23}$$

Then the parameter d^2 in (A-22) can be expressed as

$$d^2 = 2\,M\,R. \tag{A-24}$$

More generally, if

$$a_m = A_m \cos \Theta_m, \quad b_m = A_m \sin \Theta_m, \tag{A-25}$$

where $\{A_m\}$ are arbitrary constants, then (A-1) reduces to

$$d^2 = \frac{1}{\sigma^2} \sum_{m=1}^{M} A_m^2 . \tag{A-26}$$

Again, presuming $\{\Theta_m\}$ to be uniformly distributed random variables over 2π, if we define the individual component signal-to-noise ratios as

$$R_m = \frac{\overline{a_m^2}}{\overline{x_m^2}} = \frac{\overline{b_m^2}}{\overline{y_m^2}} = \frac{A_m^2/2}{\sigma^2} , \qquad \text{(A-27)}$$

then (A-26) can be expressed as

$$d^2 = 2 \sum_{m=1}^{M} R_m . \qquad \text{(A-28)}$$

These relations, (A-24) and (A-28), afford an alternative interpretation of the "total" parameter d^2 in terms of component signal-to-noise ratios.

APPENDIX B. TABULATION OF P_{CD} AND $Q_M(d,T)$

For the eight possible combinations of M=1,10 with N=2,10,100,1000, values of the exact value of P_{CD} and the approximation afforded by $Q_M(d,T)$ are tabulated here. An explanation of table B-1, which pertains to M=1, N=2, follows:

For threshold T = 2.40, the false alarm probability P_F = .10912. Holding these values fixed, then as d is varied from 2.2 to 5.4, the detection probabilities vary over the values .5, .9, .99, .999 (approximately). This case is covered by the top four lines in table B-1.

When the threshold T is changed to 3.25, the new false alarm probability is P_F = .01015, and the second group of four lines in table B-1 pertains. This procedure is continued for all the M,N combinations, while P_F ranges over the values .1, .01, .001 (approximately). The comparisons for smaller P_F values are not conducted because the discrepancies are very small, as may be seen by inspection of the tables.

The greatest discrepancies between probabilities P_{CD} and $Q_M(d,T)$ occur in tables B-3 and B-4, where N=10. These particular cases are plotted in figure B-1, for false alarm probabilities in the .1 and .01 regime. For example, the two curves labelled by A, which pertains to M=1, N=10, $P_F \approx .1$, show a very slight difference between the two probabilities over the range (.5,.999). The label B actually pertains to two overlapping curves for M=1, N=10, $P_F \approx .01$; that is, the plotted values for P_{CD} and

$Q_M(d,T)$ are indistinguishable at this level of false alarm probability The situation for C and D is exactly similar, except that in these latter cases, we have M=10, N=10.

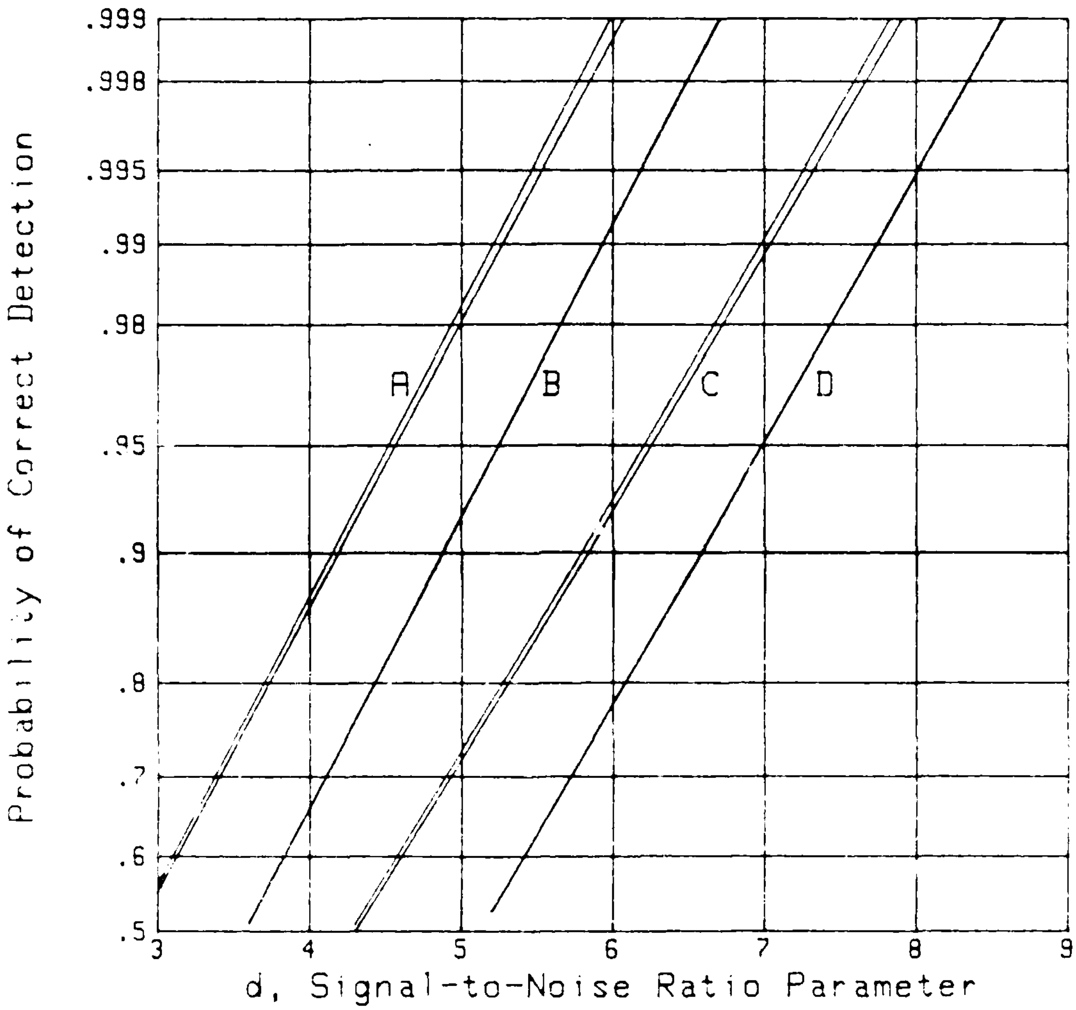

A: Table B-3, P_F =.10272
B: Table B-3, P_F =.01021
C: Table B-4, P_F =.10175
D: Table B-4, P_F =.01002

Figure B-1. Comparison of Probabilities

	d	P_{CD}	$Q_M(d,T)$
$T = 2.40$	2.2	.50220	.51005
$P_F = .10912$	3.6	.91017	.91506
	4.6	.98935	.99062
	5.4	.99890	.99915
$T = 3.25$	3.1	.50353	.50409
$P_F = .01015$	4.4	.89997	.90032
	5.5	.99099	.99106
	6.3	.99920	.99921
$T = 3.89$	3.8	.51653	.51658
$P_F = .00104$	5.0	.88951	.88954
	6.2	.99205	.99206
	6.9	.99905	.99905

Table B-1. Probability Comparison for M=1, N=2

	d	P_{CD}	$Q_M(d,T)$
$T = 5.59$	3.5	.49914	.50646
$P_F = .10129$	5.1	.89637	.90120
	6.4	.99083	.99185
	7.3	.99913	.99931
$T = 6.32$	4.6	.51111	.51166
$P_F = .01013$	6.1	.90493	.90526
	7.3	.99132	.99138
	8.1	.99905	.99906
$T = 6.89$	5.3	.49032	.49036
$P_F = .00101$	6.8	.90322	.90325
	8.0	.99162	.99162
	8.8	.99913	.99913

Table B-2. Probability Comparison for M=10, N=2

	d	P_{CD}	$Q_M(d,T)$
$T = 3.01$	2.9	.51382	.52498
$P_F = .10272$	4.2	.90180	.90857
	5.3	.99074	.99213
	6.1	.99909	.99933
$T = 3.71$	3.6	.51050	.51140
$P_F = .01021$	4.9	.90404	.90457
	6.0	.99161	.99171
	6.8	.99927	.99929
$T = 4.29$	4.2	.51145	.51153
$P_F = .00101$	5.5	.90544	.90548
	6.6	.99188	.99189
	7.3	.99903	.99903

Table B-3. Probability Comparison for M=1, N=10

	d	P_{CD}	$Q_M(d,T)$
$T = 6.11$	4.3	.49943	.51032
$P_F = .10175$	5.9	.90911	.91532
	7.1	.99133	.99257
	7.9	.99898	.99921
$T = 6.73$	5.2	.52682	.52769
$P_F = .01002$	6.6	.90232	.90282
	7.8	.99133	.99143
	8.6	.99908	.99910
$T = 7.23$	5.8	.51336	.51344
$P_F = .00104$	7.2	.90126	.90131
	8.4	.99160	.99160
	9.2	.99914	.99914

Table B-4. Probability Comparison for M=10, N=10

	d	P_{CD}	$Q_M(d,T)$
$T = 3.70$	3.6	.50535	.51547
$P_F = .10105$	4.9	.90037	.90628
	6.0	.99080	.99193
	6.8	.99914	.99931
$T = 4.29$	4.2	.51067	.51153
$P_F = .01003$	5.5	.90499	.90548
	6.6	.99180	.99189
	7.3	.99901	.99903
$T = 4.79$	4.7	.50637	.50645
$P_F = .00104$	6.0	.90378	.90382
	7.1	.99170	.99170
	7.8	.99900	.99900

Table B-5. Probability Comparison for M=1, N=100

	d	P_{CD}	$Q_M(d,T)$
$T = 6.72$	5.2	.52240	.53217
$P_F = .09974$	6.6	.89913	.90471
	7.8	.99064	.99169
	8.6	.99895	.99913
$T = 7.23$	5.8	.51258	.51344
$P_F = .01033$	7.2	.90082	.90131
	8.4	.99152	.99160
	9.2	.99913	.99914
$T = 7.68$	6.4	.52928	.52936
$P_F = .00102$	7.8	.91140	.91144
	8.9	.99112	.99113
	9.7	.99910	.99910

Table B-6. Probability Comparison for M=10, N=100

	d	P_{CD}	$Q_M(d,T)$
$T = 4.27$	4.2	.51031	.51962
$P_F = .10403$	5.5	.90369	.90884
	6.6	.99141	.99233
	7.3	.99892	.99909
$T = 4.79$	4.7	.50564	.50645
$P_F = .01036$	6.0	.90337	.90382
	7.1	.99162	.99170
	7.8	.99899	.99900
$T = 5.25$	5.2	.51839	.51846
$P_F = .00103$	6.5	.90916	.90920
	7.5	.99008	.99009
	8.3	.99911	.99911

Table B-7. Probability Comparison for M=1, N=1000

	d	P_{CD}	$Q_M(d,T)$
$T = 7.22$	5.8	.50897	.51785
$P_F = .10332$	7.2	.89822	.90320
	8.4	.99098	.99185
	9.2	.99903	.99917
$T = 7.68$	6.3	.49278	.49354
$P_F = .01017$	7.8	.91105	.91144
	8.9	.99105	.99113
	9.7	.99909	.99910
$T = 8.08$	6.8	.50022	.50029
$P_F = .00105$	8.2	.90129	.90133
	9.3	.98975	.98976
	10.1	.99894	.99894

Table B-8. Probability Comparison for M=10, N=1000

APPENDIX C. PROGRAM LISTING

```
10    M=10                       !  NUMBER OF FILTER OUTPUTS SUMMED
20    N=1000                     !  NUMBER OF CHANNELS OR-ED
30    DIM U(100),Do(1:10,0:3)     !  THRESHOLD VALUES
40    COM Pf(100),Pd1(100),Pd2(100),Pd3(100),Pd4(100),Pd5(100)
50    COM Pd6(100),Pd7(100),Pd8(100),Pd9(100),Pd10(100)
60    COM Pd11(100),Pd12(100),Pd13(100),Pd14(100),Pd15(100)
70    COM Pd16(100),Pd17(100)
80    DOUBLE M,N,I,J             !  INTEGERS
90    DATA 2,3,4,4,3,3,4,5,3,4,4,5,3,4,4,5,3,4,5,5
100   DATA 3,4,5,5,4,4,5,5,4,4,5,6,4,5,5,6,4,5,5,6
110   READ Do(*)                 !  STARTING VALUES FOR d
120   U=0.
130   U=U+.01
140   Pf=FNPf(U,M,N)
150     IF Pf>.1 THEN 130        !  UPPER LIMIT ON Pf
160   U1=MAX(U-.01,.01)
170   U=U+.01
180   Pf=FNPf(U,M,N)
190     IF Pf>1E-10 THEN 170     !  LOWER LIMIT ON Pf
200   U2=U
210   Delu=(U2-U1)/100.
220   FOR I=0 TO 100
230   U=U1+Delu*I
240   U(I)=U
250   Pf(I)=FNPf(U,M,N)
260   NEXT I
270   I=LGT(N)
280   Do=Do(M,I)
290     PRINTER IS PRT
300     PRINT M,N,Do
310     PRINTER IS CRT
320   FOR J=1 TO 17
330     Ds=Do+(J-1)*.5           !  TOTAL DEFLECTION PARAMETER d
340   FOR I=0 TO 100
350   U=U(I)                     !  THRESHOLD
360   Pd=FNPd(Ds,U,M)
370   Pd=MIN(Pd,.99999)
380   IF J=1 THEN Pd1(I)=Pd
390   IF J=2 THEN Pd2(I)=Pd
400   IF J=3 THEN Pd3(I)=Pd
410   IF J=4 THEN Pd4(I)=Pd
420   IF J=5 THEN Pd5(I)=Pd
430   IF J=6 THEN Pd6(I)=Pd
440   IF J=7 THEN Pd7(I)=Pd
450   IF J=8 THEN Pd8(I)=Pd
460   IF J=9 THEN Pd9(I)=Pd
470   IF J=10 THEN Pd10(I)=Pd
480   IF J=11 THEN Pd11(I)=Pd
490   IF J=12 THEN Pd12(I)=Pd
500   IF J=13 THEN Pd13(I)=Pd
510   IF J=14 THEN Pd14(I)=Pd
520   IF J=15 THEN Pd15(I)=Pd
530   IF J=16 THEN Pd16(I)=Pd
540   IF J=17 THEN Pd17(I)=Pd
550   NEXT I
560   NEXT J
```

```
570     FOR I=0 TO 100
580     Pf(I)=FNInvphi(Pf(I))
590     Pd1(I)=FNInvphi(Pd1(I))
600     Pd2(I)=FNInvphi(Pd2(I))
610     Pd3(I)=FNInvphi(Pd3(I))
620     Pd4(I)=FNInvphi(Pd4(I))
630     Pd5(I)=FNInvphi(Pd5(I))
640     Pd6(I)=FNInvphi(Pd6(I))
650     Pd7(I)=FNInvphi(Pd7(I))
660     Pd8(I)=FNInvphi(Pd8(I))
670     Pd9(I)=FNInvphi(Pd9(I))
680     Pd10(I)=FNInvphi(Pd10(I))
690     Pd11(I)=FNInvphi(Pd11(I))
700     Pd12(I)=FNInvphi(Pd12(I))
710     Pd13(I)=FNInvphi(Pd13(I))
720     Pd14(I)=FNInvphi(Pd14(I))
730     Pd15(I)=FNInvphi(Pd15(I))
740     Pd16(I)=FNInvphi(Pd16(I))
750     Pd17(I)=FNInvphi(Pd17(I))
760     NEXT I
770     CALL A
780     END
790     !
800     DEF FNInvphi(X)                 !   AMS 55, 26.2.23
810     IF X=.5 THEN RETURN 0.
820     P=MIN(X,1.-X)
830     T=-LOG(P)
840     T=SQR(T+T)
850     P=1.+T*(1.432788+T*(.189269+T*.001308))
860     P=T-(2.515517+T*(.802853+T*.010328))/P
870     IF X<.5 THEN P=-P
880     RETURN P
890     FNEND
900     !
910     DEF FNPf(U,DOUBLE M,N)          !   FALSE ALARM PROBABILITY
920     T=FNE(.5*U*U,M-1)
930     Pf=1.-(1.-T)^N
940     RETURN Pf
950     FNEND
960     !
970     DEF FNPd(Ds,U,DOUBLE M)         !   DETECTION PROBABILITY
980     Pd=FNQm(M,Ds,U)                 !   UPPER BOUND ON Pcd
990     RETURN Pd
1000    FNEND
1010    !
1020    DEF FNE(X,DOUBLE N)             !   exp(-x) e n(x)
1030    DOUBLE K                        !   INTEGER
1040    T=S=EXP(-X)
1050    FOR K=1 TO N
1060    T=T*X/K
1070    S=S+T
1080    NEXT K
1090    RETURN S
1100    FNEND
1110    !
```

```
1120    DEF FNQm(DOUBLE M,REAL A,B)      !   QM(A,B)
1130    Error=1.E-17
1140    DOUBLE M1,J                      !   INTEGERS
1150    Q3=.5*A*A
1160    Q4=.5*B*B
1170    Q5=EXP(-.5*(Q3+Q4))
1180    Q6=Q7=Q5
1190    M1=M-1
1200    FOR J=1 TO M1
1210    Q7=Q7*Q4/J
1220    Q6=Q6+Q7
1230    NEXT J
1240    Qm=Q5*Q6
1250    FOR J=1 TO 300
1260    Q5=Q5*Q3/J
1270    Q7=Q7*Q4/(J+M1)
1280    Q6=Q6+Q7
1290    Q9=Q5*Q6
1300    Qm=Qm+Q9
1310    IF Q9<=Error*Qm THEN 1340
1320    NEXT J
1330    PRINT "300 TERMS IN FNQm(M,A,B) AT ";M;A;B
1340    RETURN MIN(Qm,1.)
1350    FNEND
1360    !
1370    SUB A       !   PLOT PD VS PF ON NORMAL PROBABILITY PAPER
1380    COM Pf(*),Pd1(*),Pd2(*),Pd3(*),Pd4(*),Pd5(*)
1390    COM Pd6(*),Pd7(*),Pd8(*),Pd9(*),Pd10(*)
1400    COM Pd11(*),Pd12(*),Pd13(*),Pd14(*),Pd15(*)
1410    COM Pd16(*),Pd17(*)
1420    DIM A$[30],B$[32]
1430    DIM Xlabel$(1:30),Ylabel$(1:30)
1440    DIM Xcoord(1:30),Ycoord(1:30)
1450    DIM Xgrid(1:30),Ygrid(1:30)
1460    DOUBLE N,Lx,Ly,Nx,Ny,I      !   INTEGERS
1470    !
1480    A$="Probability of False Alarm"
1490    B$="Probability of Correct Detection"
1500    !
1510    Lx=12
1520    REDIM Xlabel$(1:Lx),Xcoord(1:Lx)
1530    DATA E-10,E-9,E-8,E-7,E-6,E-5,E-4,E-3,.01,.02,.05,.1
1540    READ Xlabel$(*)
1550    DATA 1E-10,1E-9,1E-8,1E-7,1E-6,1E-5,1E-4,1E-3,.01,.02,.05,.1
1560    READ Xcoord(*)
1570    !
1580    Ly=18
1590    REDIM Ylabel$(1:Ly),Ycoord(1:Ly)
1600    DATA .01,.02,.05,.1,.2,.3,.4,.5,.6,.7,.8,.9
1610    DATA .95,.98,.99,.995,.998,.999
1620    READ Ylabel$(*)
1630    DATA .01,.02,.05,.1,.2,.3,.4,.5,.6,.7,.8,.9
1640    DATA .95,.98,.99,.995,.998,.999
1650    READ Ycoord(*)
1660    !
1670    Nx=14
1680    REDIM Xgrid(1:Nx)
1690    DATA 1E-10,1E-9,1E-8,1E-7,1E-6,1E-5,1E-4,1E-3,.002,.005,.01,.02,.05,.1
1700    READ Xgrid(*)
1710    !
```

```
1720    Ny=18
1730    REDIM Ygrid(1:Ny)
1740    DATA .01,.02,.05,.1,.2,.3,.4,.5,.6,.7,.8,.9
1750    DATA .95,.98,.99,.995,.998,.999
1760    READ Ygrid(*)
1770    !
1780    FOR I=1 TO Lx
1790    Xcoord(I)=FNInvphi(Xcoord(I))
1800    NEXT I
1810    FOR I=1 TO Ly
1820    Ycoord(I)=FNInvphi(Ycoord(I))
1830    NEXT I
1840    FOR I=1 TO Nx
1850    Xgrid(I)=FNInvphi(Xgrid(I))
1860    NEXT I
1870    FOR I=1 TO Ny
1880    Ygrid(I)=FNInvphi(Ygrid(I))
1890    NEXT I
1900    X1=Xgrid(1)
1910    X2=Xgrid(Nx)
1920    Y1=Ygrid(1)
1930    Y2=Ygrid(Ny)
1940    Scale=(Y2-Y1)/(X2-X1)
1950    GINIT 200./260.                             !  VERTICAL PAPER
1960    PLOTTER IS 505,"HPGL"
1970    PRINTER IS 505
1980  ! PRINT "VS2"
1990    LIMIT PLOTTER 505,0.,200.,0.,260.           !  1 GDU = 2 mm
2000  ! VIEWPORT 20.,20.+103./Scale,19.,122.
2010    VIEWPORT 20.,85.,19.,122.
2020  ! VIEWPORT 22.,85.,59.,122.                  !  TOP OF PAPER
2030  ! VIEWPORT 22.,85.,19.,62.                   !  BOTTOM OF PAPER
2040    WINDOW X1,X2,Y1,Y2
2050    FOR I=1 TO Nx
2060    MOVE Xgrid(I),Y1
2070    DRAW Xgrid(I),Y2
2080    NEXT I
2090    FOR I=1 TO Ny
2100    MOVE X1,Ygrid(I)
2110    DRAW X2,Ygrid(I)
2120    NEXT I
2130    PENUP
2140    CSIZE 2.3,.5
2150    LORG 5
2160    Y=Y1-(Y2-Y1)*.02
2170    FOR I=1 TO Lx
2180    MOVE Xcoord(I),Y
2190    LABEL Xlabel$(I)
2200    NEXT I
2210    CSIZE 3.,.5
2220    MOVE .5*(X1+X2),Y1-.06*(Y2-Y1)
2230    LABEL A$
2240    MOVE .5*(X1+X2),Y1-.1*(Y2-Y1)
2250       LABEL "Figure 42. ROC for M=10, N=1000"
```

```
2260    CSIZE 2.3,.5
2270    LORG 8
2280    X=X1-(X2-X1)*.01
2290    FOR I=1 TO Ly
2300    MOVE X,Ycoord(I)
2310    LABEL Ylabel$(I)
2320    NEXT I
2330    LDIR PI/2.
2340    CSIZE 3.,.5
2350    LORG 5
2360    MOVE X1-.15*(X2-X1),.5*(Y1+Y2)
2370    LABEL B$
2380    PENUP
2390    PLOT Pf(*),Pd1(*)
2400    PENUP
2410    PLOT Pf(*),Pd2(*)
2420    PENUP
2430    PLOT Pf(*),Pd3(*)
2440    PENUP
2450    PLOT Pf(*),Pd4(*)
2460    PENUP
2470    PLOT Pf(*),Pd5(*)
2480    PENUP
2490    PLOT Pf(*),Pd6(*)
2500    PENUP
2510    PLOT Pf(*),Pd7(*)
2520    PENUP
2530    PLOT Pf(*),Pd8(*)
2540    PENUP
2550    PLOT Pf(*),Pd9(*)
2560    PENUP
2570    PLOT Pf(*),Pd10(*)
2580    PENUP
2590    PLOT Pf(*),Pd11(*)
2600    PENUP
2610    PLOT Pf(*),Pd12(*)
2620    PENUP
2630    PLOT Pf(*),Pd13(*)
2640    PENUP
2650    PLOT Pf(*),Pd14(*)
2660    PENUP
2670    PLOT Pf(*),Pd15(*)
2680    PENUP
2690    PLOT Pf(*),Pd16(*)
2700    PENUP
2710    PLOT Pf(*),Pd17(*)
2720    PENUP
2730    BEEP 500,2
2740    PRINTER IS CRT
2750    PLOTTER 505 IS TERMINATED
2760    SUBEND
```

REFERENCES

1. C. W. Helstrom, Statistical Theory of Signal Detection, Second Edition, Pergamon Press Inc., New York, NY, 1968.

2. A. H. Nuttall and R. Garber, "Receiver Operating Characteristics for Phase-Incoherent Detection of Multiple Observations," NUSC Technical Memorandum TC-179-71, Naval Underwater Systems Center, New London, CT, 28 September 1971.

3. A. H. Nuttall and E. S. Eby, Signal-To-Noise Ratio Requirements for Detection of Multiple Pulses Subject to Partially-Correlated Fading with Chi-Squared Statistics of Various Degrees of Freedom, NUSC Technical Report 7707, Naval Underwater Systems Center, New London, CT, 2 June 1986.

4. R. F. Dwyer, Or-ing Data Reduction Model with Applications in Passive Sonar, NUSC Technical Report 5231, Naval Underwater Systems Center, New London, CT, 3 October 1975.

5. Handbook of Mathematical Functions, U. S. Department of Commerce, National Bureau of Standards, Applied Mathematics Series No. 55, U. S. Government Printing Office, Washington, D.C., June 1964.

6. A. H. Nuttall, Exact Performance of General Second-Order Processors for Gaussian Inputs, NUSC Technical Report 7035, Naval Underwater Systems Center, New London, CT, 15 October 1983.

7. I. S. Gradshteyn and I. M. Ryzhik, Table of Integrals, Series and Products, Academic Press, Inc., New York, NY, 1980.

INIITAL DISTRIBUTION LIST

Addressee	No. of Copies
ADMIRALTY UNDERWATER WEAPONS ESTAB., DORSET, ENGLAND	1
ADMIRALILTY RESEARCH ESTABLISHMENT, LONDON, ENGLAND (Dr. L. Lloyd)	1
APPLIED PHYSICS LAB, JOHN HOPKINS	1
APPLIED PHYSICS LAB, U. WASHINGTON	1
APPLIED RESEARCH LAB, PENN STATE	1
APPLIED RESEARCH LAB, U. TEXAS	1
APPLIED SEISMIC GROUP, CAMBRIDGE, MA (R. Lacoss)	1
A & T, STONINGTON, CT (H. Jarvis)	1
APPLIED SEISMIC GROUP, (R. Lacoss)	1
ASTRON RESEARCH & ENGR, SANTA MONICA, CA (Dr. A. Piersol)	1
ASW SIGNAL PROCESSING, MARTIN MARIETTA BALTIMORE AEROSPACE (S. L. Marple)	1
AUSTRALIAN NATIONAL UNIV. CANBERRA, AUSTRALIA (Prof. B. Anderson)	1
BBN, Arlington, Va. (Dr. H. Cox)	1
BBN, Cambridge, MA (H. Gish)	1
BBN, New London, Ct. (Dr. P. Cable)	1
BELL COMMUNICATIONS RESEARCH, Morristown, NJ (J. Kaiser)	1
BENDAT, JULIUS DR., 833 Moraga Dr., LA, CA	1
BROWN UNIV., PROVIDENCE, RI (Documents Library)	1
CANBERRA COLLEGE OF ADV. EDUC, BELCONNEN, A.C.T. AUSTRALIA (P. Morgan)	1
COAST GUARD ACADEMY, New London, CT (Prof. J. Wolcin)	1
COAST GUARD R & D, Groton, CT (Library)	1
COGENT SYSTEMS, INC, (J. Costas)	1
COLUMBIA RESEARCH CORP, Arlington, VA 22202 (W. Hahn)	1
CONCORDIA UNIVERSITY H-915-3, MONTREAL, QUEBEC CANADA (Prof. Jeffrey Krolik)	1
CNO, Wash, DC	1
DAVID W. TAYLOR NAVAL SHIP R&D CNTR, BETHESDA, MD	1
DARPA, ARLINGTON, VA (A. Ellinthorpe)	1
DALHOUSIE UNIV., HALIFAX, NOVA SCOTIA, CANADA (Dr. B. Ruddick)	1
DEFENCE RESEARCH ESTAB. ATLANTIC, DARTMOUTH, NOVA SCOTIA (Library)	1
DEFENCE RESEARCH ESTAB. PACIFIC, VICTORIA, CANADA (Dr. D. Thomson)	1
DEFENCE SCIENTIFIC ESTABLISHMENT, MINISTRY OF DEFENCE, AUCKLAND, N Z. (Dr. L. Hall)	1
DEFENCE RESEARCH CENTRE, ADELAIDE, AUSTRALIA	1
DEFENSE SYSTEMS, INC, MC LEAN, VA (Dr. G. Sebestyen)	1
DTNSRDC	1
DTIC	2
DREXEL UNIV, (Prof. S. Kesler)	1
ECOLE ROYALE MILITAIRE, BRUXELLES, BELGIUM (Capt J. Pajot)	1
EDO CORP, College Point, NY	1
EG&G, Manassas, VA (Dr. J. Hughen)	1
ENGINEERING SOCIETIES LIBRARY, NY, NY	1
FUNK, DALE, Seattle, Wn	1

GENERAL ELECTRIC CO. PITTSFIELD, MA (Mr. J. Rogers)	1
GENERAL ELECTRIC CO, SYRACUSE, NY (Mr. R. Race)	1
HAHN, WM, Apt. 701, 500 23rd St. NW, Wash, DC 20037	1
HARRIS SCIENTIFIC SERVICES, Dobbs Ferry, NY (B. Harris)	1
HARVARD UNIV, CAMBRIDGE, MA (Library)	1
HONEYWELL, INC., Seattle, WN (D. Goodfellow)	1
HUGHES AIRCRAFT, Fullterton, CA (S. Autrey)	1
IBM, Manassas, VA (G. Demuth)	1
INDIAN INSTITUTE OF SCIENCE, BANGALSORE, INDIA (N. Srinivasa)	1
JOHNS HOPKINS UNIV, LAUREL, MD (J. C. Stapleton)	1
M/A-COM, BURLINGTON, MA (Dr. R. Price)	1
MAGNAVOX GOV & IND ELEC CO, Ft. Wayne, IN (R. Kenefic)	1
MARINE BIOLOGICAL LAB, Woods Hole, MA	1
MASS INSTITUTE OF TECH, Cambridge, MA (Library and (Prof. A. Baggaroer)	2
MAXWELL AIR FORCE BASE, ALABAMA (Library)	1
MBS SYSTEMS, NORWALK, CT (A. Winder)	1
MIDDLETON, DAVID, 127 E. 91st ST, NY, NY	1
MIKHALEVSKY, PETER, SAIC, 803 W. Broad St., Falls Church, VA.	1
NADC	1
NASC, NAIR-03	1
NATIONAL RADIO ASTRONOMY OBSERVATORY (F. Schwab)	1
NATO SACLANT ASW RESEARCH CNTR, APO, NY, NY (Library, E. J. Sullivan and G. Tacconi)	3
NAVAL INTELLIGENCE COMMAND	1
NAVAL INTELLIGENCE SUPPORT CTR	3
NAVAL OCEANOGRAPHY COMMAND	1
NAVAL OCEANOGRAPHIC OFFICE	1
NAVAL POSTGRADUATE SCHOOL, MONTEREY, CA (C. W. Therrien)	1
NAVAL RESEARCH LAB, Orlando, FL	1
NAVAL RESEARCH LAB, Washington, DC (Dr. P. B. Abraham; W. Gabriel, Code 5372; A Gerlach; and N. Yen (Code 5135)	4
NAVAL SYSTEMS DIV., SIMRAD SUBSEA A/S, NORWAY (E. B. Lunde)	1
NCEL	1
NCSC	1
NICHOLS RESEARCH CORP., Wakefield, MA (T. Marzetta)	1
NOP-098	1
NORDA (R. Wagstaff)	1
NORTHEASTERN UNIV. (Prof. C. L. Nikias)	1
NOSC, (F. J. Harris)	1
NPRDC	1
NPS	3
NRL, Washington, DC (Dr. P. Abraham, W. Gabriel, A. Gerlach and Dr. Yen)	4
NRL, UND SOUND REF DET, ORLANDO	1
NSWC	1
NSWC DET FT. LAUDERDALE	1
NSWC WHITE OAK LAB	1
NUSC DET FT. LAUDERDALE	1
NUSC DET TUDOR HILL	1
NUSC DET WEST PALM BEACH (Dr. R. Kennedy Code 3802)	1
NWC	1
OCNR-00, -10, -11, -12, -13, -20(2), -122, -123-, -124	10
OFFICE OF NAVAL RESEARCH, Arlington, VA (N. Gerr, Code 411)	1
ORI CO, INC, New London, CT (G. Assard)	1

PENN STATE UNIV., State College, PA (F. Symons)	1
PDW-124	1
PMS-409, -411	2
PROMETHEUS, INC, Sharon, MA (Dr. J. Byrnes)	1
PSI MARINE SCIENCES, New London, Ct. (Dr. R. Mellen)	1
RAN RESEARCH LAB, DARLINGHURST, AUSTRALIA	1
RAYTHEON CO, Portsmouth, RI (J. Bartram)	1
ROCKWELL INTERNATIONAL CORP. Anaheim, CA (L. Einstein	
and Dr. D. Elliott)	2
ROYAL MILITARY COLLEGE OF CANADA, (Prof. Y. Chan)	1
RCA CORP, Moorestown, NJ (H. Upkowitz)	1
SAIC, Falls Church, VA (Dr. P. Mikhalevsky)	1
SAIC, New London, CT (Dr. F. Dinapoli)	1
SANDIA NATIONAL LABORATORY (J. Claasen)	1
SCRIPPS INSTITUTION OF OCEANOGRAPHY	1
SEA-63, -63D,	2
SONAR & SURVEILLANCE GROUP, DARLINGHURST, AUSTRALIA	1
SOUTHEASTERN MASS. UNIV (Prof. C. H. Chen)	1
SPERRY CORP, GREAT NECK, NY	1
SPWAR-05	1
TEL-AVIV UNIV, TEL-AVIV, ISRAEL (Prof. E. Winstein)	1
TRACOR, INC, Austin, TX (Dr. T Leih and J. Wilkinson)	1
TRW FEDERAL SYSTEMS GROUP (R. Prager)	1
UNDERSEA ELECTRONICS PROGRAMS DEPT, SYRACUSE, NY (J. Rogers)	1
UNIV. OF ALBERTA, EDMONTON, ALBERTA, CANADA (K. Yeung)	1
UNIV OF CA, San Diego, CA (Prof. C. Helstrom)	1
UNIV OF CT, (Library and Prof. C. Knapp)	2
UNIV OF FLA, GAINESVILLE, FL (D. Childers)	1
UNIV OF MICHIGAN, Cooley Lab, Ann Arbor, MI (Prof T. Birdsall)	1
UNIV. OF MINN, Minneapolis, Mn (Prof. M. Kaveh)	1
UNIV. OF NEWCASTLE, NEWCASTLE, NSW, CANADA (Prof. A. Cantoni)	1
UNIV OF RI, Kingston, RI (Prof. S. Kay, Prof. L. Scharf,	
Prof. D. Tufts and Library)	4
UNIV. OF STRATHCLYDE, ROYAL COLLEGE, Glasgow, Scotland	
(Prof. T. Durrani)	1
UNIV. OF TECHNOLOGY, Loughborough, Leicestershire, England	
(Prof. J. Griffiths)	
UNIV. OF WASHINGTON, Seattle (Prof. D. Lytle)	
URICK, ROBERT, Silver Springs, MD	
VAN ASSELT, HENRIK, USEA S.P.A., LA SPEZIA, ITALY	
WEAPONS SYSTEM RESEARCH LAB, ADELAIDE, AUSTRALIA	
WESTINGHOUSE ELEC. CORP, WALTHAM, MA (D. Bennett)	
WESTINGHOUSE ELEC. CORP, OCEANIC DIV, ANNAPOLIS, MD	
(Dr. H. L. Price)	
WINDER, A. Norwalk, CT	
WOODS HOLE OCEANOGRAPHIC INSTITUTION	
Dr. R. Spindel and Dr. E. Weinstein	
YALE UNIV (Library and Prof. P. Schu[illegible]	